M R D division

GENERAL AMERICAN TRANSPORTATION CORPORATION

7501 NORTH NATCHEZ AVENUE • NILES 48, ILLINOIS • NILES 7-7000

NASA

NONDESTRUCTIVE TESTING FOR EVALUATION OF STRENGTH OF BONDED MATERIAL

By Gerald Schmitz and Louis Frank

September 1965

Prepared under Contract No. NAS 8-11456 by
GENERAL AMERICAN RESEARCH DIVISION
General American Transportation Corporation
Niles, Illinois

Marshall Space Flight Center

NATIONAL AERONAUTICS AND SPACE ADMINISTRATION

FOREWORD

This report was prepared by the General American Research Division under Contract NAS 8-11456, Nondestructive Testing, for the George C. Marshall Space Flight Center of the National Aeronautics and Space Administration. The work was administered under the technical direction of the Quality & Reliability Assurance Laboratory of the George C. Marshall Space Flight Center with James B. Beal acting as project manager.

ABSTRACT

The theoretical and experimental investigation of various techniques for nondestructively testing for bond strength are described. Existing nondestructive test techniques are mainly effective for detecting complete lack of bond in adhesively bonded structures. Techniques investigated included: acoustic emission, bond line electrical parameters, strain sensitive coatings, and ultrasonic attenuation as a function of bond stress. The ultrasonic emission of a bond line under stress was found to be a reliable indication of bond strength. A definite need was found for a widely applicable bond stress method.

TABLE OF CONTENTS

TABLE OF CONTENTS (CONTINUED)

TABLE OF CONTENTS (CONTINUED)

LIST OF FIGURES

LIST OF FIGURES (CONTINUED)

LIST OF TABLES

SECTION 1

INTRODUCTION

The needs of the aerospace industry have rapidly accelerated the use of adhesive bonding in structural applications. Composite structures, particularly those using honeycomb, are to a large extent adhesively bonded today. The advantages of adhesive bonding over welding, brazing, riveting, etc. are well known. Perhaps the major problem posed by their use has been the variability of bond strength sometimes obtained. The exact reasons for these variations are larely obscure although in many cases they can be related to material and adhesive handling and processing procedures. This problem is further complicated by the fact that no suitable nondestructive testing (NDT) technique exists for measuring the strength of the bonds in complex structures. Methods have been developed for determining whether or not a bond exists, and in some cases the character of the bond line, but experience has shown that none are effective for determining bond strength. This program was undertaken to investigate nondestructive testing methods capable of quantitatively determining bond strength. All NDT methods were considered within the legitimate domain of the program.

To maximize the immediate return from the program attention was focused on adhesives and structures currently under consideration and use under the Saturn 5 program. Adhesives considered were:

1) HT-424 Bloomingdale Rubber Co.
2) FM-1000 Bloomingdale Rubber Co.
3) Metlbond 329 Narmco Materials Division
4) 7343/7344 Narmco Materials Division

The types of structures considered included:

1) Aluminum honeycomb core with aluminum face sheets.
2) Phenolic honeycomb core with aluminum face sheets.
3) Metal to metal bonds.

Guide lines established by NASA for the equipment development included:

1) The equipment should be portable to permit use for both spot check and automatic scanning.
2) Equipment should be useable on curved surfaces.
3) Liquid couplants or abrasive surface contacts should be avoided.
4) Instruments developed should be as inexpensive and simple in operation as the techniques permit.
5) Where equipment utilizes vibration inputs to structures, the use of sonic as well as ultrasonic transmission of vibration frequencies and frequency scans should be considered.
6) Original ideas and approach were emphasized.

The program was divided into three phases: a survey phase, a theoretical investigation of adhesive bonding, and an experimental phase. The survey included a literature search and numerous discussions with manufacturers and users of adhesives. It was conducted to determine the NDT needs of the bonding industry and to ascertain the present practices. The survey showed little NDT was being used on bonded structures; and a method of determining the strength of a bonded structure was definitely needed. The adhesive type failure at or near the material-adhesive interface was found to be more troublesome than the cohesive type failure resulting from a condition such as excessive bond porosity. This is due to the low strength of the bond, the wide area affected, and the difficulty in detecting the adhesive type of weakness.

The second phase of the program (the theoretical investigation), consisted of a literature review, a brief analytical study, and discussions with theoretical people and engineers working in the field. Its purpose was to examine current theories and identify those parameters that can be related to bonding strength. This knowledge would form the starting point for later equipment development.

Under the third phase of the program, techniques for simulating variable strength bonds were to be developed and NDT techniques applicable to bond inspection were to be investigated. The variable bond strength simulation investigation resulted in a new technique which we have labeled photomicroflaw. This technique is capable of producing bond strengths from zero to 100% with the repeatability obtainable in manufacturing good bonds. The NDT investigation uncovered a number of promising inspection techniques applicable to various kinds of bonds. Of these, the sonic emission from a stressed bond was found to be a reliable indication of the bond condition and has possible uses in whole structure tests.

The sonic emission technique has immediate application to proof tests. It is recommended that a program to adapt this technique to the static or dynamic tests of subsections or stages be undertaken. This program would determine the ultrasonic emission characteristics of large structures under stress and determine optimal instrumentation. Such instrumentation could, for a modest additional cost, greatly increase the amount of data available from the hydraulic or dynamic tests of large structures.

The investigation of NDT techniques demonstrated that stressing of the bond line is required to discern bonds of different strength. A program to investigate all methods of bond stress is recommended. The bond stress method investigated could be used for all present methods of NDT, including the strain sensitive coatings and the ultrasonic emission technique. They would also be useful as a proof test of critical bond areas.

The remainder of this report treats the various phases of the investigation in detail and presents the results obtained and the conclusion reached relative to the feasibility of inspecting adhesive bonded structures.

SECTION 2

SURVEY PHASE RESULTS

This phase consisted of a literature search followed by a survey of the adhesive manufacturers, the fabricators using adhesive bonding, and the manufacturers of NDT equipment. The survey was conducted to determine the state of art of adhesive bonding and nondestructive testing of adhesive bonds.

The number of papers published on the subject of bond nondestructive testing is relatively limited. Those papers that are available are largely concerned with particular equipment. A report[1*] of work done for the Navy Bureau of Aeronautics compares several of the nondestructive test instruments for inspecting bonds and is informative. The reports of development work on the instrumentation were, in cases, sources of information.[2,3,4] Some of the operating manuals for the bond nondestructive testing instrumentation were also useful.

The literature search pointed out several facts. First, an urgent need exists for a true bond strength inspection system. Secondly, a need exists for a consistent method of simulating a poor bond. Thirdly, existing NDT equipment is adequate for detecting understrength bonds caused by large voids in the adhesive, complete unbond due to inaccurate mating surfaces of serious contamination, bond line porosity, and bond line thickness. This equipment is completely inadequate for detecting poor adhesive type bonds.

The specific information sought from the adhesive manufacturers and users included: What are the main problems in producing a good bond? What are the critical parameters affecting a good bond? What are the NDT techniques now in use? What additional NDT test would be useful?

The adhesive manufacturers often gave different answers to these questions than the users because of a different point of view. Both the adhesive manufacturer and the user agree that very strict control over every portion of the adhesive bonding process is necessary. However, from the manufacturers point of view, if all the precise steps are carried out properly, a good bond will result. From the users point of view, unavoidable and often unknown process variables will affect the strength of a bond. Thus the main problems in producing a good bond from an adhesive manufacturer's point of view are related to process variables. Fitting of faying surfaces, heat rate, and bonding pressure are the important problem areas. As examples, if the parts to be bonded are misfitted or the pressure while bonding is insufficient, the adhesive will not wet the surfaces and a poor bond will be formed. If the adhesive is brought up to temperature too slowly so that there is improper filleting action a weak drum peel test on honeycomb panel results.

---

* The numbers refer to the list of references at the end of this report.

Both the manufacturer and the user stress the importance of proper cleaning, etching, and elimination of any chance of contamination during the process. An instance of a difficult bonding situation occurred when one manufacturer was producing understrength bonds during humid weather. Although subsequently portions of the bonding operation were humidity controlled, the bonds remained understrength, and bonding had to be suspended for the humid months. Poor bonds can also be produced by unavoidable delays in the monitoring of the cleaning and etching bath.

Most of the more serious poor bond situations resulted from "adhesive" failures; these are characterized by almost all of the adhesive remaining on one faying surface when the bond is broken. The surface of the adhesive will often have a very shiny surface when the bond is broken in this way. These failures are attributed to contamination of some type, sometimes from unknown sources.

The critical considerations for a good bond as determined from the survey include the formation of a strong wettable oxide surface on the metal to be bonded, proper wetting of the surface with the adhesive, elimination of contaminants, and control of the fitting, temperature, and pressure of the bond.

The users of the adhesives were more concerned about the need for an NDT technique for determining bond strength as they are surer of the many fabrication variables that can affect a bond. The types of NDT equipment now available are well known to most manufacturers of bonded structures and are used mainly for critical bonds. However, the shortcomings of the best equipment available are serious and often they will not detect an understrength bond. It is significant that at least one adhesive user uses the "coin tapping" test. In this test a skilled operator taps the bonded panel with a coin and determines from the sound the soundness of the panel. This technique will detect the larger bonding voids. The weak bonds detected by any available NDT technique are those originating from faulty cure, or excess porosity. However, the very serious problem of the "adhesive" failures cannot be detected.

A review of the existing NDT instruments showed that most of them fall into two major categories. The first category is the ultrasonic or sonic instrument. It is characterized by such instruments as the Fokker bond tester, the Coinda-Scope and the Stubmeter. The second major type of NDT technique includes means for physically stressing all or part of the bond line. These are either proof tests which do not damage a good bond or plug tests where a small portion of the bond line is removed, stressed to destruction and the section repaired. The Porta-shear and Porta-pull techniques are examples of the small destructive test.

The results of the survey phase indicate that a nondestructive technique to determine bond strength is urgently needed. A versatile instrument would have to detect the adhesive type of failure in addition to voids, porosity, improper cure, etc. Of course, the desirable attributes of any NDT system always include a low initial cost, low inspection cost, simple operation and portability.

SECTION 3

THEORETICAL INVESTIGATION

The object of this phase of the program was to identify the properties of a bond that determine its strength and from this information to determine the NDT technique best suited for measuring these properties. The investigation was conducted through a survey of the books and literature in the field and discussions with people knowledgeable in the field of bonds and bonded structures. This was followed by an analysis of current bonding theories to determine whether they provided any clues which would relate measurable parameters to bonding strength.

Conferences were held with Dr. R. F. Blomquist of the U.S. Department of Agriculture, Forest Products Laboratory, Madison, Wisconsin, and with Dr. L. H. Sharp of Bell Telephone Laboratories, Murray Hill, New Jersey. These discussions were very informative and contributed signficantly to the conclusions drawn in this investigation.

References 4, 5, 6, 7, and 8 contain information about the theoretical nature of the adhesive forces at work in a bond. Some of the older adhesive theories have been superseded, and the present adsorption theory is gaining more acceptance. It was not, however, the purpose of this investigation to appraise the attributes of current bonding theories or to develop a new bonding theory; accordingly, these theories will not be discussed in detail.

Current bonding theories state that all of the forces involved in giving strength to an adhesive bond attenuate very rapidly with increasing distance; therefore, there is great difficulty in measuring them from a distance. Furthermore, except in those theories which hold that the mechanical interlocking of the adhesive or the exclusion of air from the bond layer are responsible for the strength of a bond, the theoretical strength of a bond is higher than the actual measured strength. The results of this investigation further indicated that the theoretical bonding forces were not responsible for the failure of bonds. Since theoretically the bond forces in an adhesive joint are stronger than the cohesive forces in the weaker of the two materials, i.e., the adherand or the adhesive, there is theoretically no bond failure in adhesion.

The apparent failure of a bond in adhesion must then be attributed to other causes, such as surface contaminants, either of a low cohesive force, or of such a chemical composition that the layer of adhesive near the surface is greatly weakened. It is theorized that small areas of contamination can cause stress risers that propagate cracks parallel with and close to the surface of the adherand. Thus, what appears to be an adhesive failure is actually a cohesive failure and a thin film of adhesive is left on the adherand.

Another reason for such a failure could be a weakening of the oxide surface of the adherend which might be due to the etching process or adverse chemical effects after the etching process. Of course, a thin film of a weak contaminant could also cause a weak bond resulting in a cohesive failure of the contaminant.

If these theories are true, the NDT method would have to test for contaminants or the formation of a weak oxide layer. The difficulty of detecting these conditions after the bond is formed in a true nondestructive manner is evident from the configuration of an adhesive bond. The inspection of these surfaces before bonding could be helpful if done immediately before the bonding operation. Some consideration was given to this type of process control and it is a good area for future investigation.

The results of this phase indicated that an NDT technique probably should not be based on the molecular parameters of the theoretical nature of a bond. In any case, the extremely short range of these forces virtually eliminates such a system in a completed bond. If the contamination and discontinuities in the bond layer cause stress risers and contribute to the failure of a bond, it is possible to have perfect adhesion over the greater portion of the area being interrogated and still have a weak bond.

These considerations do suggest areas for investigation into NDT techniques. The possibility of small contaminated areas effecting the total bond strength to a large degree suggests that some method of stressing the bond to fail these portions would be necessary to detect them. For this reason many of the NDT technqiues investigated utilize some bond stress technique. Additionally, as the small contaminant areas will be exposed to very high stresses when the bond line is loaded, it is expected that they will emit sonic and ultrasonic vibrations that can be detected by suitable listening devices long before the complete bond line reaches the point of failure. This phenomenon can lead to proof test.

The change of dielectric properties of the adhesive during cure can be predicted theoretically; thus, with suitable instrumentation, any curing of the adhesive prior to fabrication can be determined. Also, dielectric constant, resistivity, and piezoelectric effect are potentially useable for the measurement of bond interface conditions, particularly for nonconducting composites.

Weak areas caused by poor bonds will manifest themselves by the effect they produce on the stress patterns on the surface of the composite during loading. Stress sensitive coatings which have been used for many years to detect such stress patterns should be applicable for variable strength bond determination within the limitations they impose.

Finally, we would expect that poor bonds will influence the propagation of ultrasonic waves through the part, particularly under loading. Ultrasonic

Lamb waves which can be propagated for short distances in bonded structures offer a potential tool for determining variable bond strength due to their great sensitivity to surface and interface conditions.

A further effort carried out during this phase of the program was an analysis of the forces of attraction in a molecular bond. This analysis is contained in Appendix 1, and was performed to uncover any theoretical molecular parameters capable of being analyzed by nondestructive methods. Although idealized, it is helpful in the consideration of NDT techniques.

Note from the analysis the extremely rapid fall-off of the bond forces. This emphasizes the need for close contact or good wetting. It also emphasizes the difficulty of measuring these forces. Also, according to the analysis, different surfaces will yield different bond strengths. The analysis does show an advantage to the oxide coating on an aluminum surface.

Other considerations indicate that the cause of weak bonds is not the weaking of these forces, but rather the failure to form the bond in the first place. Thus, the cohesive strength of the surface layer of the adhesive is more important than the nature of its bonding forces. The analysis also shows the importance of the molecules of adhesive very close to the surface of the adherand. Because of this any contamination effecting the strength of this very first layer of adhesive is most important.

SECTION 4

UNDERSTRENGTH BOND SIMULATION

In any nondestructive test system an important consideration is the production of sample flaws. This is particularly difficult in the testing of bond strength because the flaw mechanism is not clearly known. In practice poor bonds can be caused by a failure in the cohesive strength of the bulk of the adhesive or in an "adhesive failure". As discussed earlier, it is probable that there is no real adhesive failure because the theoretical adhesive bond is stronger than the cohesive strength of the weaker of the two materials taking part in the bonding. However, any failure that takes place very close to one faying surface is often called an adhesive failure. Such failures are serious in adhesive bonding production.

The unsatisfactory bonds which cause these failures and which must be detected by the inspection system, seem to result from such factors as:

1) improper cleaning and etching,
2) interposition of a weak interface in the bond line through contamination,
3) degradation of the cohesive strength of the adhesive adjacent to the bond line due to contamination, and
4) small contaminations which act as stress risers causing the failure to progress along the bond line.

These bond imperfections are brought about by the following conditions:

1) "smutting" - a film on the surface of aluminum that results from the etching bath for some batches of certain alloys,
2) excess moisture caused in some cases by high humidity,
3) contaminated cleaning and etching bath,
4) excess exposure of the oxide surface before priming or applying the adhesive, and
5) various contaminants (can be airborne or introduced at various stages in the manufacture).

These conditions must, therefore, be simulated to produce bond imperfections.

It is possible to produce weak bonds by allowing the oxide surface to be exposed to the atmosphere for a long period, or by partially curing the adhesive. The strength of the bond produced under these conditions is difficult to control.

Weak bond simulation has previously been accomplished by either changing the process variables or by introducing a sheet of foreign material in the bond line. Polyethylene or TFE plastic strips or paper have been included in the bond line to reduce the bond strength. However, in the latter cases it was found that the adhesive bonded well enough to the plastic strip that

a good bond was registered on NDT equipment. Also, the inclusion of a foreign material of significant thickness and bulk in the bond detracts from the value of the simulation.

Since the object of the program was to investigate weak bonds, several techniques were investigated to simulate them. Several methods of direct contamination of the faying surface before bonding were tried. The most successful method was one in which a pattern of very small dots of contaminant was produced on the surface with a photo emulsion technique. The techniques investigated are described below.

4.1 Contamination

Several means of selectively contaminating the surfaces to be bonded were investigated experimentally. In one, the surface was simply exposed to high humidity. Water and water solutions of salt were also employed to produce weak bonds. These methods were unpredictable and often had no effect on bond strength.

The most successful contamination scheme utilized an oil dissolved in a volatile solvent. Various oils and greases were used with a benzene solvent. As the ratio of oil to benzene was increased, the amount of residual oil remaining on the surface to be bonded after the solvent evaporated also increased. This was found to be a very good method of varying the amount of soil contamination on a faying surface. However, even a uniform coating affects the various adhesives in a different manner. For example, a light coat of mineral oil on the surface to be bonded did not affect the lap shear values of FM-1000, whereas, HT-424 was 20.9% degraded and Metlbond 329 was 38.3% degraded. When a hydrocarbon grease was used, all adhesives were affected. When a high temperature stable silicon grease was used as the contaminant, none of the adhesives were affected.

When the test specimens were bonded without any etching in a chromic-sulfuric acid bath, FM-1000 was again unaffected and Metlbond 329 and HT-424 were degraded. Table 1 summarizes some of the results for three of the adhesives. The low good bond strength (about 1500 psi) of Metlbond 7343/7139 made similar data on this adhesive very difficult to obtain. Figure 1 shows the amount of bond degrading as a function of contaminant-to-solvent ratio for one adhesive. The wide variations in results, the dependency of the results on the adhesive and contaminant used, and the limited percent of degradation possible, limit the value of this type of bond degradation.

4.2 Photomicroflaw

The photomicroflaw technique overcomes many of the difficulties of the previously described approach. The technique simulates more closely the actual role of contaminant in a manufactured bond. As discussed in the first portion of this report, it is believed that contaminants representing

Table 1

Results of Contaminants for Bond Degradation

Resin	Contaminant					
	None	Coated with Dow 331 Silicone Oil No Dilution	% Deviation from Uncontaminated Bond	Coated with Mineral Oil No Dilution	% Deviation from Uncontaminated Bond	Coated with Caldron #1 E.P. by Sinclair Dilute 5.9 gms-in 50 cc of Benzene	% Deviation from Uncontaminated Bond
FM-1000	6320 psi	6320 psi	0%	6320 psi		1940 psi	69%
HT-424	3110 psi	3000 psi	3%	2550 psi	21%	2120 psi	32%
Metlbond-329	2300 psi	2170 psi	6%	1420 psi	28%	1370 psi	40%

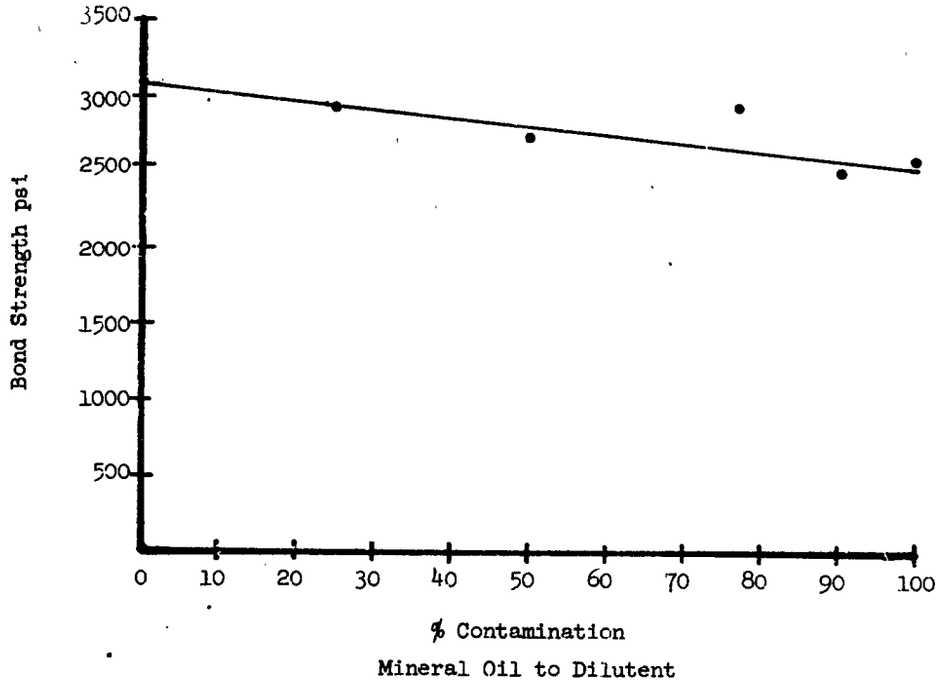

Figure 1 HT-424 BOND DEGRADATION VS CONTAMINANT-TO-SOLVENT RATIO

a small surface area can have a large effect on the strength of the bond as a result of the stress risers produced by the discontinuity of the contaminant. The photomicroflaw technique uses a photographic process for selectivity contaminating the surface area of the adherends.

The technique consists of the following steps which are described in detail below:

1) coat bonding surfaces with photo emulsion,
2) expose coating to light through a grid,
3) immerse exposed coating in appropriate developer, and
4) wash off developer.

The result is a surface which has a grid of uniform contamination and thus, when bonded, produces a sample of predictable strength.

Coating

The photo sensitive emulsion used is called "PHOTO RESIST" made by Eastman Kodak Company of Rochester, New York. Its primary application is as an acid resist for making photoengraved nameplates and printing plates. It is sensitive to ultraviolet light and daylight.

The method of coating depends on the type and shape of the part but a few general rules can be applied to all samples. First, uniform coating is important. For optimum results it is recommended by Eastman Kodak that the emulsion be filtered before using.

In many instances, the best method for coating the samples is by dipping. The lap shear samples are dipped in a pool of emulsifier to a height of approximately one inch and the excess allowed to run off to an edge. It is also helpful to rotate the lap shear samples in the vertical plane to allow the excess emulsifier to run across the surfaces a few times to assure a good coating. The drum peel face sheets and other test blocks can be coated by spilling the emulsion over the surface. The samples are then dried at room temperature for approximately fifteen minutes; this is followed by an oven dry at 100-150°F for an additional fifteen to thirty minutes. This procedure assures a good hard coating.

Sample cleanliness is also important. The samples should be cleaned with a sodium dichromate bath as specified in MIL-A-9067C (paragraph 6.1 "Suggested Procedure for Treatment of Metal Faying Surfaces"). Care must also be taken so as not to contaminate the samples either before, while, or after the coating is applied.

Exposure

The setup for exposing the emulsion to light is shown in Figure 2.

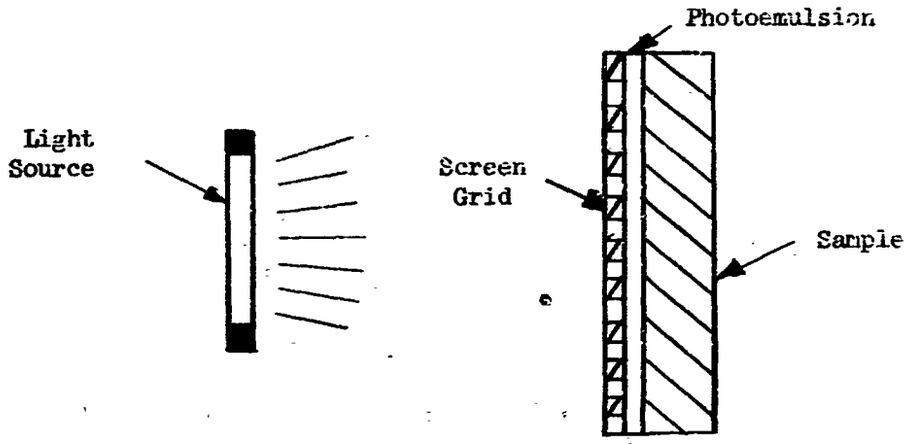

Figure 2 EXPOSURE OF PHOTOEMULSION

The controlling factor in setting the degree of contamination is the grid. Since the emulsion is light sensitive, the areas which are irradiated by the ultraviolet light will stay on the sample surface, and conversely those areas which fall within the shadow of the blackened areas of the grid will be removed after applying the developer.

Photographer's "Screen-tints" were used as grids. These are polyester-base films containing a grid of finite dots of uniform distribution. Both the size and number of dots can be varied by appropriate selection of film transmission percentage and dot number, respectively; e.g., 10%-65 corresponds to a dot diameter allowing 10% light transmission and a population of 65 dots per inch. It was found that a close grid spacing with small dots was necessary for good bond degradation, especially for drum peel tests. An illustrator's toner called Zip-A-Tone manufacturered by Para-Tone Inc. was used. The dot pattern was photographed and the negative used as the exposure control grid.

The uniformity of the dot contamination is illustrated in Figure 3, where three lap shear surfaces are shown after test. Figures 3a and 3b also show the light circles which are areas where the emulsion was exposed to light, thus contaminating these areas. The failure was "adhesive" in these areas while around the circles where the emulsion was not exposed to light and washed away by the developer, the failure was cohesive in the adhesive resin.

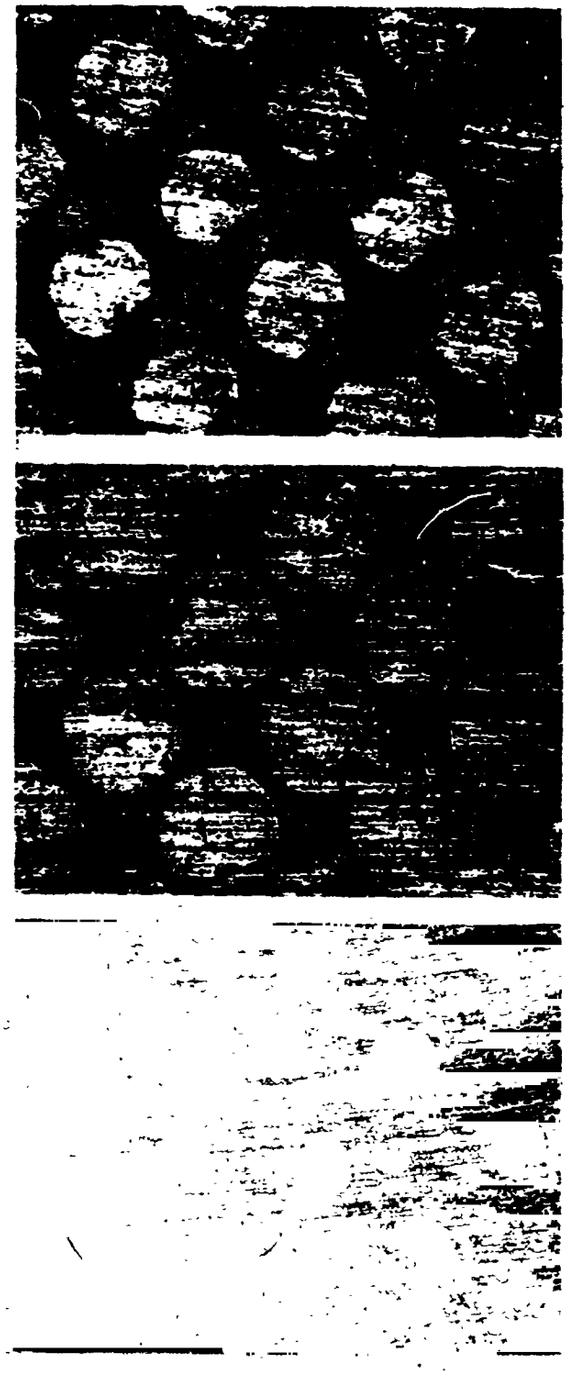

a
10%

b
30%

c
60%

Figure 3 UNIFORMITY OF DOT CONTAMINATION FOR PHOTOMICROFLAW TECHNIQUE.

The exposure time was 3 minutes using a carbon arc high intensity light source. The grid and sample should be closely coupled to minimize the penumbra area.

Developing

After the samples have been exposed they are developed with Kodak's "Photo-Resist Developer" or "Developing Solution" by Kepro Circuit Systems Inc., St. Louis, Missouri. Further details of the techniques applicable to the use of "Photo-Resist" can be found in the booklet "Photosensitive Resists for Industry", Industrial Data Book, P.7, from Eastman Kodak Company, Rochester 4, N. Y.

The plots of Figures 4 and 5 give the calibration curves for this type of bond degradation. These curves are similar for each type of adhesive. This suggests that the dot pattern of photo emulsion is acting only as a low cohesive strength film and is not influencing the cohesive strength of the adhesive. In addition, the strength is much more sensitive to percent light exposure at the zero end of the scale (i.e. smallest contaminant dots). This tends to confirm the stress riser concept.

All of the degraded bond tests in this report were treated in the above manner. The amount of degradation is referred to as the "grid spacing" and the percent light transmission of the "exposure grid".

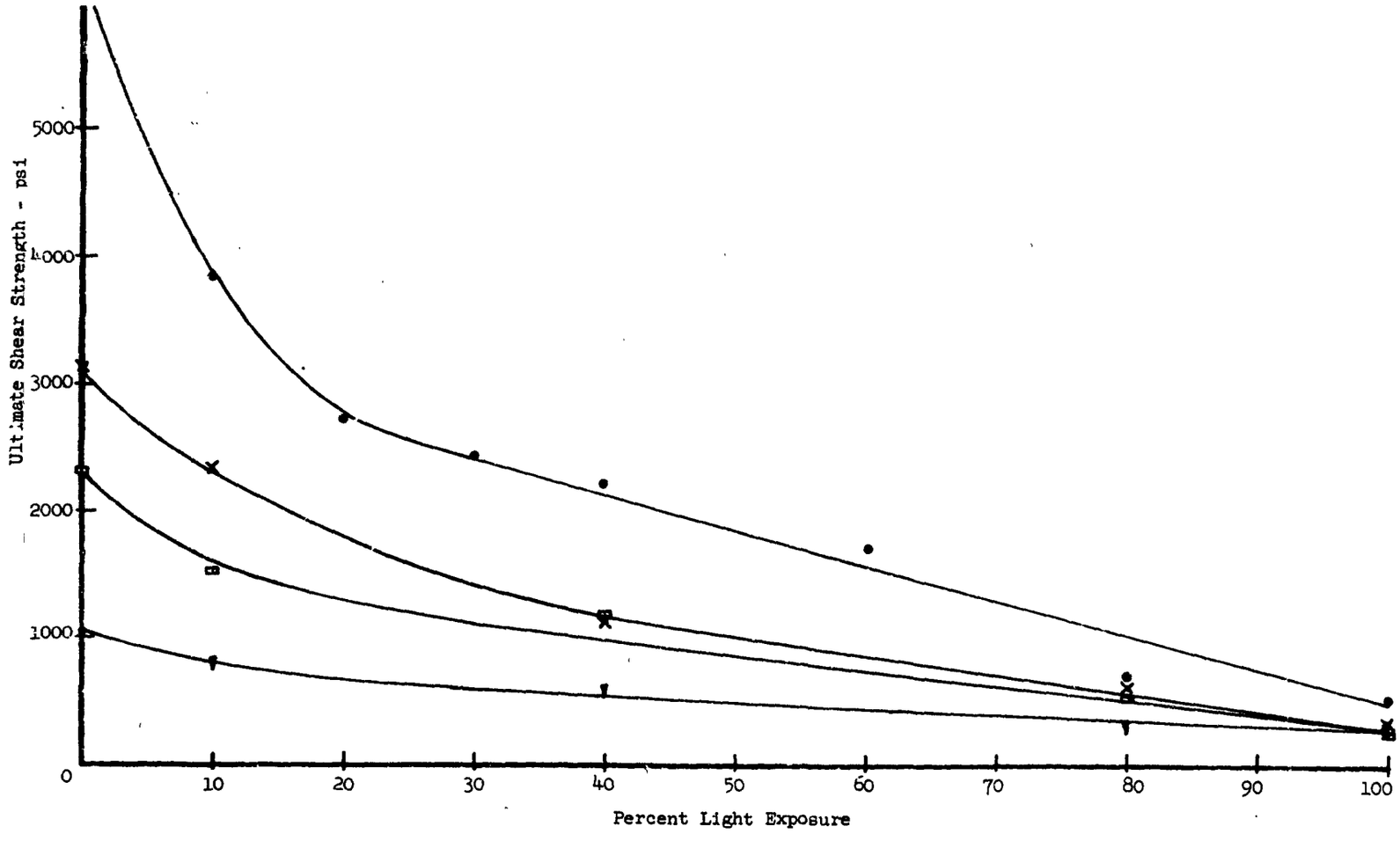

Figure 4 PHOTOMICROFLAW CONTROL OF BOND STRENGTH WITH LAP SHEAR SAMPLES

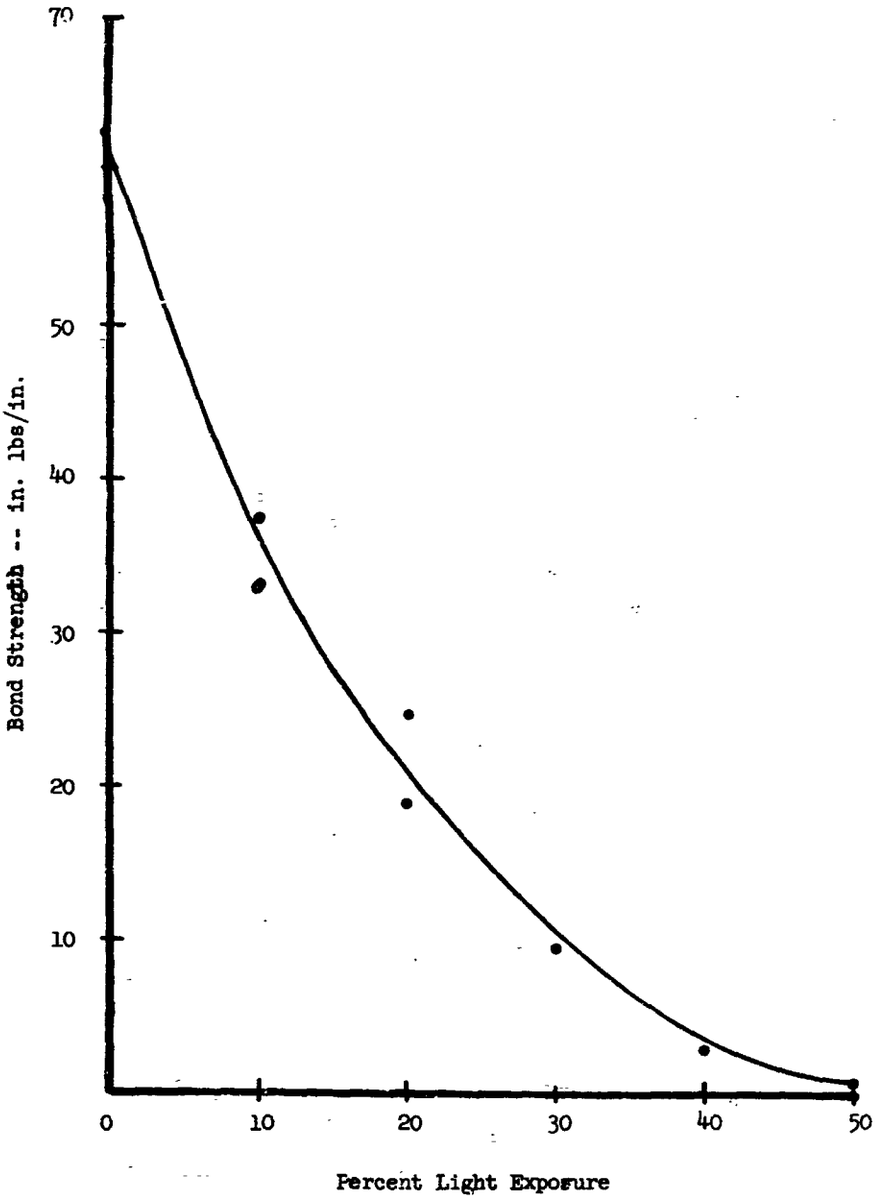

Figure 5 PHOTOMICROFLAW CONTROL OF BOND STRENGTH WITH DRUM PEEL SAMPLES

SECTION 5

BOND TESTS

A prerequisite to the nondestructive testing of bonds is the availability of specimens with bonds of known strength. Therefore, the ability to fabricate sample bonds with some level of confidence as to their strength is required before NDT techniques can be investigated. Information gathered concerning any difficulties in fabricating samples would be of interest to both the program and to NASA.

Initial effort was expended in producing good bonds which would serve as a reference for variable strength bonds that were fabricated later. Preparation, fabrication and testing of samples was done according to Mil-A-25463(ASG) and Mil-A-00509 (Wep.). It was decided early in the program that the lap shear test and the climbing drum peel test would be used to determine the strength of a sample bond. The results of these tests for the good samples is shown in Table 2. No difficulty was encountered with three of the adhesives: FM-1000, HT-424 and MB-329. However, with the fourth adhesive, the two part resin, difficulty was experienced in meeting the manufacturer's specifications. The problem and its solution will be covered later in this section.

5.1 Good Bonds

The samples were fabricated according to Mil specifications in order to produce good standard bonds. Figure 6 is a block diagram showing the steps used in preparing samples for bonding. The sample parts were cleaned, then stored in a drying oven until bonding. The storage time does not exceed one hour. A heated platen press (350°F) was used for the bonding operation. The platen was at times coated with a high temperature silicon grease to prevent sample sticking. A jig was used to obtain consistent registration with the lap shear samples. The following sections discuss information of interest about each adhesive.

5.1.1 Adhesive FM-1000

The adhesive FM-1000 is a polyamide epoxy resin manufactured by Bloomingdale Rubber Company. The sheet used had a weight of 0.6 lbs/ft^2. FM-1000 has the highest design strength of the four adhesives tested. The results of the good bond tests can be seen in Figure 7. The dotted lines show the extremes in the data points. The average lap shear strength of this adhesive is 6320 psi and the average value from the drum peel test is 39.2 in. lbs/in. When the etching bath was not used in the cleaning, there was no appreciable decrease in bond strength, likewise when the vapor degreasing was eliminated at the same time (for one test only), and just the alkaline cleaning was used, there was no decrease in bond strength. This adhesive is not as sensitive to surface contamination as some of the other resins.

TABLE 2

RESULTS OF TESTS

	Lap Shear Test Results (RT) psi		Manufacturer's Published Value No Primer (RT) psi	Drum Peel (RT) inch lbs/inch		Manufacturer's Published Value No Primer (RT) inch lbs/inch
	Test	Gvt. Spec.		Test	Gvt. Spec.	
BLOOMINGDALE RUBBER						
FM-1000	6320	2250	6408	39.2	8.5	58
HT-424	3110	2250	3350	8.3	8.5	11
NARMCO						
7343/713	970	2250	1600 psi RT -423°F-8000 psi -320°F-5100 psi 67°F-4600 psi 125°F-800 psi	30.1	8.5	None given
Metlbond-329	2300	2250	3000	12.2	8.5	14.9

RT = Room Temperature

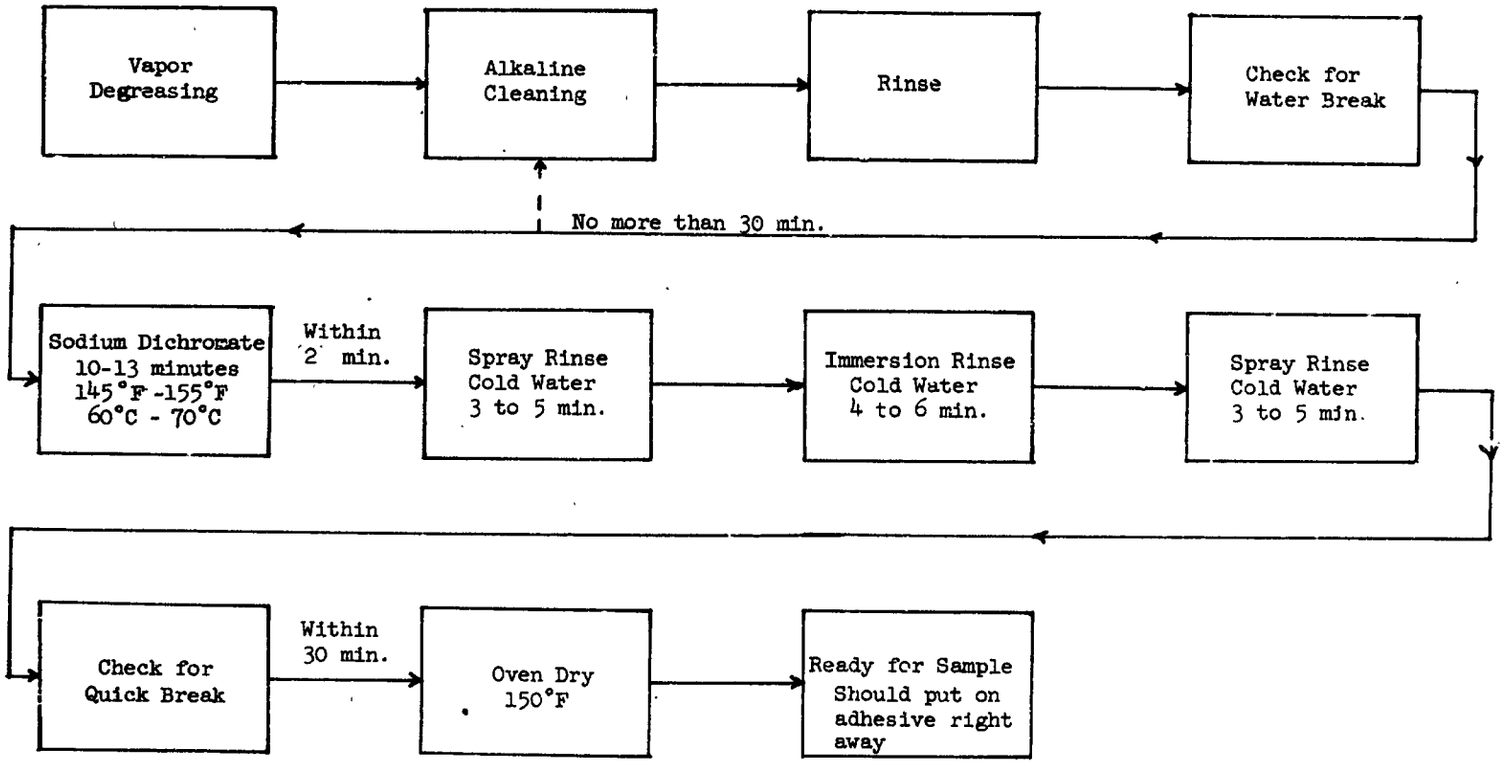

Fig. 6 STEPS IN SAMPLE PREPARATION

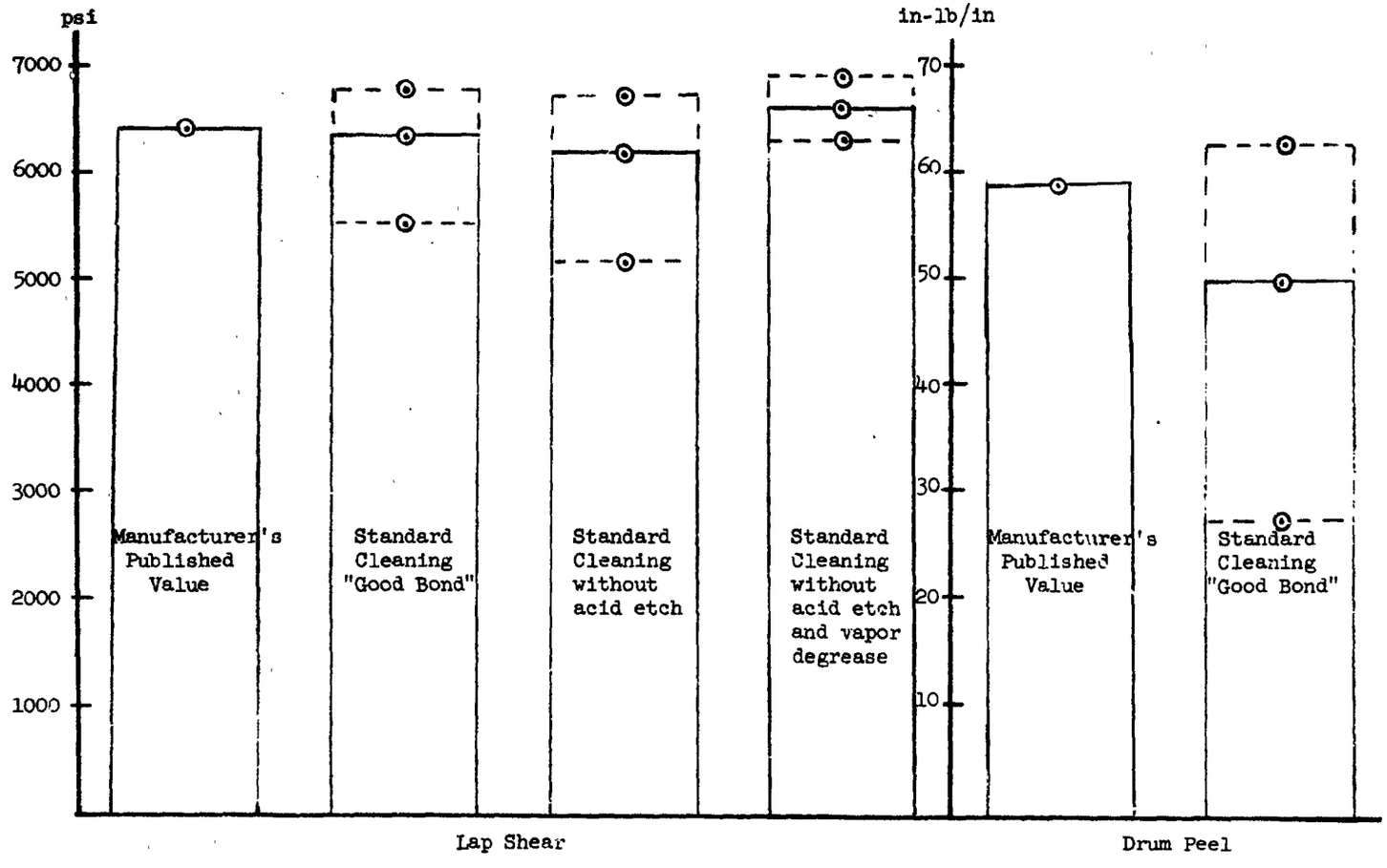

Figure 7 GOOD BOND RESULTS - FM-1000

5.1.2 Adhesive HT-424

HT-424 is an epoxy phenolic also manufactured by Bloomingdale Rubber Company and is intended for high temperature applications. It is a skrim supported adhesive. The adhesive used had a weight of .135 #/in^2. The results of bond tests can be seen in Figure 8. The dotted lines on the bar graphs indicate the extreme failures of the data. The average value of the lap shear strength of this adhesive is 3110 psi compared to the Mil Spec. of 2250. The results of the drum peel tests indicate an average value of 8.3 in. lbs/in. When the acid etch was eliminated from the cleaning cycle the bond strength was not affected. However, when both the acid etch and vapor degreasing were eliminated the bond strength dropped approximately 7%.

5.1.3 Adhesive MB-329

This adhesive, MB-329, is a modified epoxy manufactured by Narmco Materials Division and is a skrim supported adhesive. It is also intended for high temperature applications. The average value of the lap shear test is 2300 psi which is greater than the spec. value of 2250 psi. The results of the climbing drum peel test indicate an average strength of 12.2 in/lb/in. The test results are shown in Figure 9. This resin is more sensitive to surface contaminations: when the acid etch was eliminated, the average value for the lap shear decreased by 20%.

5.1.4 Adhesive Narmco 7343/7139

The 7343/7139 adhesive is a polyurethane epoxy manufactured by Narmco Materials Division. This is a two part resin which requires mixing before bonding. Several problems were encountered in producing samples to meet the manufacturer's specifications. It was found there was a problem in obtaining a homogeneous mixture of the resin and the catalyst, if the two were combined too slowly. To overcome this problem the resin was melted in a beaker that was placed in a silicon oil bath at 250°F $\pm$ 2°. The resin and catalyst were weighed beforehand, then combined quickly. This adhesive is very moisture sensitive (reported by the manufacturer). Entrapped air is also a problem. A vacuum was pulled over the mixed resin to remove the entrapped air and minimize exposure to moisture. Extreme care must be taken in all steps. If the opened adhesive is not kept in a dry nitrogen atmosphere, the remainder of the adhesive must be discarded.

There are two cure cycles recommended for this two part adhesive. The fast cure produced very low strength bond. The bond strength was improved with the slow cure; however, military specifications were not achieved. The bond strength improves at room temperature for several days. Thus very long cure cycles will result in better values than given in Figure 10. The 7343/7139 adhesive has been developed for cryogenic applications and the manufacturer does not claim Mil. Spec. performance at room temperature in the lap shear test. The climbing drum peel test results were very high. This is attributed to the exaggerated filleting action between the honeycomb core and the face sheet. Because of the high

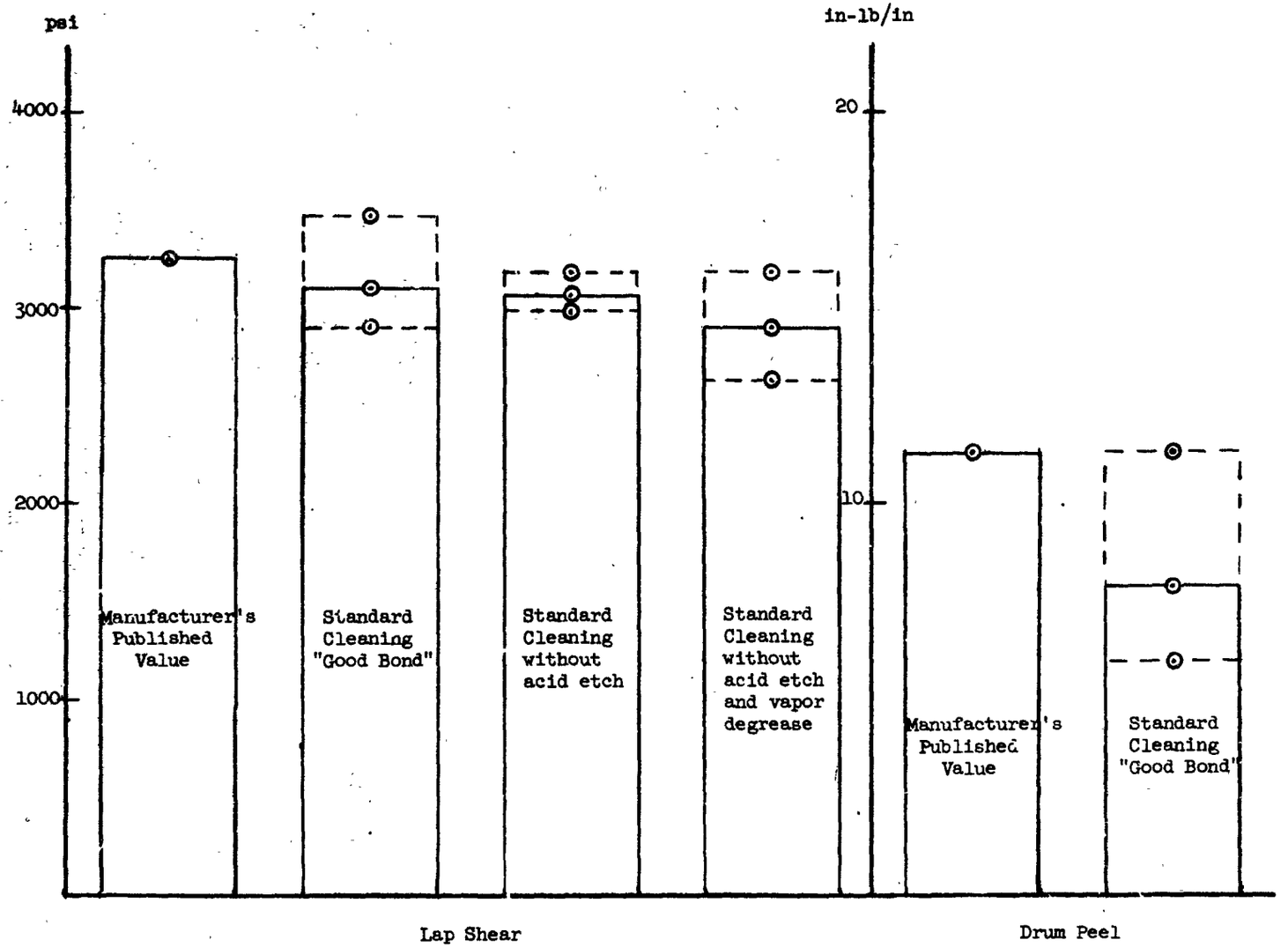

Figure 8 GOOD BOND RESULTS HT-424

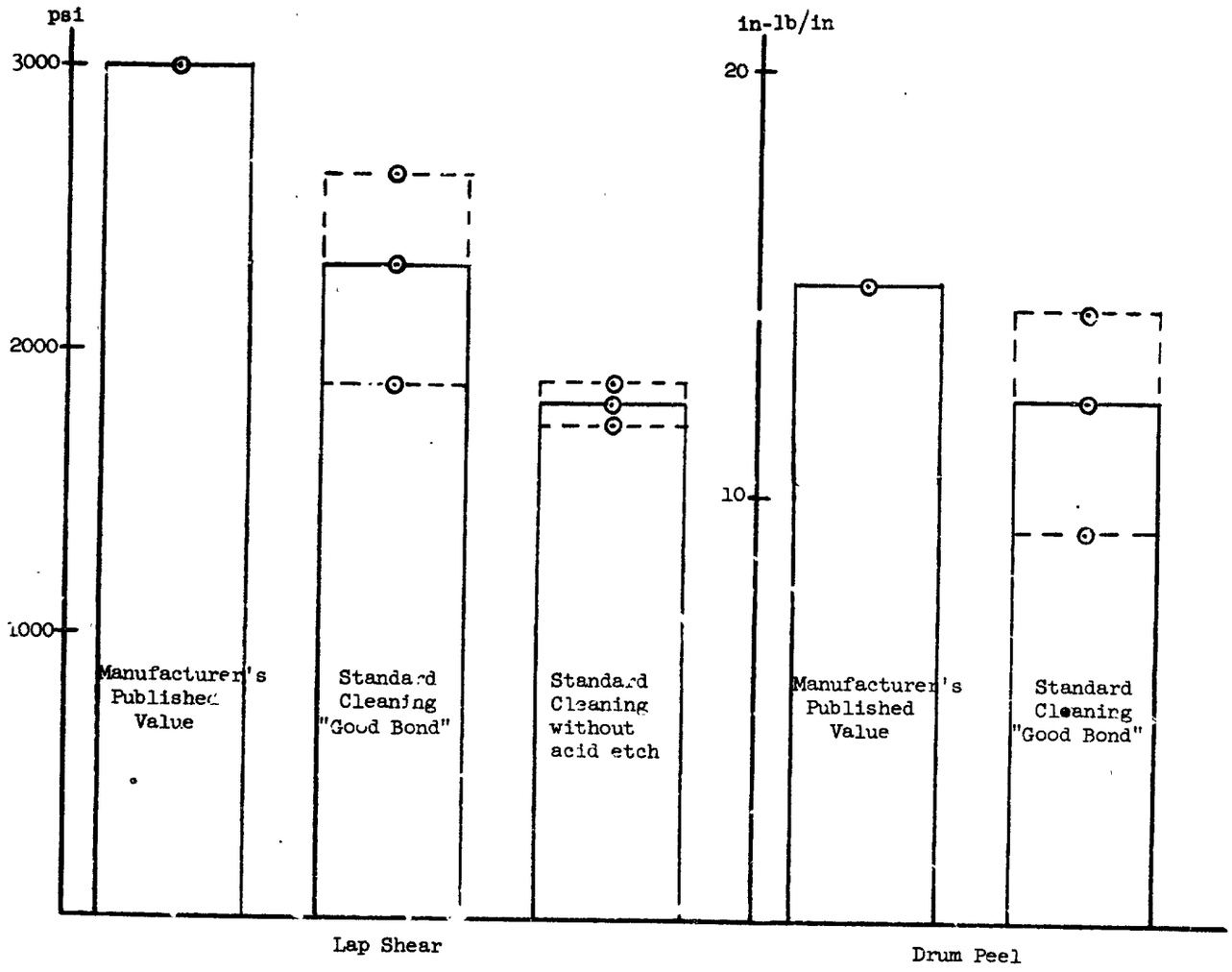

Figure 9 GOOD BOND RESULTS - METLBOND 329

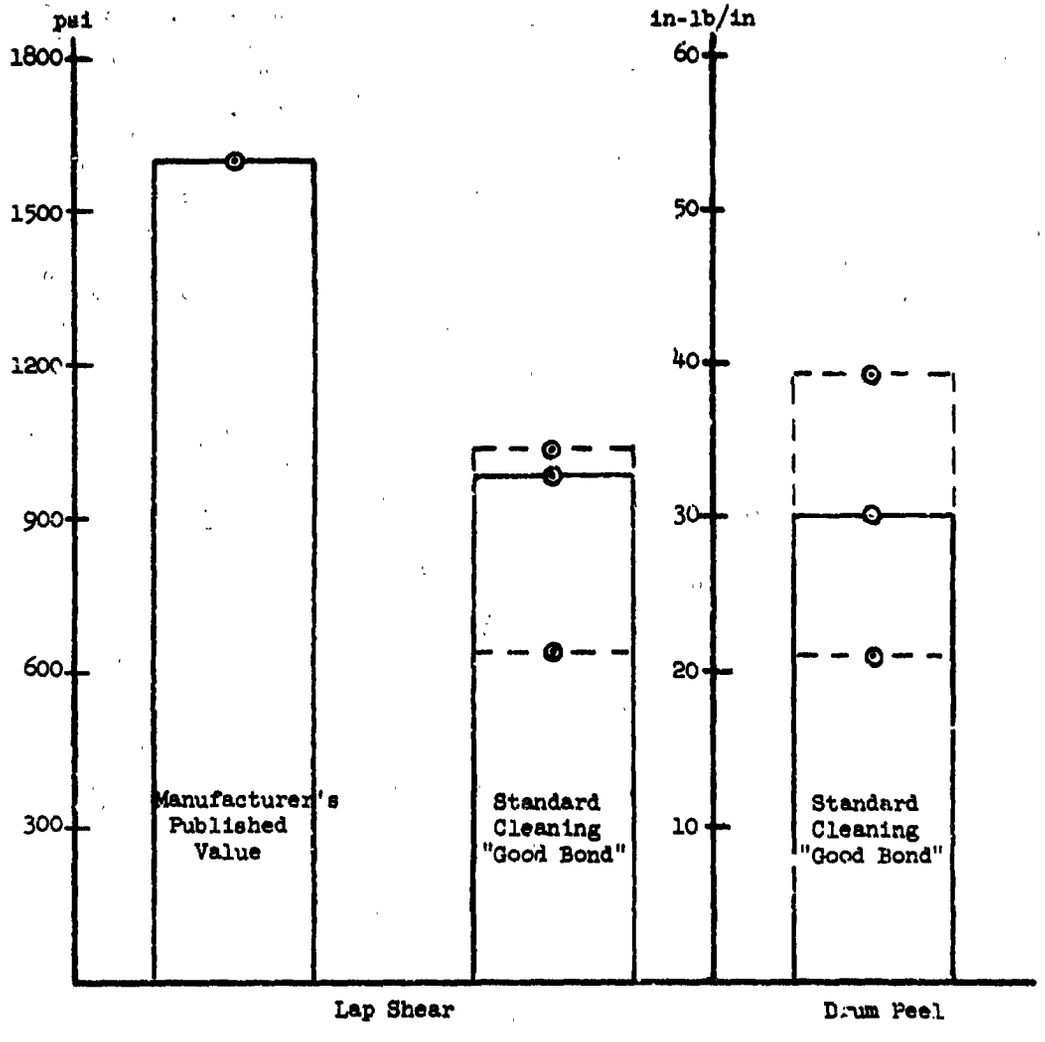

Figure 10. GOOD BOND RESULTS - NARMCO 7343/7139

elasticity of this adhesive at room temperature when the primary bond area broke the fillets remained. It appeared as if the face sheet was connected to the honeycomb core by rubber bands. Results from these tests are shown in Figure 10.

5.2 Environmental Tests

Of the four different adhesives used on the program, only one is intended for room temperature applications. As indicated earlier two were developed for high temperature applications and one for low temperature applications. High temperature (500°F) also a combination low temperature (approximately -320°F) vacuum environment was used to expose samples. The object was to determine if there was any residual degradation in a bond after exposure to these environments. If there had been any degradation of the bond then it would have been measured with the developed techniques of testing that are described in Section 6.

The following conditions were used in each of the environments for sample exposure:

Condition 1 - High temperature - 500°F for 15 minutes
Condition 2 - High temperature - 500°F for 2 hours
Condition 3 - Low temperature - -320°F in a vacuum chamber at a pressure of 10^{-9} Torr for 2 hours
Condition 4 - Low temperature - -320°F in vacuum chamber at a pressure of 10^{-9} Torr for 15 minutes

For the last two conditions the samples were placed in the chamber for a period of 24 hours on a cold plate during pump down prior to the start of the test. The desired vacuum conditions could not be achieved because of sample outgassing. Actual environments attained are given in the test report in Appendix 2.

For each of the conditions the set of samples consisted of 4 lap shear samples and 1 drum peel sample made with each of the four adhesives. In addition a control set of samples were fabricated at the same time. The sample sets used in the high temperature tests did not contain samples with the Narmco 7343/7139 resin since it is intended for cryogenic applications.

The results of the drum peel and lap shear tests on the samples after exposure are shown in Table 3. There was no degradation of the samples after exposure to these environments.

TABLE 3

ENVIRONMENTAL TEST RESULTS

	Control	High Temperature 500°F 15 Min.	High Temperature 500°F 2 Hours	Low Temperature -297°F 1.5×10^{-6} torr 15 Min.	Low Temperature -308°F 8×10^{-7} torr 2 Hours
DRUM PEEL (in-lbs/in)					
FM-1000	27.4	31.7	20.6	24.9	16.6
HT-424	6.0	----	9.6	17.7	----
MB-329	16.6	18.4	19.2	12.6	14.4
7343/7139	39.2	----	----	14.6	49.1
LAP SHEAR (lbs/in^2)					
FM-1000	5960	6680	7350	6340	6800
HT-424	2950	3020	2860	2760	2910
MB-329	2740	2750	2700	2550	2840
7343/7139	655	----		582	857

SECTION 6

BOND STRENGTH NONDESTRUCTIVE TEST METHODS

The present theories on bonds and the models for them suggest that weak bonds can be attributed to cohesive failure of the adhesive. The survey phase has revealed that users and manufacturers of adhesives attribute weak bonds to "adhesive" failure. A bond that has separated with only one or a few molecular layers of the adhesive on one faying surface would be classified as an "adhesive" failure from a visual inspection, yet from theoretical considerations it would be a cohesive failure. This type of adhesive-characterized failure presents the biggest problem in bonding. It is usually attributed to contamination of the faying surfaces which results in a weakened bond.

As discussed earlier, NDT methods were examined for their capabilities in determining the strength of a bond. Nearly all of the test methods investigated required stressing of the bond line during the test. Techniques for accomplishing this are treated in the next section. The significance of the stress on a partially contaminated bond suggests that such methods would be most applicable. The following section will discuss the NDT methods examined during the program. All possible methods could not be experimentally examined within the limits of the program. However, every attempt was made to examine as many diverse and potentially useable methods as possible.

6.1 Sonic and Ultrasonic Emission

Acoustical energy is generated when stresses are applied to materials. This effect is presently being used to detect evidences of plastic deformation in metal structures. Tests were conducted to determine its applicability to investigation of adhesive bonds.

The principle of sonic emission testing is very simple. A transducer or microphone capable of detecting or measuring ultrasonic vibrations is mounted to the surface of the test specimen in the vicinity of the bond. For a large complex structure, several transducers may be required. The transducer output is amplified and selectively filtered so that only vibrations in a particular frequency band are passed on to the data translation system. The latter may be a device which converts these signals to frequencies in the audio spectrum permitting the signals from the specimen to be heard via a set of earphones or a loudspeaker. Alternatively the data can be suitably processed for display on an oscilloscope or a recorder.

In practice, the test specimen is exposed to a differential force or pressure such that the bond lines are stressed in tension. This stress causes the bond interface to emit ultrasonic vibrations which can be detected by the above means. The amplitude of the emission becomes significantly stronger as the yield stress is approached, and the point of initiation of this emission change can be used to predict the yield point very accurately without noticeable damage to the structure.

To evaluate this technique, test samples capable of being stressed to measurable levels in a hydraulic test fixture were fabricated. The test samples consisted of aluminum blocks of the same alloy used for the face sheets of the honeycomb sample. The aluminum blocks were drilled and threaded to facilitate mounting on rods for use in a tensile tester or on a hydraulic cylinder. The hydraulic cylinder mounted on a test stand is shown in Figure 11.

To achieve minimum system noise for the initial tests, a hand pump was used to generate the pressure in the cylinder and, hence, stress the samples. For each sample which consisted of 2 aluminum blocks 3" in diameter, one of the blocks is cut on the end to form an annulus of 3 or 5 square inches. The 3 square inch area is used for sample bonds of FM-1000 and the 5 square inch area is used for sample bonds of MB-329 and HT-424.

The transducer used to detect the acoustical energy generated by the adhesive was a ceramic disk of barium titanate-lead zirconate mounted in an aluminum housing (Clevite Corp., Piezoelectric Div., Bedford, Ohio; Model No. PZT-5). It is one inch in diameter and 1/2 inch thick. The frequency response of this transducer is higher than 100 kHz.

A block diagram of the initial test setup is shown in Figure 12. The output from the transducer was amplified and recorded by an Ampex CP-100 tape recorder, using wide band (100 Hz - 200 kHz) electronics and at a tape speed of 30 inches per second. The hydraulic pressure signal (a measure of bond stress) was recorded on another channel using the FM electronics (dc-100 Hz). The tape recorder was run at a speed of 3-3/4 inches per second on playback. Corrections were made for the change in frequency of the data that resulted from the change in tape speed. An x-y plotter was used for data presentation. Plots were made of average acoustical energy in various frequency bands as a function of bond stress for many samples of FM-1000, HT-424 and MB-329 adhesive bonds. This data is presented in Appendix 3. A sample with no bond was also tested to determine the noise generated by the test fixture.

Results indicate that ultrasonic emission by the adhesive above 16 kHz can be used to predict where a bond will fail. Acoustic emission also occurs at lower frequencies; however, considerable noise is generated below 16 kHz by the test fixture. For each of the different types of adhesives there is a large increase in noise above 16 kHz as the ultimate strength of the bond is approached. Thus, if a method of stressing a bond is available, this technique provides a means of determining bond strength.

The use of the tape recorder obviated a real time display of the data. To facilitate the collection of data in real time, an "Ultrasonic Emission Detector" was constructed as shown in Figure 13. A block diagram of this unit appears in Figure 14. The output of the transducer is amplified with a gain of 5000 at a center frequency of 31 kHz and a bandwidth of 5 kHz. This allows energy in a frequency band of 28 kHz to 32 kHz to be amplified

Figure 11 HYDRAULIC STRESSING FIXTURE

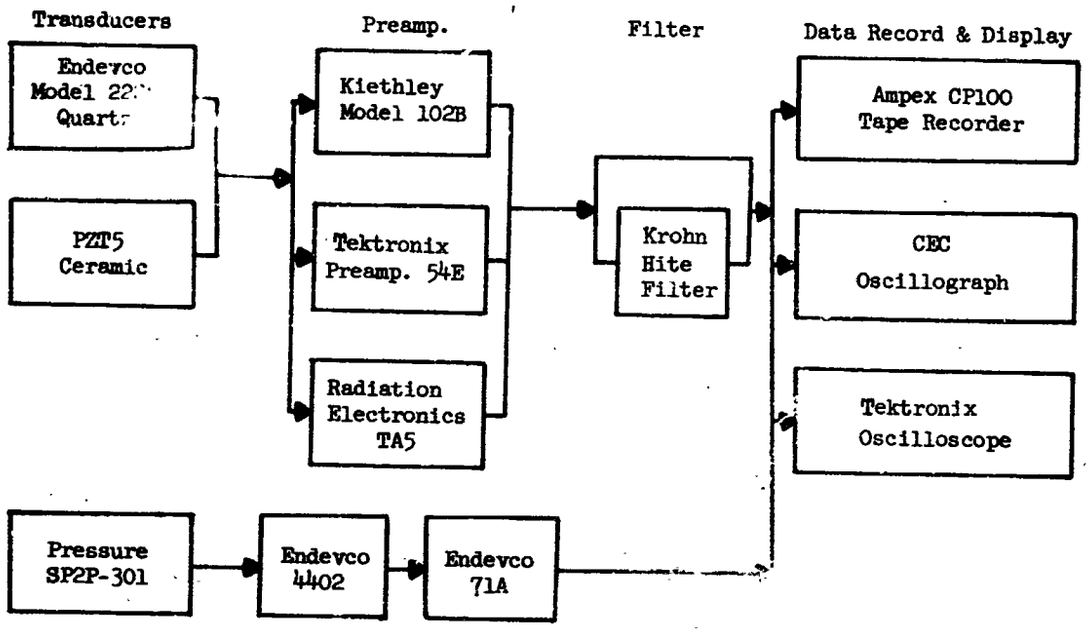

Data Recording System

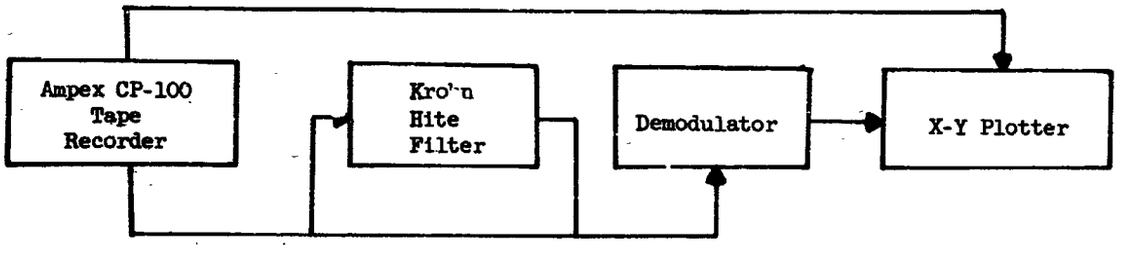

Data Processing System

Figure 12 DIAGRAM OF SONIC/ULTRASONIC EMISSION DETECTING SYSTEM

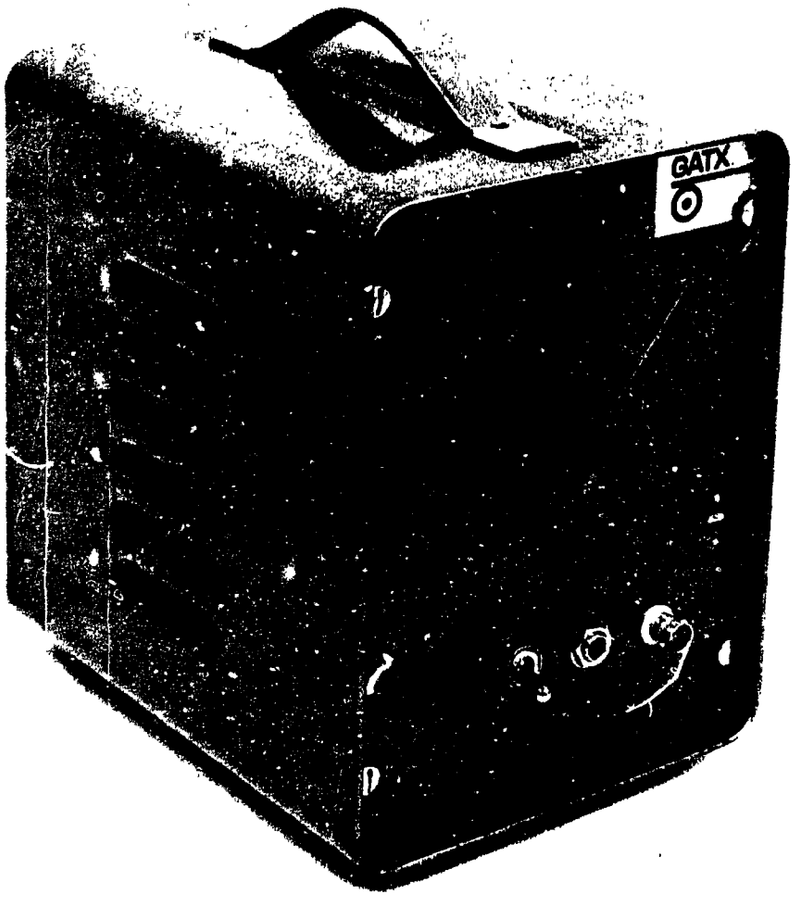

Figure 13 ULTRASONIC EMISSION DETECTOR

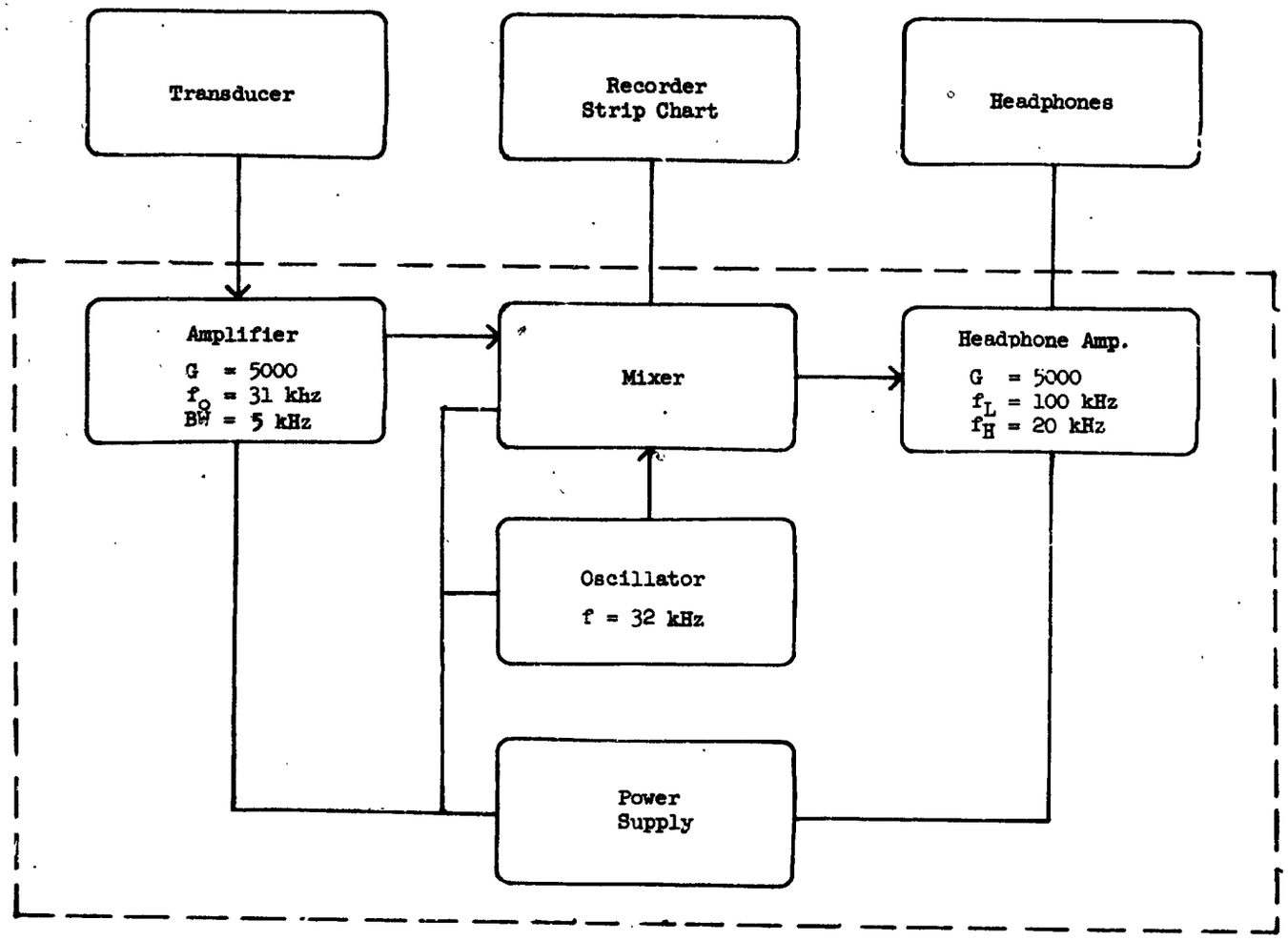

Figure 14 BLOCK DIAGRAM OF ULTRASONIC EMISSION DETECTOR

and processed. The input of this amplifier can handle large signals below 28 kHz without distortion. This allows noise pulses either from the test fixture or a shop environment which are below 28 kHz, to be attenuated and not disturb the system. The amplifier output is fed to a mixer along with a signal from a 32 kHz oscillator. The mixer produces the sum and difference frequencies of the two inputs, although only the difference frequency is used. The output frequency of the transducer is now translated to a range of 100 Hz to 4 kHz. This is detected and used to drive a recorder (x-y plotter) to plot average noise as a function of applied stress in real time. Thus the data can be interpreted while the sample is being stressed. The output of the mixer is also connected to a headphone amplifier. A set of headphones was used to listen to the acoustical noise generated by the adhesive under stress.

The acoustical energy generated by the adhesive can easily be distinguished from the sounds of the test stand or environment. The adhesive produces many very short duration bursts of energy that sound like a high pitched crackling noise. The data from the first series of tests (Appendix 3) reveals a characteristic increase in acoustical energy above 16 kHz when the applied force on the adhesive is about 90% of the value at which it failed.

Using the above criterion, samples of each adhesive were tested. However, because of the difficulty in preparing samples of Narmco 7343/7139, it was not generally used for these tests. The adhesive's room temperature flexibility precluded testing by sonic/ultrasonic emission; it was anticipated that the level of acoustical energy would be significantly lower than the other adhesives used. Further, tests were not conducted at the low operating temperatures normally associated with Narmco 7343/7139.

In actual test, the stress on the bond was applied slowly with an hydraulic hand pump. The first few samples were broken so the operator while listening with the headphones, could become familiar with the sounds preceding bond breakage. The bond force on the remaining samples was increased to the point at which the bond was about to break as judged by the operator. The maximum force applied to the bond was then increased by 10% and this value was considered the predicted bond failure point. The results of this series of tests are shown in Table 4.

The prediction errors ranged from 3% to 30% (i.e. deviation of predicted breaking point from actual failure). The size of this range is influenced by the fact that the ultrasonic emission testing is combined with a tensile test of the sample. The predicted failure value was determined when the sample was stressed at a constant rate. Those samples that failed during the ultrasonic attenuation measurements were being stressed at a varying rate due to the dynamics required for the test. As a result, this varying stress rate influenced the point at which the failure occurred and accounts for the larger errors.

Adhesive	Contamination	Maximum Bond Pressure Attained psi	Predicted Breaking Point Pressure psi	Actual Breaking Point Pressure psi	Precent Deviation of Predicted Breaking Point from Actual Breaking Point
MB-329	20%	2100	2310	2520	-8%
	20%	2100	2310	2180*	+6%
	30%	1600	1760	1900*	-7%
	40%	1400	1540	1500	+3%
	40%	1000	1100	1150	-4%
	Good	2500	2750	3750	-27%
HT-424	20%	3550	3900	3200*	+22%
	20%	2180	2400	2075	+16%
	40%	2360	2600	2670*	-3%
	40%	3700	4070	3120*	+30%
	Good	5800	6380	5400*	+18%

* ±5% accuracy; all others ±1%

TABLE 4 BOND STRENGTH PREDICTION RESULTS

The test results presented in Table 4 are for MB-329 and HT-424 resins only, using the instrument developed on the project. Limitations of the test fixture prevented the use of FM-1000 at that time. Previous investigation using this adhesive (see Appendix 3) verify that it has similar acoustic emission response characteristics.

The method described provides a means of predicting the strength of a bond and could be employed quite easily with any proof test presently in use, such as the pressure test of a fuel tank.

The application of the above test method of predicting bond strength to honeycomb panel required a means of stressing the bond line. A suction cup would be suitable except that it is limited in force per unit area to the pressure of the environment. To achieve large bond stresses, a suction cup was fabricated with an ultrasonic transducer spring mounted in its center, for use in a pressure chamber. This transducer is shown in Figure 15. With the inside of the vacuum cup open to ambient (14.7 psia), the force on the bond is equivalent to the internal pressure in the chamber. Honeycomb panels using each of the three adhesives were fabricated for this test.

Any method employing internal pressure to stress the face sheet of honeycomb panel has to take into account the porosity of the adhesive if the integrity of the bond between the adhesive and the face sheet is to be verified. When the face sheet is separated from the panel with the climbing drum peel test, the degradation of the bond is apparent. However, when this same panel was previously tested with the high pressure vacuum cup, the degraded bond was not detected. Results of the test are shown in Table 5. There is a problem with this method of stressing the bond line because the thickness of the face sheet determines what portion of the force is absorbed in the face sheet and what portion of the force stresses the bond. With a thicker face sheet, the samples failed at a substantially higher value.

The testing of honeycomb panel with a phenolic core revealed that the phenolic material generates more ultrasonic energy than the adhesive. The phenolic core was not perforated to relieve internal pressure as was the metal honeycomb core. Therefore, when the pressure was increased, it was possible to detect the phenolic cell walls breaking and the air rushing into the cell. The use of a perforated phenolic core would eliminate this problem. Further testing revealed that the phenolic core always failed before the bond, even for degraded bonds.

The sonic/ultrasonic emission method of testing is very practical for establishing whether any portion of a structure has failed during a proof test.

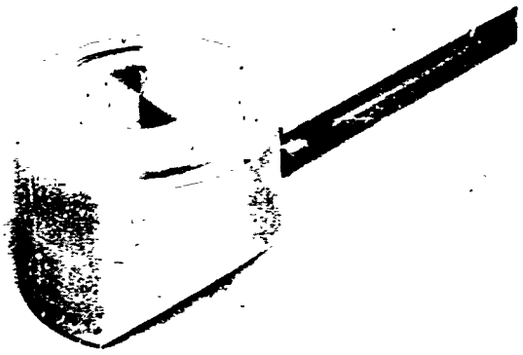

Figure 15 HIGH PRESSURE VACUUM CUP

Table 5

HIGH PRESSURE VACUUM CUP TECHNIQUE

Adhesive Type	Contamination	Breaking Point Pressure
MB-329	Good Bond	650 psi
MR-329	20%	619 psi
MB-329	30%	645 psi
MB-329	40%	570 psi
HT-424	Good Bond	405 psi
HT-424	20%	305 psi
HT-424	30%	310 psi
HT-424	40%	320 psi
FM-1000	Good Bond	405 psi
FM-1000	20%	260 psi
FM-1000	30%	240 psi
FM-1000	40%	265 psi

6.2 Ultrasonic Attenuation

Curently available techniques for bond testing using ultrasonics can detect adhesive voids and areas where the adhesive may be present but no bond exists. In some instances, excessive porosity which would result in an understrength bond can be detected, but with little certainty. However, none of the present ultrasonic systems will find a weak unstressed bond.

Analysis of bonding theory and discussions with bonding specialists pointed out the possibility that a weak bond might be detectable with ultrasonics if the bond line is stressed. It was reasoned that the stressing might affect, among other things, thickness, density, damping, and attenuation. An experimental program was therefore initiated to investigate these possibilities. To determine the characteristic of the adhesive in a bond under stress, a method of applying a known force to the bond was needed. For laboratory evaluation a hydraulic cylinder was used to supply the stressing force. This was the same mechanical system used for the ultrasonic emission tests. Other techniques applicable to actual structures are discussed in Section 7.

The test blocks used for ultrasonic experiments were the same as those used for the sonic emission investigation. Each sample bond is constructed with two aluminum blocks, one of which has an annulus cut on the bonding surface to provide known bonding areas of 3 or 5 square inches. The blocks were 1-1/2 and 2-1/2 inches thick, respectively. When ultrasonic energy is passed through the specimens, reflections occur at each interface so that there are many path lengths. For the preliminary tests, it was important that the length of a path where multiple reflections occur is not an integral multiple of the fundamental path. Since blocks had to be designed to stress a bond in a known manner, it was not possible to measure the parameters of resonant frequency or "Q" of the bond line-face sheet combination due to the block thickness.

The attenuation is measured using through transmission of an frequency modulated ultrasonic wave in the frequency range of 5 MHz to 10 MHz. A block diagram of the ultrasonic inspection system initially used is shown in Figure 16. A sweep generator provides a recurrent voltage which is used to modulate the voltage controlled oscillator (VC); the power amplifier serves to increase the magnitude of this voltage so as to produce the desired output intensity of ultrasonic waves generated by the piezoelectric transmitting transducer. The electrical output signal of the receiving transducer is directed to an amplifier with a sufficiently wide bandwidth such that all frequencies in the band are received equally. After about 75 db amplification, the received signal is combined in a mixer with a portion of the VCO signal to produce new frequencies through the heterodyning action of the mixer. One component is the sum while the other is the difference of the transmitted and received frequencies. The mixer is followed by a low-pass filter which accepts the difference frequency component while rejecting the other, and produces an output essentially in synchronism with

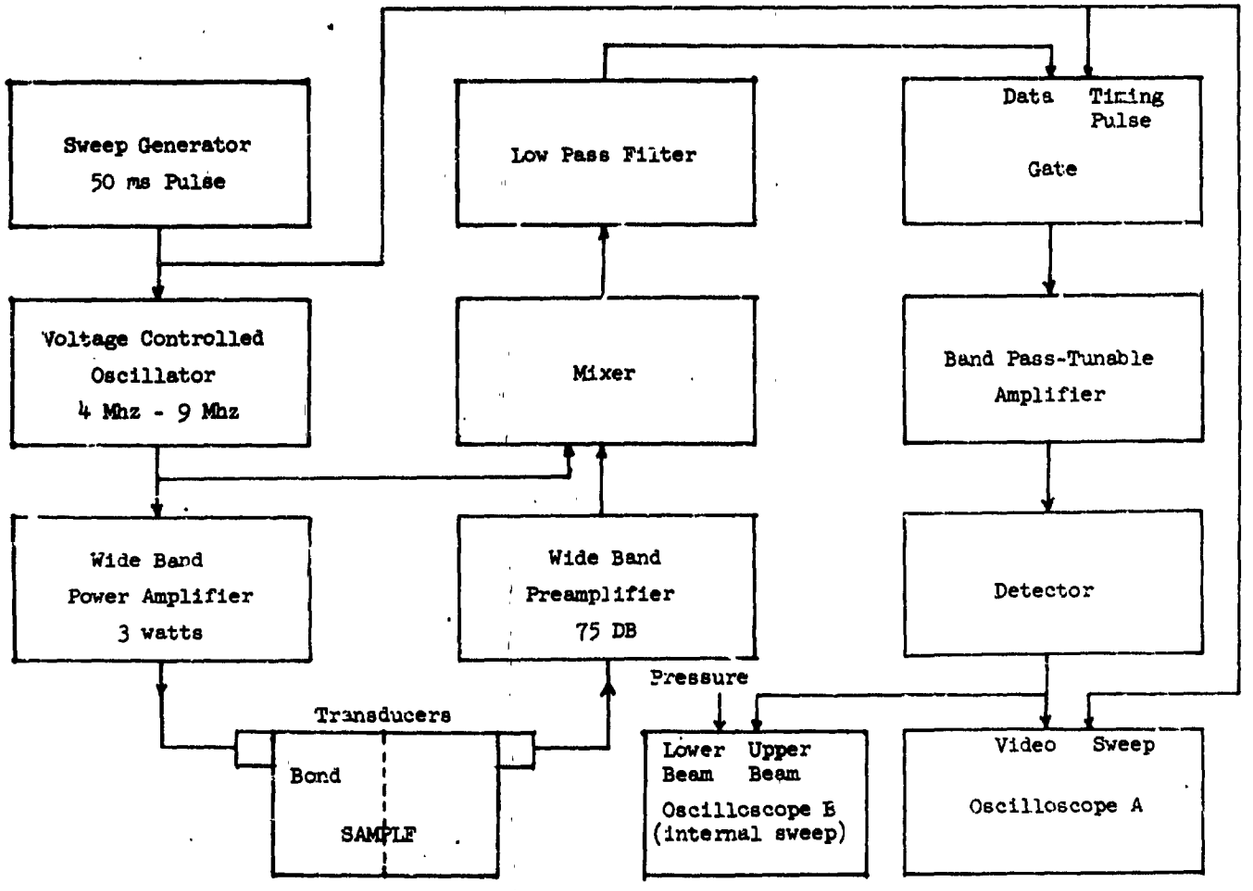

Figure 16 BLOCK DIAGRAM OF ULTRASONIC INSPECTION SYSTEM

the frequency of the generated wave. Because of the inherent time required for the generated wave to traverse a path from the transmitting to the receiving transducer, and the fact that the transmitted frequency is continuously increased at a constant rate, a constant frequency difference exists between the transmitted and received waves for a particular path. The shortest path length will have the minimum travel time and will result in the lowest frequency component from the mixer. The tunable band pass amplifier is adjusted to just pass this component. The data shown in Figure 17 is representative of that gathered during the test to measure ultrasonic attenuation as a function of bond stress. There are four traces shown in each of the four pictures. The top trace represents the output of the tunable band-pass amplifier and the sampling circuit. A portion of this signal is sampled by the gating circuit and is shown in the second trace. The top two traces display the amplitude of the ultrasonic signal as a function of frequency. The bottom two traces display the amplitude of the bond stress and the ultrasonic signal as a function of time. The third trace is the attenuation signal while the fourth represents the bond stress signal. The bond stress signal is calibrated in terms of hydraulic pressure on the cylinder which is 500 psi per division.

Initial results showed a change of attenuation with applied stress. To obtain quantitative results it was necessary to use more complex techniques of data processing. The pulse sampling technique required a zero order hold circuit. This circuit provided a signal which was equal in magnitude to the peak value of the sampled signal. It was then possible to record the attenuation of the signal on a strip chart recorder. The system was calibrated so that 1/2 DB change in attenuation through the bond resulted in a 15% change in signal level on the strip chart recorder. During the testing of the samples both the bond stress signal and the attenuation signal were recorded from the oscilloscope display as shown in Figure 17. The change of attenuation with stress can be observed on the oscilloscope screen where both attenuation and force on the bond were displayed as a function of time. In addition, the attenuation was also displayed on a strip chart recorder as a function of time.

The sample was stressed alternately in tension and compression at a rate of one-half cycle per second on the hydraulic test stand. The peak stress in each cycle was gradually increased until the sample broke. As the peak stress was increasing from cycle to cycle, the peak attenuation generally increased from cycle to cycle. However, in some samples the attenuation switched between two different but relatively constant values as the sample cycled between tension and compression. In the case of one good HT-424 bond, the switching phenomenon occurred on the first test, as can be seen in Figure 19. The transducers were moved to a new spot on the same sample and a linear change of attenuation with stress was observed, as can bee seen in Figure 19 (trial 2). When the separated bond was examined, there was no visual difference between the two areas that were tested.[2] This phenomena decreases the reliability of the indication from this test method.

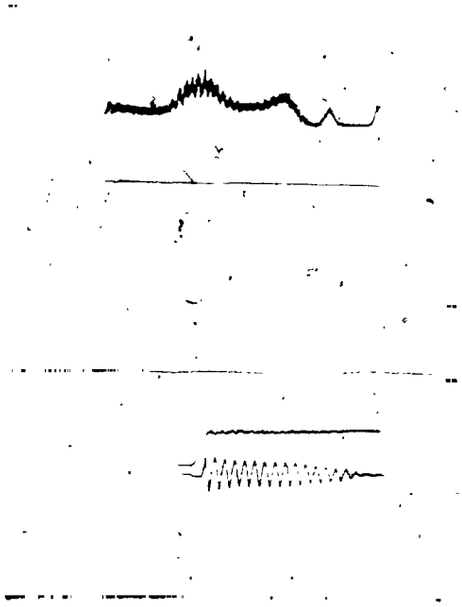

MB329 30% Cont. Failure 1900 PSI

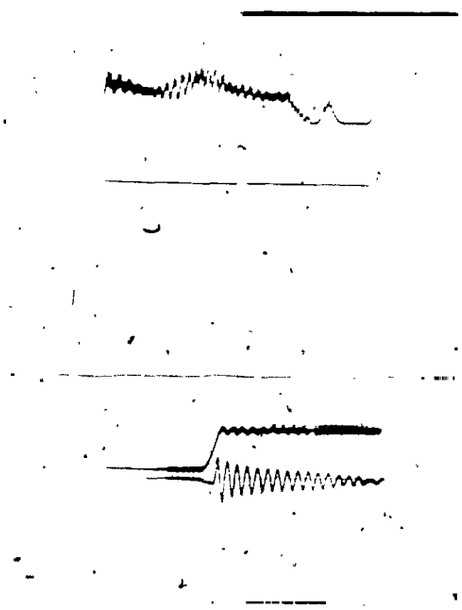

MB329 20% Cont. Failure 2520 PSI

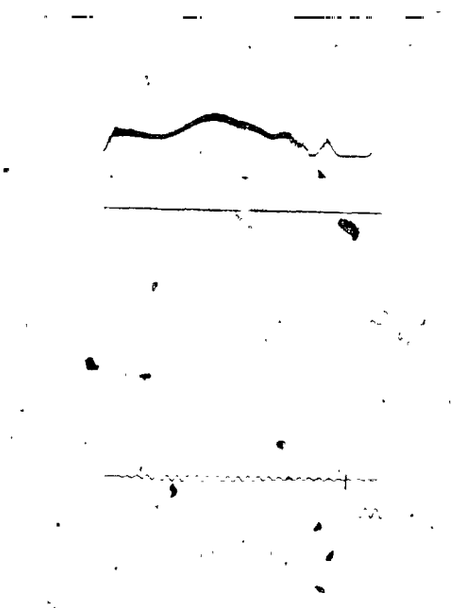

HT 424 Good Bond Failure 3400 PSI

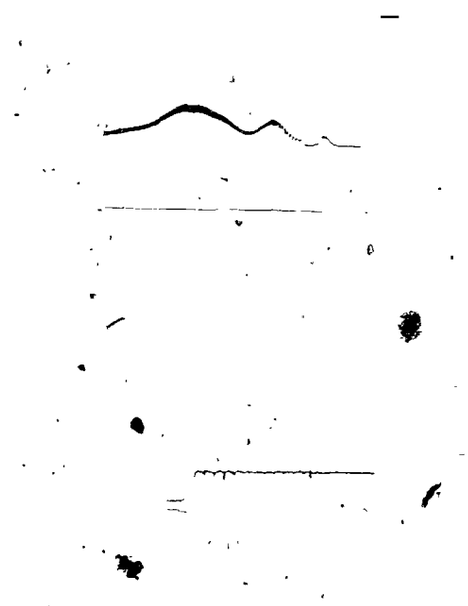

HT 427 Good Bond Failure 3400 PSI

Fig. No. 17 TYPICAL ULTRA SONIC DATA

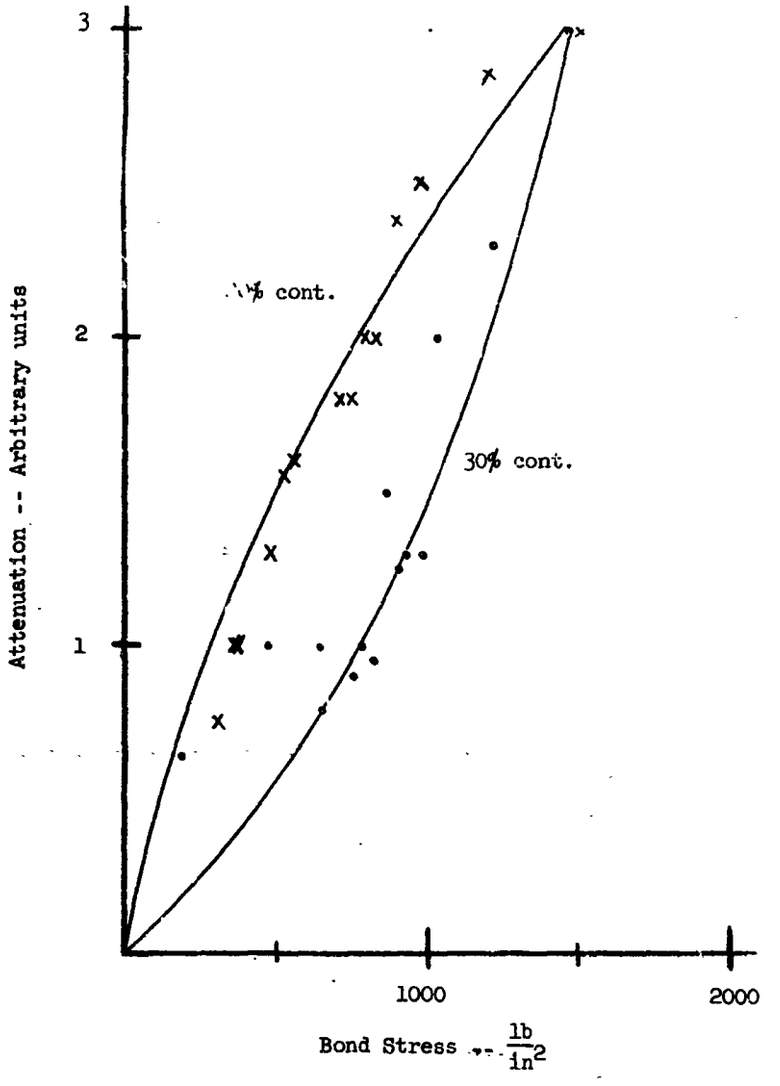

Figure 18 BOND STRESS VS. ATTENUATION -- MB329
TWO SAMPLES -- 20 and 30 PER CENT CONTAMINATED

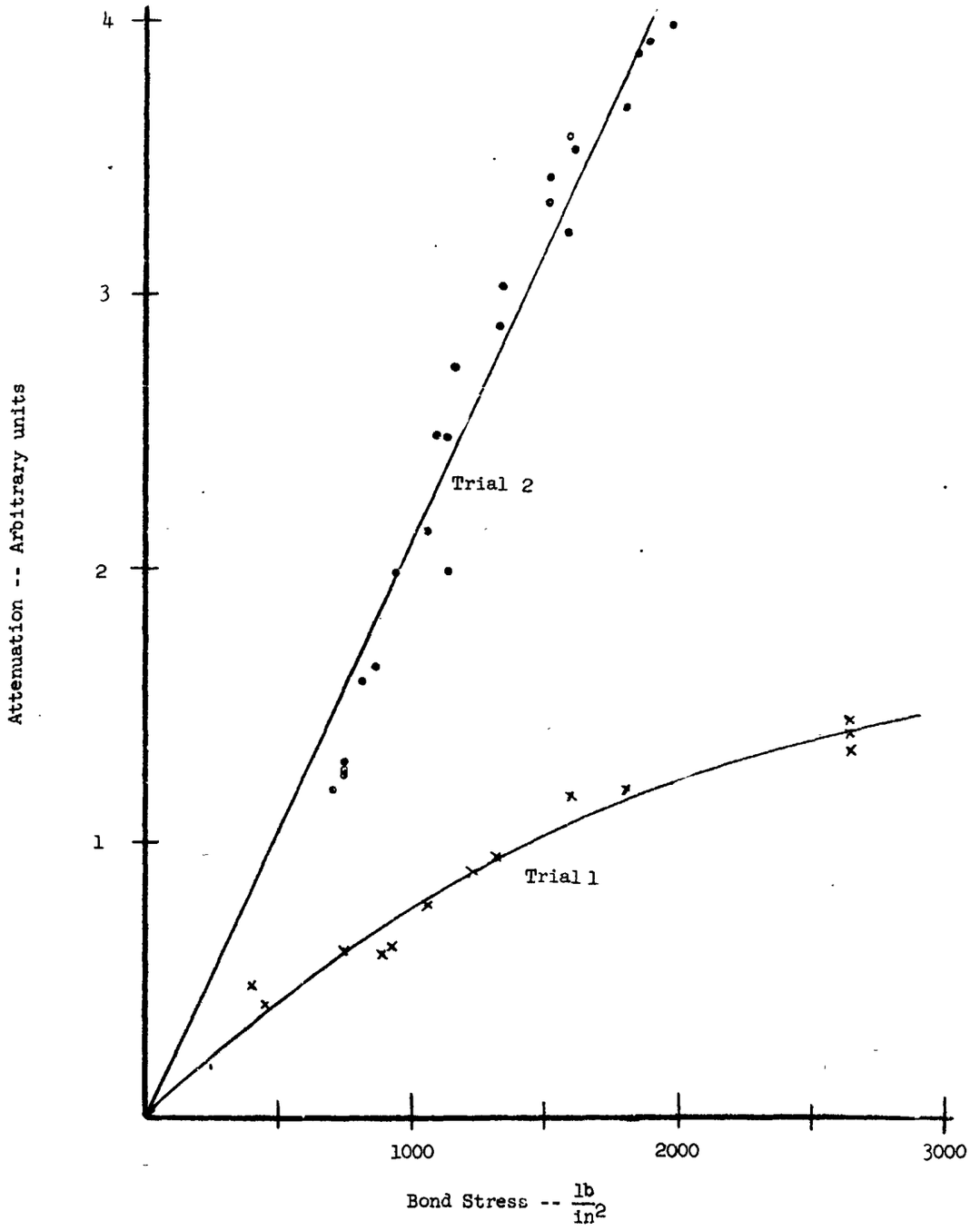

Figure 19 BOND STRESS VS. ATTENUATION--HT424

To compare the results from various samples, the change in attenuation from nominal was plotted as a function of applied stress. These plots, shown in Figures 18 and 19 indicate that the change of attenuation with applied stress is a linear function for the samples in which the switching phenomenon was not observed. It was suspected that the slope of the curves in Figures 18 and 19 (i.e. the rate of change of attenuation with stress) would be a function of bond strength.

This type of trend is, however, not noticeable in the data. For this reason, further experimental work on this method was curtailed in order to examine more favorable techniques. The reason for the change in attenuation with stress is not known, nor are the variables causing the switching phenomenon in the attenuation. These attenuation characteristics may be a function of some other bond variable instead of ultimate strength. To further understand the nature of an adhesive bond, additional work should be done in this area.

6.3 Brittle Coatings

The testing of the quality of a bond in a honeycomb panel can be accomplished by stressing the bond and detecting any concentration of stress on the surface of the face sheet. The bond between the honeycomb core and the face sheet can be stressed by sealing the edges of the panel and pressurizing it. A brittle laquer such as "Stresscoat" can detect the induced stress concentrations.

The honeycomb core is perforated with holes during manufacture to prevent buildup of internal pressure in honeycomb panels if the adhesives outgas during bonding. To achieve internal pressures in a panel, the edges of the specimen require sealing. The panel has to be pressurized slowly because of the small size of the holes that connect the cells of the core. "Stresscoat" is a very brittle coating material which fractures readily. However, under the influence of time and load, the coating tends to creep and relieve the stress within the coating which was induced by the face sheet. A method of producing a stress with a fast rise time is necessary to give the best indications with "Stresscoat". To achieve a stress with this fast rise time, rapid decompression was used.

The stresses were generated by placing the honeycomb panels in a small chamber that was pressurized at a rate of about 10 psi/minute until a suitable level was reached. During the time the chamber is pressurizing, the gas is penetrating into each cell of the honeycomb core. At equilibrium, each cell and the chamber are at the same pressure. The chamber is then rapidly decompressed by opening a one inch ball valve. The chamber decompresses at a faster rate than the honeycomb cells since the gas in the cells bleeds out through the small perforations in the cell walls. For a few milliseconds the bond is stressed by the high internal pressure in the cells and the low chamber pressure. This method generates the high rise time stress which works best with the "Stresscoat".

The initial tests were conducted with several samples using FM-1000 and MB-329 as the adhesives. "Stresscoat" 1204 (Magnaflux) was used to coat the samples. It has a threshold strain of 900 microinches per inch. The coating was applied to the face sheet with seven passes of an air gun. Spraying is continued until the color of the coating changes from clear to a definite yellowish tinge indicating the proper thickness. The coatings were dried in an oven for 6 to 18 hours at a temperature of 100°F. Before each sample was used, it was slowly brought down to room temperature. The coating is temperature sensitive and fast temperature changes will crack it. Each sample was carefully inspected for cracks before the test. The first test of a sample was at 100 psi. If no cracking appeared, the pressure was increased and the test was repeated. Pressures of 100, 200, 500, 700, 900, 1000 and 1100 psi were used. The sample with MB-329 as the adhesive produced cracks in the "Stresscoat" when decompressed from 700 psi. The faint crack pattern outlined the honeycomb, as can be seen in Figure 20. The maximum cracking seemed to occur in the center of each honeycomb cell. The panel was not damaged in this test. Similar results were noted with the FM-1000 adhesive.

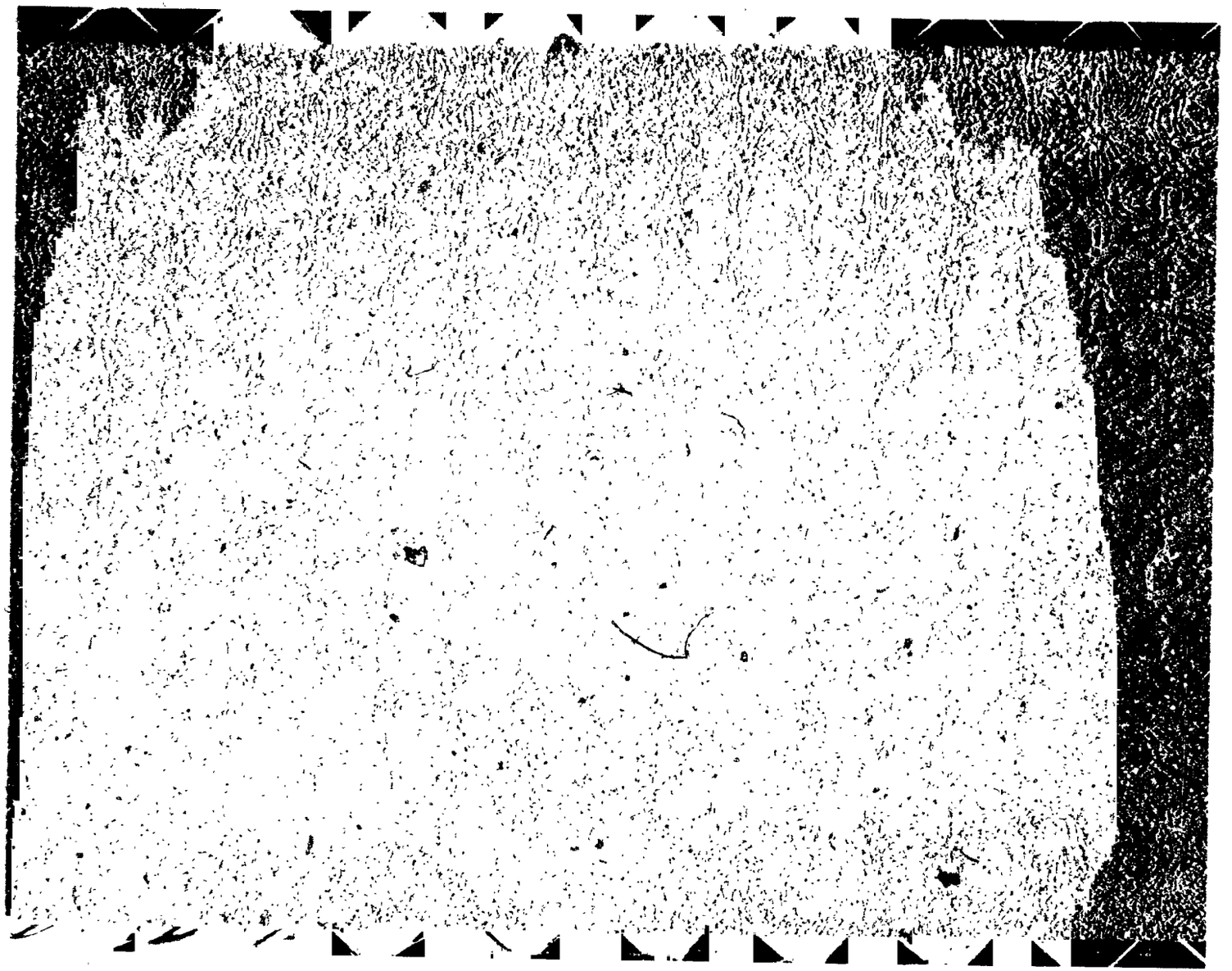

Figure 20 STRAIN SENSITIVE BRITTLE COATING TEST OF GOOD PANEL

Since like results were obtained with the FM-1000 and MB-329, only one adhesive was used for the majority of additional tests. HT-424 is also similar to the MB-329 and reacts in much the same manner. Narmco 3743/7139, however, was not used due to the difficulty in preparing samples.

Additional honeycomb sandwich samples were then prepared using MB-329 as the adhesive. The use of one adhesive eliminated one variable from the testing, thus providing quicker results. This set of samples was constructed with voids contained in the bond line. These voids were the result of a hole cut in the adhesive for some samples; for others the honeycomb core was undercut so it could not come into contact with the adhesive. With three holes in the adhesive (less than 20% of the adhesive area was removed), the panel was destroyed during a decompression from less than 300 psi. Tests on the panels with voids substantiated the fact that if there is a lack of bond over a small portion of the total area of a panel, the panel will be weakened to a greater extent than the percentage of no bond area. It required decompression from less than 100 psi for the "Stresscoat" to show where the small voids occurred in the panel, as shown in Figure 21. Therefore, small voids or lack of bond could easily be detected with this method.

Several panels were constructed using the photomicroflaw technique to degrade the bond between the adhesive and the face sheet. The degraded area consisted of two 1 inch diameter circles on the center line of the face sheet. These panels were coated with "Stresscoat" (ST 1204) and rapidly decompressed from a starting pressure of 20 psi. The starting pressure was increased in 20 psi increments to 100 psi and then in 100 psi increments until failure of the panel at 1000 psi. In a typical panel, the craze in the "Stresscoat" occurred at 600 psi. The pattern of cracks showed the configuration of the honeycomb with no apparent pattern change in the area of the contaminated bond.

Samples with the honeycomb contaminated to produce a weak bond between the core and the adhesive were also rapidly decompressed. The contaminated area could not be detected until after the panel has been decompressed from a pressure of sufficient magnitude to cause failure. The pressures required to cause failure of the panels with contaminated areas in the bond were as large as those required to cause good panels to fail. However, the failure was at the contaminated surface; that is, at the core-adhesive interface or the face sheet-adhesive interface depending on the contamination of the sample.

The thickness of the honeycomb core has very little effect on this test technique. The honeycomb core must, however, be perforated. For this reason the nonperforated, heat resistant phenolic honeycomb core samples produced no results. The method is sensitive to face sheet thickness; the thicker face sheets obscure the smaller flaws.

6.4 Birefringent Coatings

The decompression method of stressing the bond line should not leave residual stresses in the panel if it is to be useful as a nondestructive test means. Birefringent coatings can be used to determine if there were any residual stresses from this testing technique.

Figure 21 STRAIN SENSITIVE BRITTLE COATING TEST OF PANEL WITH AN ADHESIVE VOID

When a part coated with a birefringent plastic material is subjected to a load, the strain distribution is visible when the plastic is illuminated with polarized light and observed through a circular polarizer and a 1/4-wave plate. The strain distribution appears as contrasting color and black patterns (fringes) which are interpreted quantitatively in terms of strains in the part.

A sample was prepared with MB-329 as the adhesive. The face sheet contained two areas contaminated by the photomicroflaw technique. Each area was a 1 inch diameter circle located on the center line of the sample and 2 inches from the end. The contamination was accomplished using a 20% light transmission screen. A "Photo Stress" (Budd Company) plastic sheet type K1-5 (.042 inches thick) was cemented to the face sheet. The panel was tested by decompressing it from a pressure of 100 psi and slowly building the pressure up to 1300 psi where it failed in subsequent tests.

Nothing was observed until the sample had been decompressed from 600 psi where strains became apparent around the outer edge, as shown in Figure 22. Further tests from 700 and 800 psi indicate no increase in the residual strain in the sample. Even after decompression from 1150 psi there seemed to be no substantial residual stresses. The panel failed when decompressed from 1300 psi. As expected, once the panel failed, residual stresses could be observed as shown in Figure 23. This substantiates initial testing with brittle coatings ("Stress-coat") and demonstrates that there are no residual stresses to weaken the panel. The poor sensitivity of this test technique in detecting understrength areas of the bond was also demonstrated.

6.5 Bond Line Electrical Parameters

It has been noted that almost all bonds conduct electricity. This is true even though the surfaces to be bonded are finished smoothly and the adhesive is nonconductive. The effect has been used to eliminate grounding straps in telephone equipment. On the other hand, monitoring of any dielectric changes or piezoelectric effects in the bond line is made difficult. The electrical resistance of the bond line was monitored to determine if this parameter could be correlated to bond line conditions. No change in the resistivity of the bond line under stress could be noted. The bond line resistance was investigated with the hope that the parameter could be used as a measure of bond conditions or as a means of increasing the resistance to allow the investigation of any dielectric changes or piezoelectric effects.

Several other tests have been made to measure the electrical properties including resistance of a bond line during resin curing. The results show that there are changes in d-c resistance, loss tangent, and dielectric constant during cure. However, repeatable results were difficult to achieve. This is attributed to the fact that bond line thickness and percentage cure do not follow the same profile in each test. For example, from test results and published data, we know the dielectric constant and loss tangent decrease and the resistivity increases with cure. Conversely, the decreasing of bond line thickness during cure produces the opposite effects on the three variables.

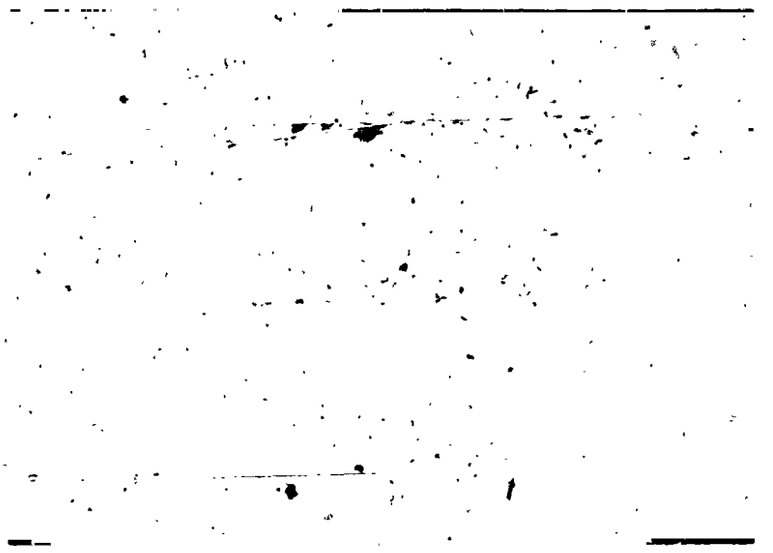

Figure 22 STRAIN SENSITIVE PHOTO COATING OF GOOD PANEL AFTER RAPID DECOMPRESSION FROM 600 PSI

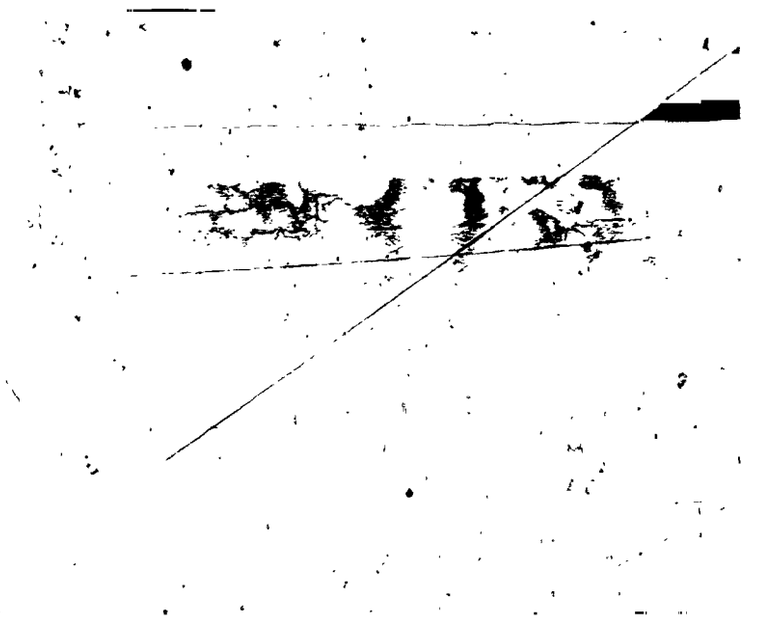

Figure 23 STRAIN SENSITIVE PHOTO COATING OF GOOD PANEL AFTER FAILURE CAUSED BY RAPID DECOMPRESSION FROM 1300 PSI

Our theoretical investigation has shown that by increasing polarizability, bond strength would be similarly increased. Since polarizability of the resin appears to be important, the dielectric constant was investigated for both stressed and unstressed bonds.

The dielectric and resistivity properties of the adhesive vary with state of cure. The decrease in dielectric constant as an epoxy resin is cured is physically explained by considering the polarizability of the resin. Although this quantity is defined as "the dipole moment of a molecule per unit polarizing field" and therefore seemingly on a microscopic scale, it can be related to the dielectric constant, K, by the Clausis-Mossotti equation which is:

$$\text{polarizability, } \alpha = \frac{3\epsilon_o}{N}\frac{(K-1)}{(K-2)}$$

where ϵ_o = permitivity of free space

N = number of molecules per unit volume,

thus giving the polarizability a macroscopic significance.

It is believed that cross linking of the basic oxygen and two carbon epoxy ring makes the resin rigid thereby freezing the molecules (i.e., the dipoles) in place with an accompanying decrease in polarizability. As shown in Figure 24, decreasing the polarizability also decreases the dielectric constant; the largest change in K for small changes in polarizability occurs at the higher dielectric constant values. The dielectric constant of epoxy resin is approximately 10 which places it in the more sensitive range for monitoring polarizability, (i.e., degree of cure or cross linking). The metal skin over the bonds investigated during this program and the low bond resistance prevent any measurements of these properties of the completed bond. However, these properties possibly can be measured before the bond is assembled. The cure state of an adhesive before the actual bonding begins cannot always be tightly controlled in the field. In a very large section it may take appreciable time to apply the adhesive. In this case, a measure of the state of cure before the complete structure is assembled may be useful.

The resistivity of manysamples was monitored. Values range from several milliohms to the megohm range. No correlation to bond strength or ultrasonic effects has been observed. It was suspected that low conductivity is due to direct contact between faying surfaces. A limited effort was directed toward confirming the cause. A sample was constructed with mica around the edges to prevent any metal-to-metal contact, but this sample did not have the characteristic resistance and the bond strength was reduced (see Figure 25). However, the bond was no longer typical.

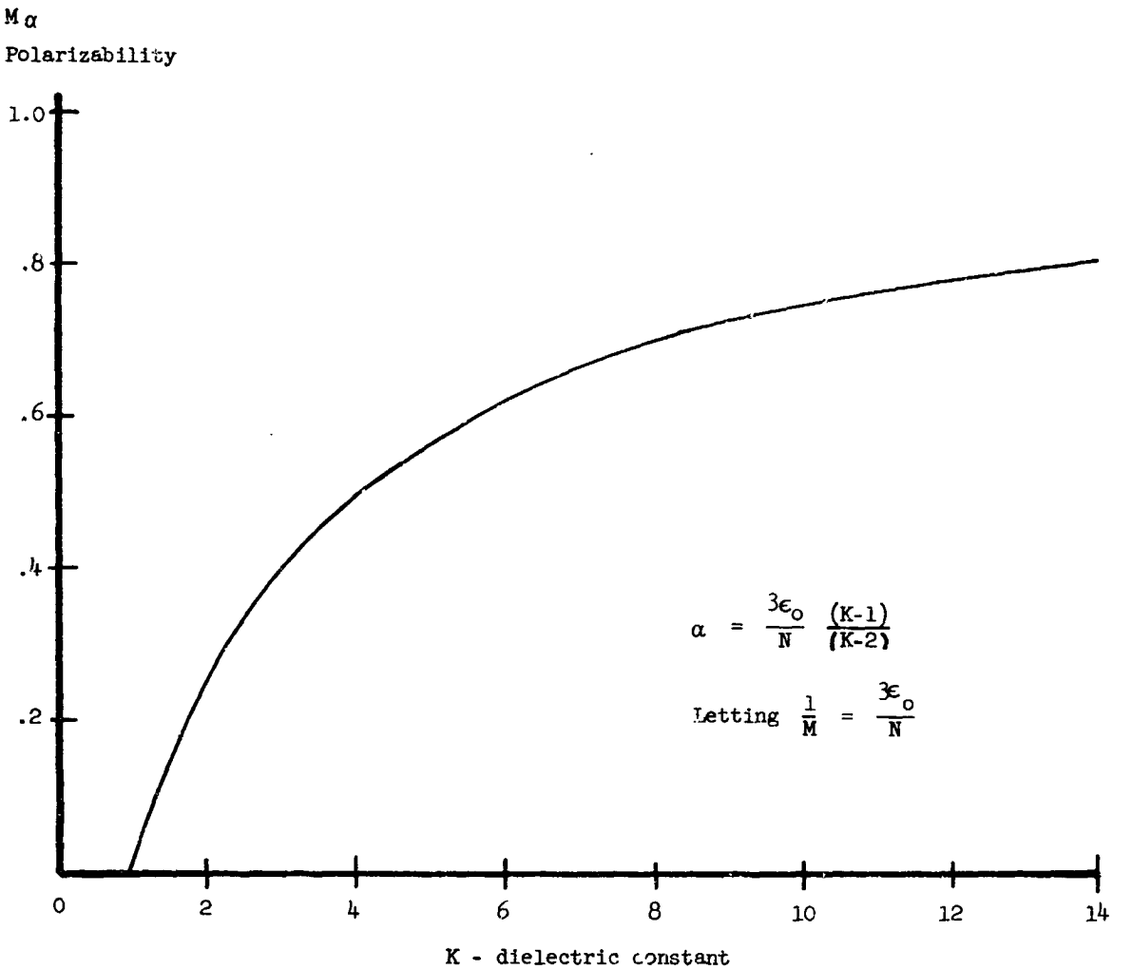

Figure 24 THE EFFECT OF POLARIZABILITY ON DIELECTRIC CONSTANT

Figure 25 SAMPLE BOND FOR RESISTANCE MEASUREMENT

SECTION 7

BOND STRESS METHODS

Most of the nondestructive test methods that have any capability of testing a weak bond require some means of stressing the bond line. This stress should be some significant percentage of the ultimate strength of the bond. The stress level is usually in the range of 1000 to 10,000 psi in tension and somewhat less in shear. Shear stress is very difficult to produce in a local area and compression is usually not useful in an NDT situation. Therefore, most bond stress methods utilize a tensile stress.

Because of the many NDT uses of a bond stress method (mentioned in Section 6), various methods of stressing a bond were investigated. The methods used for stressing bonds to gather data for this report were all basically mechanical techniques. One technique utilized a hydraulic cylinder to apply tension or compression on specially threaded test blocks. This method is unsuitable for most NDT situations. The other techniques were the rapid decompression or the high pressure vacuum cup. These were used to stress honeycomb panels for either the stress sensitive coating NDT technique, or the sonic emission NDT technique. They are however applicable to a great many situations. Other techniques were investigated theoretically.

The following section presents the results of the above and examines several approaches with regard to possible applications. The bond stressing techniques are categorized by the nature of the forces involved. The discussion is not intended to be all inclusive nor are all the methods discussed practicable in all NDT situations. Additional experimental work in this area is necessary to increase the number of situations in which the NDT techniques investigated under this program can be used.

7.1 Electrical

Perhaps the most versatile forces available in nature are electrical forces. These forces can be produced by stationary or moving charges (current) in a magnetic field. Some techniques using these forces for stress investigation are described below.

7.1.1 Forces Produced by Stationary Charges

If two groups of monoploar charges are separated, they exert a force on each other as defined by Coulomb's law:

$$F = \frac{q_1 q_2}{k r^2}$$

where

F - force
q - magnitude of charge groups
r - separation between the charge groups

If the two groups are of the same polarity they repel each other; if they are of opposite polarity, they attract each other. If one group of charges is placed on the material surface to be stressed and the other placed at some point apart from the surface, either tensile or compressive forces can be exerted by the charges on the material surface in a noncontacting manner. Since charges can be distributed on a nonconductor, the method may have use in both metallic and nonmetallic materials. However, in most cases it is limited to conductive material applications. A configuration for such a stress method is shown in Figure 26. The system consists of a plate which is maintained a fixed fistance from the surface of the bonded material surface by the use of a dielectric and an insulator.

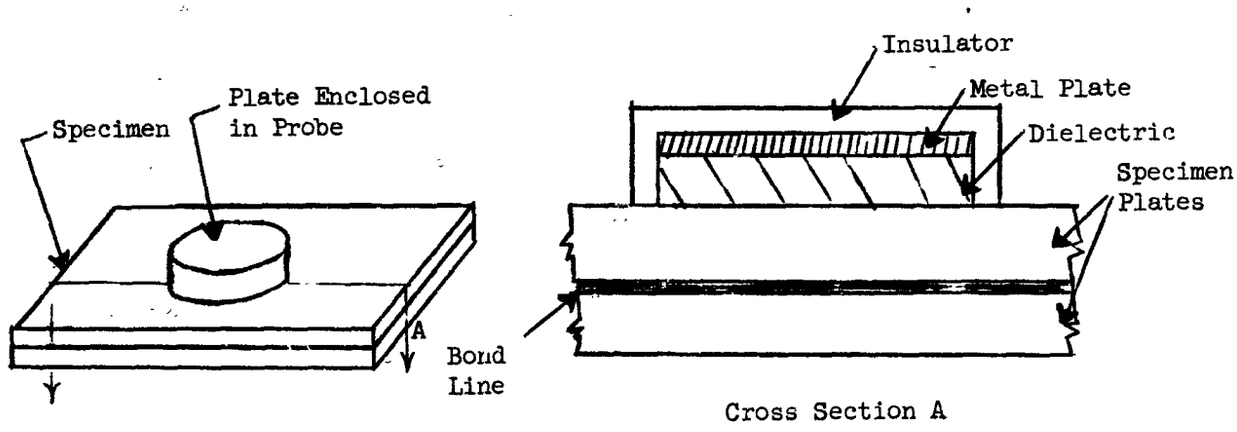

Figure 26 PROBE CONFIGURATION

The force of attraction between this metal plate in its probelike housing and the top plate at the bond line is:

$$F/A = \frac{\epsilon KV^2}{2\ell^2} \qquad \epsilon = \epsilon_o \epsilon_r \qquad 1)$$

where

F is the force in pounds
A is the area in sq. in.
ℓ is the spacing between the plates
V is the voltage between the plates
K is the conversion factor to convert newtons to lbs.
ϵ_o dielectric constant of free space
ϵ_r dielectric constant of the material used

Let us assume the metal plate is spaced .001 in. from the sample.

$$\ell^2 = (10^{-3})^2 = 10^{-6} \text{ in}^2$$
$$\epsilon_o = 8.85 \times 10^{-12}$$
$$K = .22481$$

If the dielectric of the probe is mica, it is possible to use 5 KV across the .001" gap. Then $V = 5 \times 10^3$ and $\epsilon_r = 6$

$$p = F/A = \frac{(8.85 \times 10^{-12})(6)(.22481)(5 \times 10^3)^2}{2 \times 10^{-6}} \qquad 2)$$

$$F/A = 149 \text{ psi}$$

Therefore, the applied average stress is 149 psi. This force is nearly ten times lower than the minimum force desirable for the NDT situation. However, it is 10 times greater than that presently available from devices such as suction cups, which are limited to 14.7 psi.

Obtaining a .001" gap is, of course, very difficult except for a perfectly flat surface. However, the use of a larger gap reduces the force very significantly. The use of mica as a dielectric is desirable because of its high breakdown voltage and its high dielectric constant. A disadvantage of mica is its low compliance. If the probe is used as a clamp, and force applied externally then the compliance of the mica is not significant; however, if the probe is used to stress the material between the probe edges and its center, then the dielectric has to have sufficient compliance to allow deformation of the material stressed into the cavity of the probe. If the latter method is used, a voltage breakdown problem could exist at the interface between the material to be stressed and the probe dielectric.

The applied force can be increased by using a separation material with a higher dielectric constant providing it has sufficient dielectric strength. Alternatively, a significantly higher dielectric constant would allow some reduction in applied voltage, reducing the breakdown voltage requirement.

This probe can be built as a portable system with the necessary power supply included. Considering our probe again, the voltage required is 5000 volts and the capacity per unit area is $C/A = \epsilon_o \epsilon_r / d$ (.0254) = 1344 pf per sq. in. of probe area. A 5" probe would have a capacity of 26,880 pf. The energy required to charge the capacitor at 5000 V is $1/2\ CV^2 \cong 1/2$ $(26.9 \times 10^{-9})(25) \times 10^6 \cong .34$ watt-seconds.

A 1 watt power supply would charge the probe in less than 0.6 seconds. A dc-to-dc transistor converter could be used as a power supply. With batteries it would weigh less than 5 lbs. and occupy less than .25 cubic feet, making for a very portable unit. The feasibility of this approach

is dependent to a large extent on the availability of dielectrics with suitable electrical and mechanical properties.

7.1.2 Forces Produced by Currents

Another physical phenomenon which results in the creation of forces is the interaction of two magnetic fields. A current flowing through a conductor produces a magnetic field. If two current carrying conductors are in proximity of each other, there is a net force between them, as shown in the Figure 27 below.

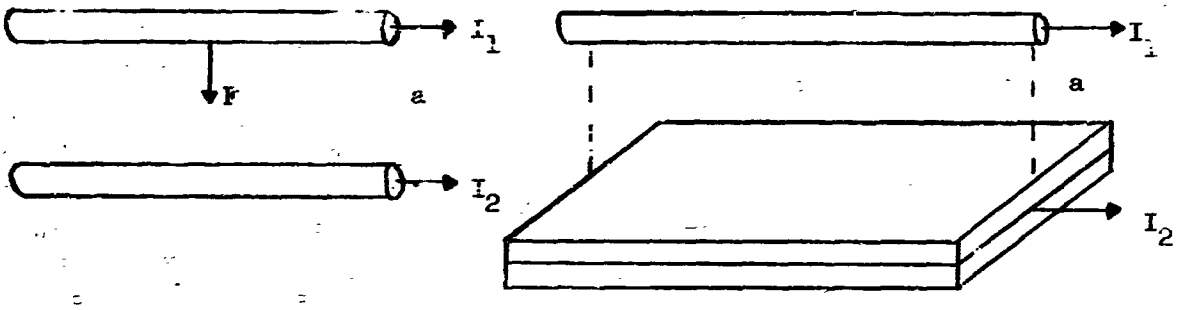

27 (A) 27 (B)

Figure 27 FORCES DUE TO CURRENT FLOW

If a current carrying conductor is suspended over a metal plate with a current passing through, there will be a force between them. Because of the current distribution in the metal plate, an exact analysis would be very involved. However, a good indication of the magnitude of the forces that could be created by this method can be gained from an analysis of the forces between two parallel current carrying conductors. If the currents are in the same direction, the force will be one of attraction between the conductors. As shown in Figure 27B, the force is:

$$F = \frac{K \mu_o 2 I_1 I_2}{4 \pi a} \qquad 3)$$

Considering the force per unit length

$$F/\ell = \frac{K \mu_o 2 I_1 I_2}{4 \pi a} \qquad 4)$$

where

F/ℓ = force per inch

$\frac{K \mu_o}{4\pi} = .225 \times 10^{-7}$ lbs/amps^2

K = .225 lbs/newton

a = spacing between conductors in inches

Suppose $I_1 = 10^4$ amp, $I_2 = 10^5$ amp and a = .01 inch;

$$F/\ell = \frac{4.48 \times 10^{-8} (10^9)}{10^{-2}}$$

$$F/\ell = 4.48 \times 10^3 \text{ lbs/in}$$

Therefore, the force of attraction will be 4.48×10^3 lbs/in or 4480 lbs/in.

The force distribution over the surface area of the plate depends on the configuration of the current carrying conductor and the mechanical and electrical characteristics of the conductive sample. These parameters could best be determined experimentally.

One method of obtaining currents of the order indicated above is through a capacitor discharge. Power supplies for this type of work are readily available. The ignition of gas discharge tubes could be used for switching the current.

In the sample of Figure 26 , 10,000 amperes are assumed flowing through the conductive sample. As is evident a major difficulty in this stress method is the passage of large currents through the sample. Very low resistance contacts would have to be used. There is a possibility of surface damage. Also, heating of the material resulting from the passage of large currents is a potential problem. However, current through the sample can be decreased if current through the external conductor is increased, with no loss in force. Because of the magnitude of current needed for this system, the power supply unit may be disadvantageously large; however, the large forces that can be generated make the method worthy of attention.

7.1.3 Forces Produced by Eddy Currents

If a coil energized by an alternating current is brought in the vicinity of a material surface, as shown in Figure 28, the alternating electromagnetic field produced by the coil will induce currents in the material which produce a field of opposite polarity.

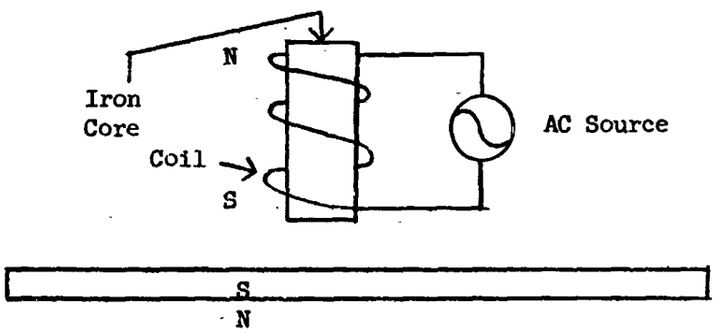

Figure 28 EDDY CURRENT METHOD

The magnitude of the induced currents is proportional to the conductivity of the material, the proximity of the coil, the applied voltage, etc. The primary current in the coil and the induced current in the material set up two effective electromagnets which produce a repelling force on each other. The repelling force can be very large and is used for metal forming. The main limitation of the eddy current approach for this application is that the forces always repel. That is, it is not possible to produce tensile forces with the present schemes being considered.

7.1.4 Mechanical and Acoustical

Under this group we include all mechanical, sonic and ultrasonic techniques for generating forces on or within a material. These are applicable to all materials. The mechanical techniques are simple in principle and have been used extensively in laboratory experiments. While the forces are relatively easy to generate, the method of coupling to produce both tensile and compressive stresses presents many difficulties.

The most direct method of applying mechanical forces is through the use of grips, bolts, etc. These generally cannot be used to produce tensile forces without damage to the structure unless special mountings or attachments are incorporated in the structure. Tensile stresses can be produced within the materials through structural bending. However, tensile stresses of the proper direction cannot be generated within the bond line in most instances.

7.1.4.1 Stress System Using Quick Acting Adhesive

One brute force method of coupling mechanical tensile forces to a material surface is through a quick acting adhesive such as Eastman 910. This adhesive is easily applied, sets in a few seconds and achieves a shear strength of over 1000 psi for materials such as aluminum. There is a solvent for this adhesive that allows it to be removed readily from a surface. To facilitate removal of the adhesive the coupling member should be removed before using the solvent. Hot water will weaken the bond sufficiently to allow the coupling member to be removed with a sharp side impact without damage to the surface.

It appears possible to design a small attachment, a large number of which could be bonded to the material surface in a relatively short period of time. A tester could then be designed which would slip over the attachment and apply a tensile force to it and the material surface of any desired amount within the limits of the adhesive. The tester could be provided with a transducer which would measure the displacement of the attachment to determine if the bond strength were adequate. Other bond tests such as the monitoring of acoustical emission, or strain sensitive coating tests can use this bond stress method. After the test, all the attachments can be quickly removed and the surfaces cleaned with a suitable solvent. While

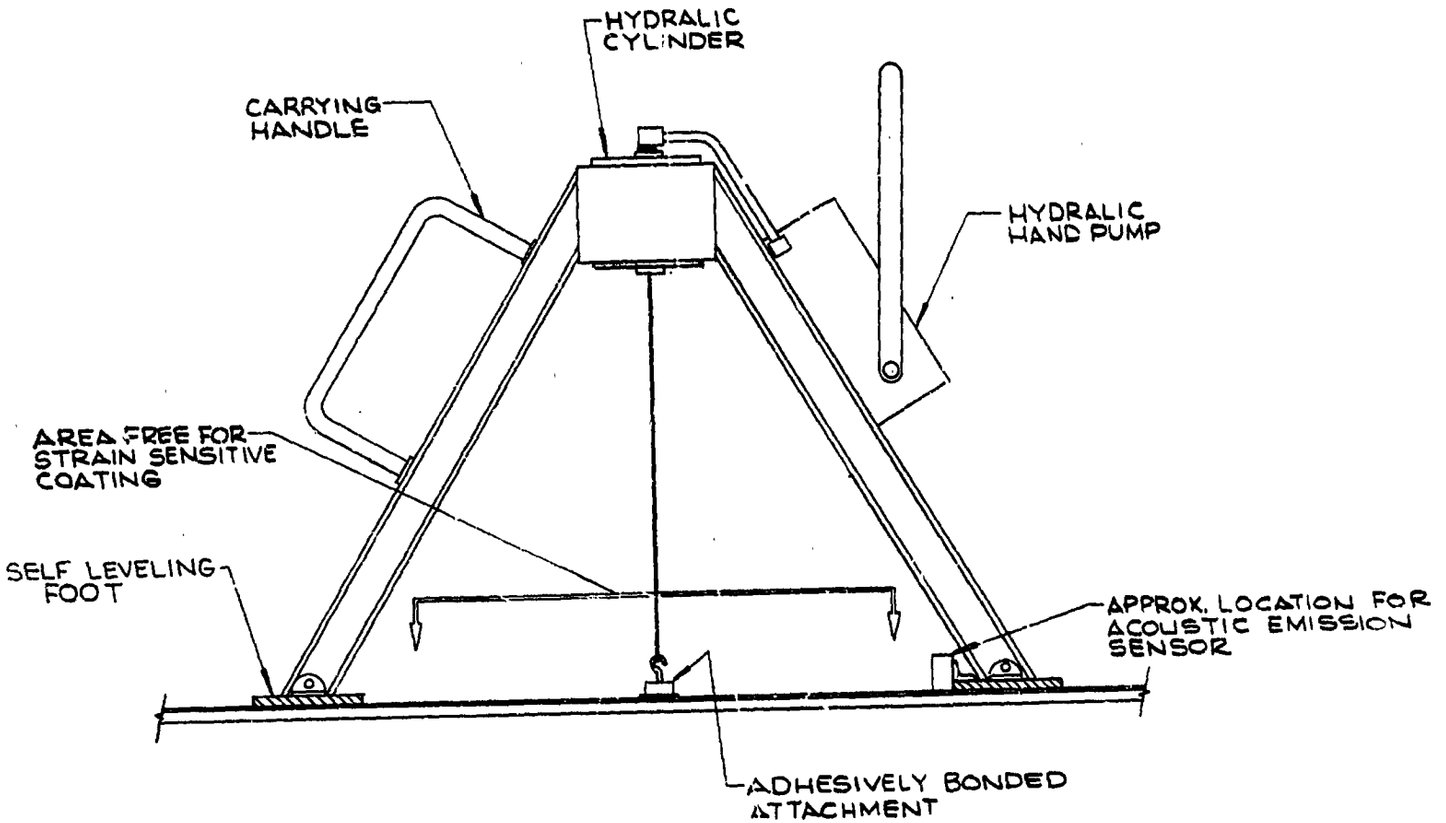

MECHANICAL BOND STRESS SCHEME

Figure 29

this approach is time consuming, it is nondestructive in the sense that good bonds are not destroyed. In addition. it is applicable in the field. A typical sensor arrangement is shown in Figure 29.

7.1.4.2 Ultrasonic Stress Systems

The passage of a sonic or ultrasonic wave through a structure does not produce tension in the material in the absolute sense unless the transducer is bonded to the surface or unless a resonance is achieved. Bonding would require a setup similar to that described for Eastman 910. The amount of tension achieved under resonance in excess of the compression needed to couple the transducer to the sample surface depends on the mechanical "Q" of the resonant system. The higher the Q the greater the stress amplification. Unfortunately, all composites are of relatively low Q. This means that the tensile stresses produced probably will not exceed the applied compression stress. In honeycomb they may be considerably lower.

Another factor of importance is the stress distribution across the cross section. For example, if the rectangular section shown in Figure 30A below is resonated, the stress pattern will approximate a half sine wave as shown.

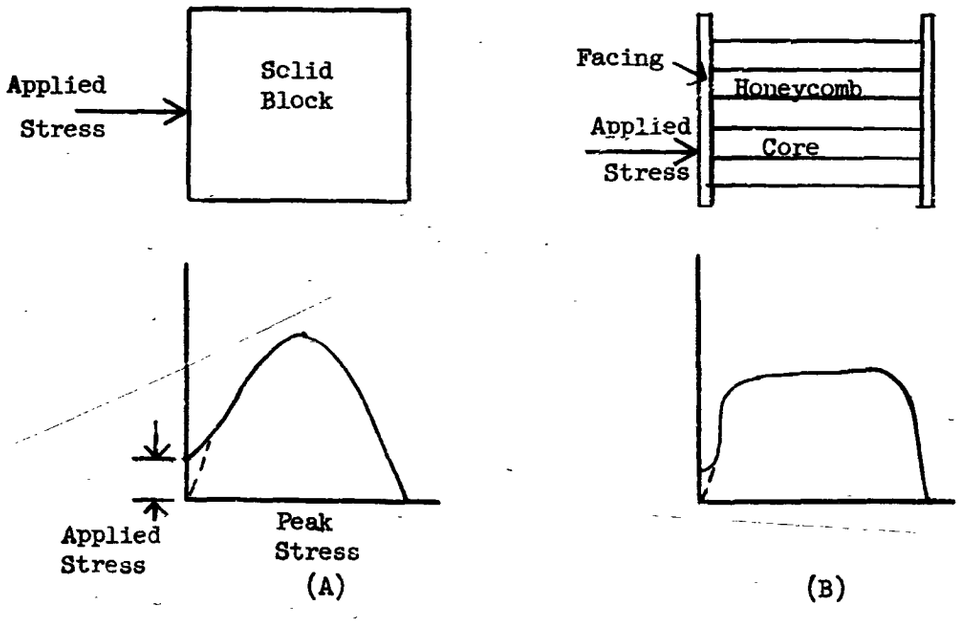

Figure 30 ULTRASONIC STRESSES

The stress and surface velocities are a maximum and minimum respectively at the center, and opposite at the edges. Thus the stress amplification near the edge will be small.

The distribution in honeycomb is much more complicated. Because of the heavier mass of the face sheet compared to the core, it is expected that the stress distribution may rise much more rapidly from the facing surface as shown in Figure 30B. The exact shape of the curve requires a detailed mathematical analysis. However, an experimental determination of the stress levels at the bond lines offers the quickest and most accurate means of determining its applicability. Suitable equipment is available at GARD for this experiment.

It is not possible in general to resonate the facing alone sufficiently to produce significant bond stress. The frequencies required lead to exceedingly high attenuation and poor energy transfer to the bond.

7.1.4.3 Shock Wave Stressing

Shock loading can produce a tensile force as is evidenced by the spalling or failing in tension of the inside of thick armor plate when a projectile or charge impinges on the outside. Figure 31 shows a plane compressional shock wave impinging on a solid medium.

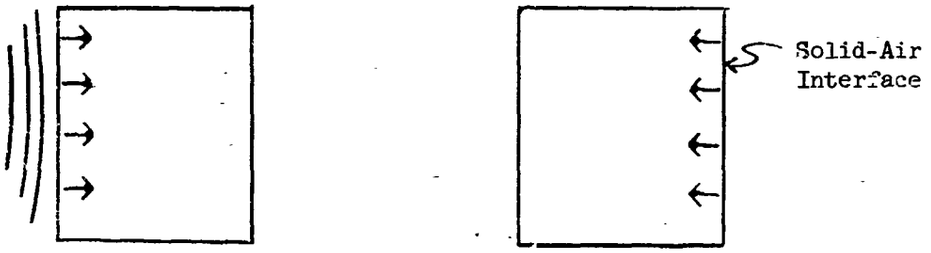

Figure 31 ACTION OF SHOCK WAVE

If the back surface of the solid is air or a medium of much lower acoustical impedance than the solid, the compressional shock wave is reflected as a dilational or tensile wave. When conditions are such that the primary shock front has ended when the reflected wave passes through, the medium at that point will be under a condition of absolute tension.

Thus a compression force, which needs no couplant, can be made to produce a tensile force. The facings are generally so thin that the reflection may occur before the initial shock wave is completed. Theoretically this limitation can be overcome by impacting with a thinner plate.

The surface that receives the shock front is, of course, obscured; however, the opposite surface is free for any tests and instrumentation. Since the wave that produces the stress on the bond line does go through the bond line, it does contain information about the bond line and can also be used as the interrogating signal for a sonic or ultrasonic attenuation type of test. For a flat or medium radius sample, the boundary conditions allow a very good analytical solution to be made. The problems of generating and controlling the incidence of a shock wave on a large structure are of course formidable; this approach has been considered primarily for completeness.

7.1.4.4 Centrifugal Forces

Another method of achieving a uniform force over a section is through the use of centrifugal forces. These forces do not alleviate the necessity of attaching to the surface of the sample unless high accelerations are employed. In some configurations the attachment may already be made. In this case the ability to generate an even force on a portion of the structure may be all that is needed.

7.1.5 Vacuum or Pressure

7.1.5.1 Internal Honeycomb Static Pressurization

If the edges of a honeycomb panel are sealed and the pressure inside increased through a valve, any value of force can be exerted on the face sheet of a honeycomb panel. This method is currently in use. Some aspects of this method are unknown at the present. Tests at GARD have shown that is has a different effect on failures between the face sheet and the adhesive than failures between the honeycomb and the adhesive. Undercut honeycomb or lack of adhesive may have still another effect. These effects are related to the strength of the adhesive cap that is formed over each cell due to the filetting action and the skrim cloth or structural strength of many adhesives.

The internal pressure method has the advantages of being applicable to all materials, of having the surface of the sample free for NDT instrumentation and providing accurate controllability over the magnitude of the stresses applied. It is limited in application to perforated core materials and has the disadvantages of requiring seals and being limited to fairly slow rates of pressure buildup.

7.1.5.2 Internal Honeycomb Dynamic Pressurization

A method of stressing honeycomb panels used in this program is the internal honeycomb dynamic pressurization. The results of these tests are discussed in Section 6. Figure 32 is a photograph of the chamber used to carry out these tests. A perforated honeycomb core sandwich sample is placed in the vessel and the pressure increased at a slow rate to a predetermined value. When the pressure is suddenly relieved by opening a

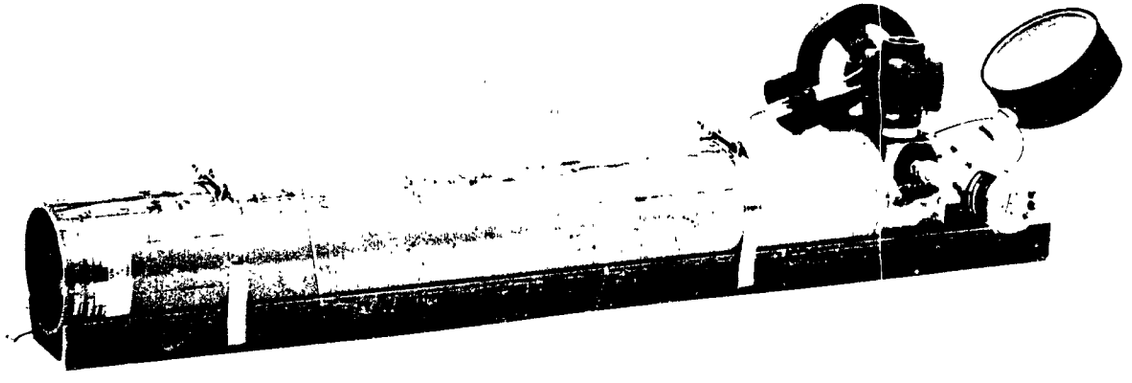

Figure 32 PRESSURE CHAMBER

large valve, the pressure in the honeycomb core cells cannot escape through the small perforation fast enough and a force is developed against the face sheet. Stresses are measured by brittle coating or photoelastic methods. Tests have shown that the force field has good uniformity across the area of the sample and is effective to the outermost row of cells. This method has most of the advantages of the internal pressure method, although viewing ports must be installed to allow direct viewing of the sample surface. Additional advantages include the ability to apply the force at a fast rate and elimination of the necessity of sealing the edges of the sample.

Its main disadvantage is the requirement for a large high pressure autoclave and large venting valves. Units capable of handling large Saturn V sections, however, can be built at reasonably low cost for pressures up to 1000 psi or higher. Venting valves present a more difficult problem but are within the state of the art.

7.1.5.3 High Pressure Vacuum Cup

Another mechanical stress method investigated experimentally under this program is the high pressure vacuum cup. It is an extension of a presently used vacuum cup technique for testing honeycomb panels. In the present method a vacuum is pulled over a honeycomb panel and the atmospheric pressure allows a stress of 14.7 psi to be applied to almost any bond configuration. This system has many advantages as it doesn't disturb the surface and is portable. Although it partially obscures the surface, it is feasible to include instrumentation within the vacuum cup for measuring bond response. The stress and the rate of stress can also be controlled, and the equipment does not usually produce electrical interference or noise that could interfere with any nondestructive test. However, the main disadvantage of low peak stress renders this method unsuitable in most instances except for nonbond areas.

One method of increasing the stress available from a vacuum is to use a higher external pressure. This necessitates a pressure chamber or autoclave; however, all of the other advantages of the vacuum cup method remain. The maximum stress available equals the capacity of the pressure chamber plus 14.7 psi. Although personnel can, and do, work under pressure to and exceeding 100 psi, an automated system for testing and scanning would be desirable. This system, except for portability, meets most of the requirements mentioned at the beginning of the proposal. The system can be used with both metallic and nonmetallic materials, and both honeycomb sandwich construction and surface construction. There is also a minimum of interference with any test medium. For surface-to-surface samples a vacuum cup can be attached to each side to impart a tensile stress to the bond using mechanical or hydraulic means. For honeycomb sandwich the vacuum cup alone can stress the bond as air under pressure is present in the cells. The provision of a sufficiently large high pressure autoclave for testing is

well within the state of the art. A photograph of the vacuum cup used for experimentation is shown in Figure 15.

7.1.6 Thermal

A method of inducing stresses in a structure is to take advantage of dimensional change effects due to heating. Honeycomb panels have been tested in this manner. The face sheet is heated quickly with a radiant source and the expansion of the face sheet disrupts any weak bonds and causes a deformation of the face sheet. Other thermal methods that can be considered include the differential expansion of two unlike materials in a surface-to-surface bond, and a pressure buildup of the air on the inside of nonperforated or sealed honeycomb sandwich at high temperatures. Radiant heating sources are available that can produce a closely controlled source of high intensity energy.

SECTION 8

CONCLUSIONS

8.1 NDT Techniques

8.1.1 Sonic Emission

The sonic emission tests have been able to determine the strength of a bond to within about 10 per cent. To utilize this test method, a tensile force must be applied to the bond line. This force should be applied in such a manner that the specimen is not damaged. This is the only true NDT technique that has thus far been able to test the strength of an adhesive bond. This method fulfills many of the characteristics set forth in the contract as desirable for a NDT technique. The major problem is the need for applying a tensile stress to the part to be tested.

This method is well suited to whole structure tests. In this manner scanning is eliminated and the test can be accomplished quickly and economically. A relatively large number of sensors would however be required to pinpoint the areas of weakness. Many structures are tested with hydraulic pressure or a static stress. This NDT method could be a very important adjunct to such tests. It requires little or no coupling and the instrumentation consisting of amplifiers and transducers is inexpensive. Tests have shown the technique to useful on honeycomb core and has virtually no dependence on face sheet or core thickness. However, phenolic honeycomb core may introduce too much noise, and mask the adhesive reaction to stress. Additional investigation is required in this area. The sonic emission was used for metal to metal bonds and good results were obtained through as much as two inches of metal.

It is recommended that the sonic emission bond test instrumentation be used on any stress or hydraulic test of large structures.

8.1.2 Strain Sensitive Coatings

This type of test is used largely for honeycomb panels. A limited investigation was carried out under this program to determine the applicability of this type of test to understrength bonds and to determine the applicability of the rapid decompression stress method to strain sensitive coatings. The technique was sensitive to adhesive void areas or nonbonds caused by undercut honeycomb. However, the sensitivity to weak bonds between either the adhesive layer and the core or the adhesive layer and the face sheet was poor. It is believed that this was due to the strength of the adhesive cap formed over each cell. The strain sensitive coatings themselves will detect any deformation of the face sheet. The variance in the sensitivity is determined by the method of applying the stress. Tests conducted to determine the residual stress left in the face sheet of a honeycomb panel showed little permanent deformation except near the edges of the sample. With a suitable means of bond stress, this method may be a good

test for critical areas of bonded structures. After the test the coatings can be easily cleaned. The brittle laquer is soluable in carbon disulphide and the photo stress can be a strippable variety.

8.1.3 Ultrasonic Attenuation

The experimental investigation of the change of ultrasonic attenuation with applied stress to the bond gave inconsistent results. Some of the data indicated a correlation between attenuation change and stress; also in some instances a rise in attenuation occurred just prior to the failure of the sample. However, the wide variance in the data between samples and between various locations on the same sample, eliminate the present method of testing from giving a reliable indication.

At present the reasons for this variation are not known. If further study discloses the reason for these variables, further correlation may result in a usable system.

8.1.4 Electrical Parameters

The high conductivity that was present between most of the metallic samples prevented any measurement of the adhesive resistivity or dielectric properties. This conductivity is thought to be unavoidable contact between the two metallic faying surfaces. No correlation was found between this conductivity and bond strength during cure, after cure, or during stress.

8.2 Bond Stress Methods

This investigation into NDT methods for determining the strength of an adhesive bond has pointed up the need for a widely applicable method of bond stressing. The experimental investigation of all of these stress methods were limited by the scope of the program. Many were theoretically investigated and some were used as a means to examine the NDT techniques under the program. It is recommended that further work in this area be undertaken to develop a good bond stress method. The following paragraphs summarize the conclusions arrived at during the program.

8.2.1 Rapid Decompression

This stress method was used with good success to test honeycomb bonds during the program. Although the experimental investigation of this method of bond stress was necessarily limited, the results and advantages are promising. The program has definitely indicated the need for a bond stress system, and this method must be one considered.

8.2.2 High Pressure Vacuum

In the experimental investigation the most convenient method of stressing a honeycomb face sheet in tension was the high pressure vacuum cup. This method is also one of the methods most applicable to production testing. The pressure chamber necessary, although not as portable as would be desired, does not present any construction difficulties for testing many sections.

8.2.3 Electrical Bond Stress Methods

These stress methods were not examined experimentally. However, their many advantages require that they be considered in any NDT bond strength testing system. The portability and lack of any contamination to the surface of the sample are among their advantages. Limited applicability to nonconductors is a disadvantage

8.2.4 Force Pulses

Mechanical force pulses either sonic or ultrasonic are very attractive as a bond stress method, however, the difficulties of coupling the force to the specimen and generating enough force are very serious.

8.2.5 Mechanical

Of the many mechanical methods available for stressing a bond such as direct threaded attachment, binding, clamps, etc. the adhesive bonded attachment point is the most promising. The simplicity and low cost of the method increase its applicability. The method could be used with many NDT systems and in many sample configurations.

8.2.6 Thermal Methods

Although these methods are now being used, primarily in brazed panels, the possibility of damage to the adhesive and the lack of control over the stresses applied are detriments to their widespread use. Their advantages are that they are portable, inexpensive, and easy to use.

8.3 Understrength Simulation

Several methods of producing degraded bonds were experimentally investigated during the program.

The photomicroflaw technique uses a pattern of contaminated dots formed photographically. This method produces the most consistent results, and, it is felt, is a close approximation to the actual flaw mechanism in many understrength bonds. It is recommended that this technique be used as an understrength bond simulation for any NDT technique for testing bond strength.

SECTION 9

RECOMMENDATIONS

9.1 Ultrasonic Emission

Additional work must be done to adapt the ultrasonic emission technique to large bonded structures. A program to run such a test is recommended. The program would determine the ultrasonic emission characteristics of a large composite structure. The optimal instrumentation with respect to the number and configuration of transducers, the amplifiers and signal processing and data presentation would also be determined by the program.

The static hydraulic pressure tests of a complete stage of a vehicle would make a good test for the system. Such a trial would add only modest cost to the work and would have the capability of providing much practical information. Information gained could include the progress of high stress points toward failure. Also small noncatastrophic failures would be readily detected. The recommended program consists of three phases. The first phase is an experimental evaluation of the response of complex structures and other problems associated with monitoring the acoustic noise emitted. The second phase is the construction phase. The number of channels of instrumentation determined necessary by the first phase would be constructed in this phase. The third phase would consist of the actual test of a vehicle stage.

9.2 Bond Stress Methods

A program to theoretically and experimentally investigate all means of stressing the bond line in a variety of configurations is recommended. As mentioned previously almost all methods of NDT for bond strength, now used or recommended for use, require some means for bond line stress. All of the capabilities of a bond stress means must be examined in light of the various NDT methods to be used.

During this program experiment has shown that all of the variables associated with the bond line stress methods now used are not well known. As an example, the bond in a honeycomb panel will react differently depending upon whether the poor bond is between the face sheet and the adhesive or between the honeycomb core and the adhesive. Voids in the adhesive and undercut honeycomb will also react differently to this type of bond stress.

The recommended program consists of two phases. The first phase is the theoretical and experimental investigation of all bond stress methods. The second phase is the construction and testing with actual NDT techniques of the most applicable bond stress method.

LIST OF REFERENCES

1. "Evaluation of Ultrasonic Test Devices for Inspection Adhesive Bonds", Reese, J. P., Boruff, V. H., Navy Bureau of Aeronautics, Contract No. 59-6266-C, Final Progress Report.

2. Nondestructive Testing of Adhesive Bonded Joints, H. M. Gonzalez and C. V. Cagle, Fourth Pacific Area National Meeting, Oct. 4, 1962.

3. "Development of Nondestructive Tests for Structural Adhesive Bonds", Arnold, J. S., WADC Tech. Report, 54-231, Part 3, April 1965.

4. "Evaluation of Fokker Bond Tester System for Nondestructive Testing of FM-47 Adhesive Bonded Honeycomb and Metal to Metal Structures", Clemens, R. E., SNT Technical Meeting, February 13, 1962.

5. Bikerman, "The Science of Adhesive Joints", Academic Press, 1961.

6. deBruyne and Houwink, "Adhesion and Adhesives", Elseview, 1951.

7. "Adhesion and Cohesion", Symposium at General Motors, Elsevier, 1962.

8. "Adhesion", Eley, Oxford U. Press, 1961.

9. "Adhesives", International Science & Technology, p. 104, April 1964.

APPENDIX 1

THEORETICAL INVESTIGATION OF BONDING FORCES

TABLE OF CONTENTS

PART I THEORY

1. Introduction

The adhesion between two materials is due almost exclusively to the forces of attraction between the molecules of the materials. These are the so-called van der Waals' forces, postulated by van der Waals to explain deviations by real gases from the perfect gas law. In most non-metallic solids, these forces are also responsible for the major portion of the cohesive strength*. It is the van der Waals' force with which the present discussion is concerned, and, in particular, that component called the London dispersion force.

2. Attractive Forces

Van der Waals' forces are a set of intermolecular forces which can perhaps best be defined as "those forces which give rise to the constants a and b in van der Waals' equation". They arise chiefly because of three different effects: (a) orientation effect of permanent electric dipoles; (b) induction effect of permanent dipoles on polarizable molecules; (c) dispersion effect of internal electron motions independent of dipole moments. The first two can be understood and described entirely in terms of classical electrodynamics. The third effect owes its existence to quantum mechanics; if Planck's constant were zero, there would be no dispersion force. The

---

* J. C. Slater, Quantum Theory of Matter

following gives a brief summary of the theory behind each of these effects.

(a) Orientation Effect

An asymmetric charge distribution in a molecule gives rise to an electric dipole moment. In an external field $\vec{E}$ the interaction energy between the dipole moment $\vec{\mu}_1$ and the field is

$$V = -\vec{\mu}_1 \cdot \vec{E} \qquad (1)$$

Now let the external field be that due to another molecule with dipole moment μ_2. The interaction energy is then

$$V = -\frac{\mu_1 \mu_2}{r^3}\left[2\cos\theta_1\cos\theta_2 - \sin\theta_1\sin\theta_2\cos(\varphi_1-\varphi_2)\right] \qquad (2)$$

where $\theta_1, \theta_2, \varphi_1, \varphi_2,$ and r are defined in Figure 1*.

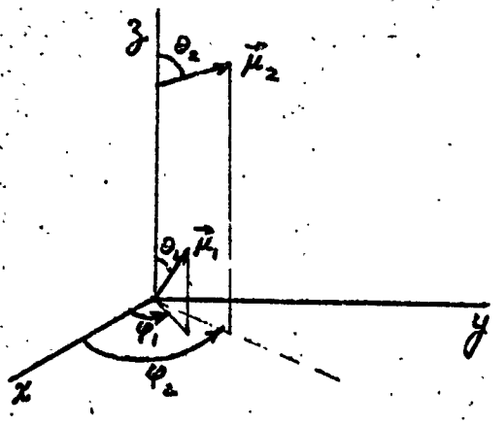

Figure 1 GEOMETRICAL RELATIONSHIPS

* F. London, Trans. Faraday Soc. 33, 9 (1937)

Depending on the relative orientations of the two molecules, the interaction energy may be either positive or negative. A positive energy corresponds to repulsion, negative to attraction. If all orientations were equally probable, the force between two molecules would, on the average, be zero, since the molecules keep shifting their orientations constantly due to thermal agitation. However, Boltzmann statistics shows that orientations of lower energy are statistically preferred, the more so the lower the temperature. Looked at another way, the torque exerted on one molecule by the field of another is always such as to turn the molecule into a position where the attractive force is a maximum. This effect is counteracted by collisions with other molecules which tend to randomize the orientations and hence nullify the attractive force. On the other hand, the lower the temperature the smaller the number collisions per unit time as well as the effect of each collision. Hence the attractive force would be expected to be more prominent the lower the temperature. Applying Boltzmann statistics, Keeson* derived the following expression for the average interaction energy between two molecules:

$$V = -\frac{2}{3}\frac{\mu_1^2\mu_2^2}{r^6}\frac{1}{kT} \qquad (3)$$

where k = Boltzmann's constant. This expression holds only for temperatures

---

* W. H. Keesor, Physik. Zeitschr. 22, 129 (1921)

such that $kT \gg \mu_1\mu_2/r^3$. For lower temperatures the energy approaches the limiting value,

$$V = -\frac{2}{3}\frac{\mu_1^2\mu_2^2}{r^3}, \qquad (4)$$

corresponding to the orientation of the two molecules parallel to each other along the line joining their centers. In this way, Keesom attempted to explain the existence of van der Waals' forces.

In addition to the dipole moment, a molecule will, in general, possess quadrupole and higher order moments. These will also give rise to interactions with other molecules. However, these interactions are generally very small and are usually neglected.

(b) Induction Effect

According to Eq. (3), the average attractive force due to dipole-dipole interaction vanishes at high temperatures. This is at variance with experience which shows that the empirical van der Waals corrections do not vanish with increasing temperatures at the rate indicated by (3). There must, therefore, be other interactions essentially independent of temperature. One of these, the so-called induction effect, was first investigated by Debye*. This treatment assumes that one of the molecules possesses a permanent dipole moment and calculates the effect of the dipole moment

* P. Debye, Physik. Zeitschr. 21, 178 (1920)

induced in the other in virtue of the second molecule's having a non-zero polarizability.

Let the second molecule have a polarizability α. In an external field $\vec{E}$ the induced dipole moment is then

$$\vec{\mu}_2 = \alpha \vec{E}, \tag{5}$$

and the energy is

$$V = -\frac{1}{2} \alpha \vec{E}^2. \tag{6}$$

The magnitude of the field due to the first molecule is

$$|\vec{E}| = \frac{\mu_1}{r^3} (1 + 3\cos^2\theta)^{1/2}, \tag{7}$$

and hence

$$V = -\frac{1}{2} \alpha \frac{\mu_1^2}{r^6} (1 + 3\cos^2\theta). \tag{8}$$

This expression is always negative and hence its average over all directions is also negative. Since $\langle \cos^2\theta \rangle = 1/3$, where $\langle\ \rangle$ denotes an average,

$$V = -\alpha \frac{\mu_1^2}{r^6}. \tag{9}$$

If the second molecule also possesses a permanent dipole moment, there is a similar term describing the polarization of the first molecule by the second. The total interaction energy is then

$$V = -\frac{1}{r^6} (\alpha_1 \mu_2^2 + \alpha_2 \mu_1^2). \tag{10}$$

If neither one of the two molecules possesses a permanent dipole moment the above effect does not occur. In such a case the first non-zero term in the interaction energy would come from the interaction between the quadrupole moment of one molecule (assuming this to be non-zero) and the dipole moment induced in the other. The energy (properly averaged as before) is

$$V = -\frac{3}{2}\alpha\frac{q^2}{r^8} \qquad (11)$$

where q is the quadrupole moment. In this way it was originally believed that the van der Waals forces could be accounted for in the cases of non-polar molecules. In fact, the empirical van der Waals corrections were used to determine (q) when no other method was available for this determination. However, when quantum mechanics later furnished a way of calculating the quadrupole moments of molecules, it was shown that they were much too small to account for the experimental facts.

(c) Dispersion Effect

In this dilemma it was shown by London* that even between neutral atomic systems with completely symmetrical charge distributions there is an attractive force due to quantum mechanical effects. As a simple model to illustrate the principles involved, consider two three-dimensional harmonic oscillators with polarizability α and no permanent moments in their rest position. If the charges (e) of these oscillators are displaced from their rest positions

* F. London, ibid.

by the displacements

$$\vec{\rho}_1 = x_1\vec{i} + y_1\vec{j} + z_1\vec{k}, \quad \vec{\rho}_2 = x_2\vec{i} + y_2\vec{j} + z_2\vec{k} \tag{12}$$

the potential energy of the system is

$$V = \frac{e^2}{2\alpha}(\rho_1^2 + \rho_2^2) + \frac{e}{r^3}(x_1x_2 + y_1y_2 - 2z_1z_2). \tag{13}$$

The first term represents the energy due to the elastic restoring force, the second the dipole interaction energy. According to classical theory, nothing would prevent these oscillators from remaining in their rest positions without interacting with each other, even if brought into close proximity. Quantum-mechanically, however, the lowest energy state of a harmonic oscillator with proper frequency ν is not zero but has the value

$$E = \frac{1}{2}h\nu, \tag{14}$$

the zero-point energy.

Let a set of normal coordinates be defined by

$$\left.\begin{aligned} \xi_1 &= \tfrac{1}{\sqrt{2}}(x_1 + x_2) & \xi_2 &= \tfrac{1}{\sqrt{2}}(x_1 - x_2) \\ \eta_1 &= \tfrac{1}{\sqrt{2}}(y_1 + y_2) & \eta_2 &= \tfrac{1}{\sqrt{2}}(y_1 - y_2) \\ \zeta_1 &= \tfrac{1}{\sqrt{2}}(z_1 + z_2) & \zeta_2 &= \tfrac{1}{\sqrt{2}}(z_1 - z_2) \end{aligned}\right\} \tag{15}$$

The expression for V then becomes, in terms of the normal coordinates:

$$V = \frac{e^2}{2\alpha}\left[\left(1+\frac{\alpha}{R^3}\right)(\xi_1^2+\eta_1^2)+\left(1-\frac{\alpha}{R^3}\right)(\xi_2^2+\eta_2^2)\right.$$
$$\left.+\left(1-2\frac{\alpha}{R^3}\right)\zeta_1^2+\left(1+2\frac{\alpha}{R^3}\right)\zeta_2^2\right]. \qquad (16)$$

This is the potential energy for a set of six independent harmonic oscillators, each with its own characteristic frequency. The zero-point energy of each oscillator is obtained from Eq. (14), and the total energy of the system is given simply by the sum of the individual energies. The frequencies are:

$$\left.\begin{aligned}
\nu_{1,2} &= \frac{e}{\sqrt{m\alpha}}\sqrt{1+\frac{\alpha}{R^3}} = \frac{e}{\sqrt{m\alpha}}\left(1+\frac{\alpha}{2R^3}-\frac{\alpha}{8R^6}+\cdots\right)\\
\nu_{3,4} &= \frac{e}{\sqrt{m\alpha}}\sqrt{1-\frac{\alpha}{R^3}} = \frac{e}{\sqrt{m\alpha}}\left(1-\frac{\alpha}{2R^3}-\frac{\alpha}{8R^6}+\cdots\right)\\
\nu_5 &= \frac{e}{\sqrt{m\alpha}}\sqrt{1-2\frac{\alpha}{R^3}} = \frac{e}{\sqrt{m\alpha}}\left(1-\frac{\alpha}{R^3}-\frac{\alpha}{2R^6}+\cdots\right)\\
\nu_6 &= \frac{e}{\sqrt{m\alpha}}\sqrt{1+2\frac{\alpha}{R^3}} = \frac{e}{\sqrt{m\alpha}}\left(1+\frac{\alpha}{R^3}-\frac{\alpha}{2R^6}+\cdots\right)
\end{aligned}\right\} \qquad (17)$$

where m is the reduced mass of each of the two elastic systems. The lowest energy state of the entire system is then

$$\begin{aligned}
E &= \frac{h\nu_0}{2}\left[2\nu_{1,2}+2\nu_{3,4}+\nu_5+\nu_6\right]\\
&= \frac{h\nu_0}{2}\left[6-(1-1-1+1)\frac{\alpha}{R^3}-\left(\frac{1}{4}+\frac{1}{4}+\frac{1}{2}+\frac{1}{2}\right)\frac{\alpha^2}{R^6}+\cdots\right]\\
&= 3h\nu_0-\frac{3}{4}h\nu_0\frac{\alpha^2}{R^6}+\cdots
\end{aligned} \qquad (18)$$

where $\nu_0 = e/\sqrt{m\alpha}$ is the proper frequency of the two elastic systems when not interacting (i. e., for $R \to \infty$).

The first term in Eq. (18) is a constant representing the combined zero-point energy of the two isolated elastic systems and does not contribute to the force between them. The second term,

$$U = -\frac{3}{4} h \nu_0 \frac{\alpha^2}{R^6}, \tag{19}$$

does represent an attractive force varying as the inverse seventh-power of the separation of the molecules. This is the force named by London the "dispersion force".

The above derivation follows along the lines of the discussion in London's paper cited previously. In the same paper a more rigorous derivation is also given, using a quantum-mechanical model of a molecule. An argument is also presented to show that the dispersion forces are additive, at least to a first approximation; i.e., that in the case of a large number of molecules the dispersion force between any given pair may be calculated independently of the presence of the other molecules.

Eq. (19) gives the dispersion force between two molecules of the same kind. The corresponding result for two dissimilar molecules is

$$U = -\frac{3}{2} h \frac{\nu_1 \nu_2}{\nu_1 + \nu_2} \frac{\alpha_1 \alpha_2}{R^6}. \tag{20}$$

3. Repulsive Forces

It is obvious that, in addition to the forces of attraction, there must also be forces of repulsion acting between molecules. Otherwise all the molecules and atoms in the world would rapidly coalesce into a single gigantic molecule. These repulsive forces have a much shorter range than the forces of attraction and are considerably more difficult to analyze and determine quantitatively. They arise primarily through the overlapping of the electron clouds of the two molecules or atoms. As a result of this overlapping, the nuclei are no longer completely screened and repel each other through the Coulomb forces between their positive charges. An additional effect arises from the Pauli exclusion principle which requires, as the overlapping starts, that energy be supplied externally in the approach of the molecules.

A quantitative treatment of the repulsive forces has been attempted by a number of workers. In many cases these attempts take the form of assuming a particular mathematical model for the intermolecular potential (including the attractive part) and using experimental data to evaluate the various constants involved by curve-fitting methods. Below are listed some of the most commonly employed forms*:

(a) Lennard-Jones Potential

$$U = 4\epsilon\left[\left(\frac{\sigma}{R}\right)^{12} - \left(\frac{\sigma}{R}\right)^{6}\right] \qquad (21)$$

* J. O. Hirschfelder, et al, Molecular Theory of Gases and Liquids, Wiley 1954

(b) Buckingham Potential

$$U = b e^{-aR} - \frac{C}{R^6} - \frac{C'}{R^8} \tag{22}$$

(c) Buckingham-Corner Potential

$$U = \begin{cases} b e^{-\alpha R/R_m} - \left(\frac{C}{R^6} + \frac{C'}{R^8}\right) e^{-4\left(\frac{R}{R_m}-1\right)^3} & R \le R_m \\ b e^{-\alpha R/R_m} - \left(\frac{C}{R^6} + \frac{C'}{R^8}\right) & R > R_m \end{cases} \tag{23}$$

(d) Modified Buckingham Potential

$$U = \begin{cases} \frac{\epsilon}{1-\frac{6}{\alpha}} \left[\frac{6}{\alpha} e^{\alpha\left(1-\frac{R}{R_m}\right)} - \left(\frac{R_m}{R}\right)^6\right] & R \ge R_m \\ \infty & R < R_m \end{cases} \tag{24}$$

The first of these forms, the Lennard-Jones potential, lends itself most readily to analytical investigations. The choice of the inverse twelfth power of the distance as the form of the repulsive potential is made as much for mathematical convenience as for any other reason, and for some substances a better fit to experimental data is obtained with a different power. The Lennard-Jones potential gives a fairly relaistic approximation to the forces between spherical non-polar molecules.

The Buckingham potential includes an inverse eighth-power in the attractive potential to account for the induced-dipole-induced-quadrupole interaction,

which may be of importance for highly non-symmetrical molecules. It also replaces the inverse twelfth-power repulsive potential with an exponential term which, according to London*, gives a quantum-mechanically more correct representation. However, the Buckingham potential approaches $-\infty$ at the origin ($R = 0$), which is certainly incorrect.

The Buckingham-Corner potential alleviates the unrealistic behavior of the Buckingham formula close to the origin. It is more complicated than the latter, since it contains an extra factor and also since two functionally different forms are used for different ranges of R.

The modified Buckingham potential, finally, is a four-parameter form which is somewhat more flexible than the Lennard-Jones potential and by which the effect of the induced-dipole-induced-quadrupole interaction can be taken into account by a suitable choice of the constant α .

Of the constants involved in these various approximations to the intermolecular potentials, some are calculated from the known values of other molecular constants (e. g., the coefficient of R^{-6} in the dispersion formula), and some are determined backwards from comparisons between theoretical predictions made on the basis of a particular model and experimental results (e. g., pressure broadening and the equation of state of a real gas).

In the applications to be made later in this section to adhesive bond strengths, the Lennard-Jones 6-12 potential will be used. It is by far

---

* F. London, ibid.

the simplest to use analytically, and by a suitable choice of the constants this function can be made to represent the intermolecular forces reasonably faithfully over the range of distances in which the adhesive forces have their greatest effect.

4. Retardation Effects

So far in this discussion of the intermolecular forces it has been assumed that the interaction between a pair of molecules depends only on the instantaneous relative positions of the two molecules. Even in cases where the force depends for its very existence on the variation with time of the states of the molecules, such as the dispersion effect which would not exist if it were not for the zero-point motions of the electrons, the effect of the state of one molecule on the other is calculated as if this effect were felt instantaneously by the other molecule. In actual fact, of course, electromagnetic interactions are propagated with the speed of light, which is large but finite. In the case of the dispersion effect, this will introduce phase lags between the induced dipole and the time-varying dipole giving rise to it. The question then arises of the effect of this phase lag on the interaction energy of the two molecules and hence on their mutual forces.

This problem has been investigated by, among others, Casimir and Polder*.

* H. B. G. Casimir and D. Polder, Phys. Rev. 73, 360(1938)

Their treatment, which is based on quantum electrodynamics, is quite and only the results pertinent to this discussion will be quoted here. The general result is that the retardation reduces the interaction, the relative effect being greater at greater distances. For the interaction of two identical neutral non-polar molecules, Casimir and Polder found for small distances the usual London dispersion formula, Eq. (19), whereas for large distances they derived a correction factor g of the general shape shown in Figure 2.

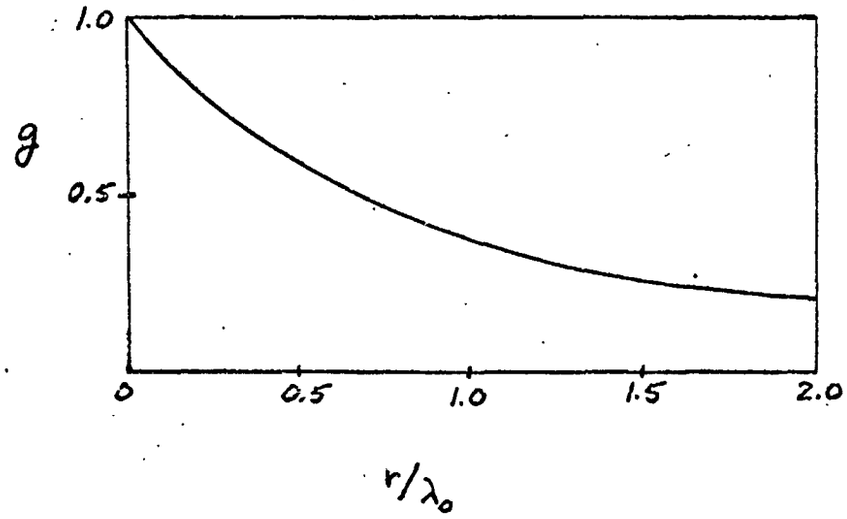

Figure 2 VARIATION OF g WITH DISTANCE

The constant λ_0 is a characteristic length defined by

$$\lambda_0 = \frac{c}{\nu_0}, \tag{25}$$

where ν_0 is the frequency of the harmonic oscillator representing the molecule. In most cases, λ_0 is of the order of 10^3 Å of 10^{-5} cm. For small molecules, the effective range of interaction is a few Å; hence retardation effects are unimportant for this case. For larger molecules or high polymers, the range of interaction may be a considerable fraction of λ_0. In these cases, the effect of retardation may have to be taken into account.

For the purposes of calculating adhesive bond strengths, the retardation effects will be ignored, at least for the preliminary calculations. It is felt that in most cases these effects represent corrections of a magnitude that will be masked by the errors introduced as a result of the simplifying assumptions made in the choice of the mathematical model.

5. General Remarks

As indicated above, the attractive forces between relatively simple, non-polar molecules are reasonably well understood and are in many cases amenable to direct calculations using well-known molecular constants. These forces are expressed as functions of the distance between the molecules and, possibly, on their relative orientation. When dealing with the interaction between large or highly asymmetrical molecules separated by distances of about the same order of magnitude as the size of the molecules, the problem is considerably more complicated. A treatment of the interaction between

molecules of a variety of different shapes and orientations is given by Hirschfelder et al*. The treatment is entirely quantum-mechanical. No attempt will be made to quote all the results, since they will not be used in the bond-strength calculations in Part II.

In addition to the intermolecular forces described above, there are the so-called reasonance forces, which are of purely quantum-mechanical origin and have no classical analogue. They arise basically when degeneracies in the wave functions of two molecules are removed through their interaction. The forces may be either repulsive or attractive. A short treatment of the resonance forces may be found in the above reference by Hirschfelder et al.

---

* J. O. Hirschfelder, et al, ibid.

PART II APPLICATIONS

1. Introduction

In this section, the theory developed above will be applied to obtain analytical expressions for the strength of an adhesive bond, and these expressions will be used to obtain numerical results for a number of adhesives and adherends. The treatment will be limited to substances with spherical, non-polar molecules. The only forces operating between the molecules are then of the London dispersion-force type, provided there is no chemical bond, and the repulsive forces. It might seem that this would exclude precisely the main problem at hand in this study, namely the bonding of epoxy resins to aluminum surfaces, since these resins are high polymers with molecules that are anything but spherical. However, the theory of the forces between such molecules is extremely difficult and far from complete. One approach to this problem is to break up a long chain-type molecule into suitable subsections, and to consider the individual interaction of each with the other parts of the same molecule as well as with similar segments of other molecules. The over-all theoretical situation in this area is rather unclear, and at present it is not possible to predict, on a purely theoretical basis, with any degree of accuracy, the bond strength of a joint utilizing a polymer-type adhesive. Nevertheless, analyses based on idealized molecular models are of considerable alue, since they help to point out general features, the way the important physical parameters enter in, and so forth. It is primarily with this objective in mind that the analyses given below are presented.

2. Adhesion Between Two Semi-Infinite Media

Let a Cartesian coordinate system be defined so that the x y plane constitutes the boundary between two media occupying the half-spaces above and below this plane (see Figure 3).

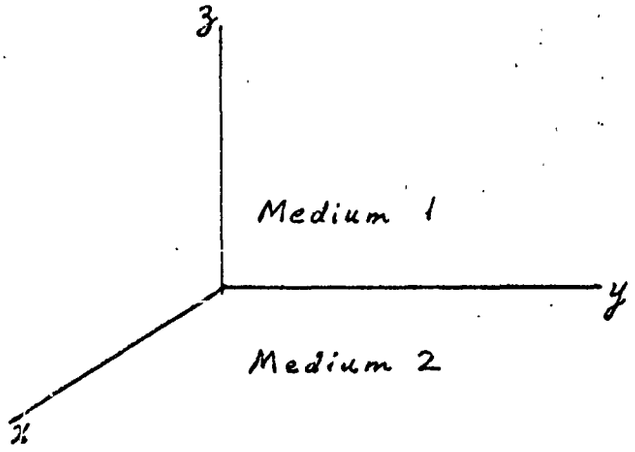

Figure 3 BASIC GEOMETRY

The two media are not supposed in actual contact but separated by a small distance δ in such a way that the boundary of Medium 1 is the plane $z = \delta$ while that of Medium 2 is $z = 0$.

Now consider a volume element $dV_1 = dx\ dy\ dz$ of Medium 1 and its interaction with a volume element dV_2 of Medium 2 in the form of a ring of radius r, thickness dr, and height $d\xi$ (see Figure 4).

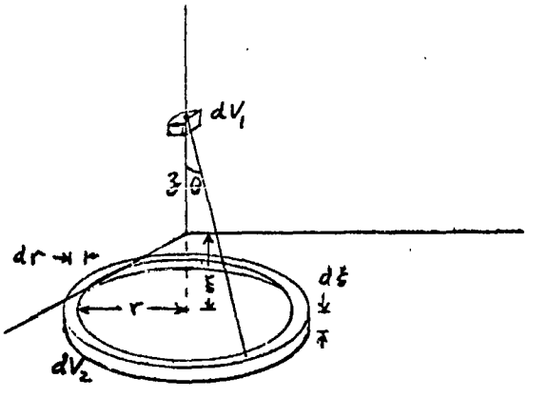

Figure 4 INTERACTION GEOMETRY

Let N_1, N_2 be the number of molecules per unit volume of the two media, respectively. Then the number of molecules in dV_1 is $N_1\,dx\,dy\,dz$, and that in dV_2 is $2\pi N_2\, r\, dr\, d\xi$. The distance between dV_1 and any point of dV_2 is given by

$$S = \left[(\zeta + \xi)^2 + r^2\right]^{1/2} = (\zeta + \xi)\sec\theta$$

Let the interaction energy between a molecule of Medium 1 and one of Medium 2 be of the form (Lennard-Jones 6-12 potential):

$$\phi = \frac{C_R}{R^{12}} - \frac{C_A}{R^6} \tag{26}$$

where R is the distance. The interaction energy between dV_1 and dV_2 is then

$$d^5\phi = 2\pi N_1 N_2 \left(\frac{C_R}{S^{12}} - \frac{C_A}{S^6}\right) r\, dr\, d\xi\, dx\, dy\, dz$$

$$= 2\pi N_1 N_2 \left[\frac{C_R \cos^{12}\theta}{(z+\xi)^{12}} - \frac{C_A \cos^6\theta}{(z+\xi)^6}\right]$$

$$\times (z+\xi)\tan\theta\,(z+\xi)\sec^2\theta\, d\theta\, d\xi\, dx\, dy\, dz$$

$$= 2\pi N_1 N_2 \left[\frac{C_R \cos^9\theta}{(z+\xi)^{10}} - \frac{C_A \cos^3\theta}{(z+\xi)^4}\right] \sin\theta\, d\theta\, d\xi\, dx\, dy\, dz.$$

The force acting on dV_1 due to dV_2 is

$$d^5 f = -\frac{\partial}{\partial z}(d^5\phi)$$

$$= 2\pi N_1 N_2 \left[10\frac{C_R \cos^9\theta}{(z+\xi)^{11}} - 4\frac{C_A \cos^3\theta}{(z+\xi)^5}\right] \sin\theta\, d\theta\, d\xi\, dx\, dy\, dz.$$

The force on dV_1 due to an infinite sheet of Medium 2 of thickness $d\xi$ is obtained by integrating the above expression over θ:

$$d^4 f = \int_0^{\pi/2} \frac{d^5 f}{d\theta}\, d\theta = 2\pi N_1 N_2 \left[-\frac{C_R \cos^{10}\theta}{(z+\xi)^{11}} + \frac{C_A \cos^4\theta}{(z+\xi)^5}\right]_0^{\pi/2} d\xi\, dx\, dy\, dz$$

$$= 2\pi N_1 N_2 \left[\frac{C_R}{(z+\xi)^{11}} - \frac{C_A}{(z+\xi)^5}\right] d\xi\, dx\, dy\, dz.$$

Finally, the force on dV_1 due to the entire half-space of Medium 2 is obtained by integrating this expression over ξ :

$$d^3f = \int_0^{-\infty} \frac{d^4f}{d\xi}\, d\xi = 2\pi N_1 N_2 \left[-\frac{C_R}{10(z+\xi)^{10}} + \frac{C_A}{4(z+\xi)^4} \right]_0^{-\infty} dx\, dy\, dz$$

$$= \frac{\pi}{10} N_1 N_2 \left(2\,\frac{C_R}{z^{10}} - 5\,\frac{C_A}{z^4} \right) dx\, dy\, dz.$$

The coefficient of dV_1 gives the force per unit volume of Medium 1 exerted by Medium 2. The quantity of interest is the force per unit area; i.e., the pressure at the interface. This may be obtained by integrating the volume force density along a column of cross-sectional area $dA = dx\, dy$ perpendicular to the xy plane from $z = \delta$ to $z = \infty$ and dividing by dA:

$$p = \int_\delta^\infty \frac{d^3f}{dx\,dy}\, dz = \frac{\pi}{10} N_1 N_2 \left[-\frac{2}{9}\,\frac{C_R}{z^9} + \frac{5}{3}\,\frac{C_A}{z^3} \right]_\delta^\infty \qquad (27)$$

$$= \frac{\pi}{90} N_1 N_2 \left(2\,\frac{C_R}{\delta^9} - 15\,\frac{C_A}{\delta^3} \right).$$

In the derivation of this result the two media have been treated as if they were continuous rather than as discrete collections of molecules. A more exact treatment would replace the various integrals by sums over all the molecules. This would require an exact knowledge of the geometrical arrangement of the molecules in both adhesive and adherend. The summation is also much more difficult to perform than the integration. Since the purpose of the analysis is primarily to bring out important parameters and to obtain order-of-magnitude results, it is felt that the errors introduced by the assumption of continuous media may be neglected.

3. Adhesion Between Two Plates

Under the assumptions made, Eq. (27) gives the force per unit area with which two semi-infinite media, interacting via the Lennard-Jones (1-12) potential, attract each other. The question now arises as to the corresponding result in the case of two plates of finite area and thickness. A little reflection shows that Eq. (27) should hold even for this case with an altogether negligible error. To be sure, the integrations involved in arriving at this formula were carried out over all space. Nevertheless, due to the extremely rapid fall-off of the intermolecular forces with distance, almost all of the adhesive force is due to the molecules in the immediate vicinity of the interface. Therefore, Eq. (27) will be taken to be the correct expression for the force of adhesion between two sheets of adhering substances.

4. Bond Strength of Two Adhering Plates

On the basis of the preceding analysis, the strength of the bond between two adhering plates will now be calculated. It must be noted that this bond strength is not given by Eq. (27). This formula gives the force which two slabs of adhering material, separated by an arbitrary distance δ, exert on each other. On the other hand, the strength of an adhesive bond is by definition the force which has to be exerted to pull the two materials apart. These are not the same thing. If the two materials are free to move under their mutual attractive (and repulsive) forces, they will seek a separation distance such that the attractive force is just balanced by the repulsive one and the total force vanishes. This distance δ_o may be obtained by

equating the right-hand side of (27, to zero and solving for δ .

At the separation δ_0 , the force between the two slabs is zero. If one tries to separate them, restoring forces arise which reach a maximum at some separation δ_m and then decay to zero as $\delta \to \infty$. The strength of the bond is thus the value of p at $\delta = \delta_m$. To obtain δ_m , Eq. (27) is differentiated with respect to δ and the result is set equal to zero:

$$\frac{dp}{d\delta} = \frac{\pi}{10} N_1 N_2 \left(2 \frac{C_R}{\delta^{10}} - 5 \frac{C_A}{\delta^4} \right) = 0 ;$$

$$\therefore \quad \delta_m = \left(\frac{2}{5} \frac{C_R}{C_A} \right)^{1/6} . \tag{28}$$

The bond strength is now obtained by substituting from Eq. (28) into (27):

$$p_m = \frac{\pi}{90} N_1 N_2 \left(2 \frac{C_R}{\delta_m^9} - 15 \frac{C_A}{\delta_m^3} \right)$$

$$= \frac{\pi}{90} N_1 N_2 \left(\frac{5}{2} \frac{C_A}{C_R} \right)^{1/3} \left(2 C_R \frac{5}{2} \frac{C_A}{C_R} - 15 C_A \right) = -\frac{\pi}{9} N_1 N_2 \left(\frac{5}{2} \frac{C_A}{C_R} \right)^{1/2} C_A . \tag{29}$$

An alternative form for p_m may be obtained by solving Eq. (27) for C_R with $\delta = \delta_0$, the distance at which p = 0:

$$p_{\delta = \delta_0} = \frac{\pi}{90} N_1 N_2 \left(2 \frac{C_R}{\delta_0^9} - 15 \frac{C_A}{\delta_0^3} \right) = 0 ;$$

$$\therefore \quad C_R = \frac{15}{2} \delta_0^6 C_A$$

Hence

$$p_m = -\frac{\pi}{9} \left(\frac{1}{3} \right)^{1/2} \frac{N_1 N_2}{\delta_0^3} C_A . \tag{30}$$

From Eq. (20), the expression for C_A is

$$C_A = \frac{3}{2} h \frac{\nu_1 \nu_2}{\nu_1 + \nu_2} \alpha_1 \alpha_2 .$$

Substituting this into (30) yields

$$P_m = \frac{\pi}{6}\left(\frac{1}{3}\right)^{1/2} h \frac{\nu_1 \nu_2}{\nu_1 + \nu_2} \alpha_1 \alpha_2 \frac{N_1 N_2}{\delta_o^3} . \qquad (31)$$

Now, the quantity $h\nu$ is, in most cases, approximately equal to the ionization potential of the molecule in question*. Hence, setting $h\nu_1 = I_1$, $h\nu_2 = I_2$, Eq. (31) becomes

$$P_m = \frac{\pi}{6}\left(\frac{1}{3}\right)^{1/2} \frac{I_1 I_2}{I_1 + I_2} \alpha_1 \alpha_2 \frac{N_1 N_2}{\delta_o^3} . \qquad (32)$$

This gives an expression for the adhesive bond strength in terms of the fundamental molecular constants $I_1, I_2, \alpha_1, \alpha_2$, the densities N_1, N_2 and the separation of adhesive and adherend δ_o. The quantity δ_o is, strictly speaking, a function of the thicknesses of the slabs of adhesive and adherend. However, due to the extremely rapid fall-off of the intermolecular forces the variation is very slight, and in this discussion δ_o will be treated as a constant. An exact determination of δ_o is still very difficult, however. This difficulty is immediately traced to the fact that δ_o was introduced to eliminate C_R from Eq. (29). This merely substituted one unknown quantity for another, since C_R, as discussed in Part I, is very difficult to determine theoretically. Nevertheless, a reasonable estimate

---

* S. J. Czyzak, Adhesion and Adhesives: Fundamentals and Practice, Wiley 1954

of δ_o may be obtained as follows. Let a_1 and a_2 be the intermolecular distances in the two media, respectively. The number of molecules per unit volume N_1 and N_2 are then connected with a_1, a_2 by the approximate relations

$$N_1 \cong a_1^{-3}, \quad N_2 \cong a_2^{-3} .$$

The equality is exact if the molecules are arranged in cubical lattices with a molecule at each corner of every cube. In any case, the products $a_1^3 N_1$ and $a_2^3 N_2$ are of the order of unity, whatever the molecular arrangement, and hence one may assume approximately that the following relations hold:

$$a_1 = N_1^{-1/3}, \quad a_2 = N_2^{-1/3} .$$

Now, a_1 represents, esentially, the equilibrium distance of two molecules of Medium 1, i. e., the distance at which the repulsive and attractive forces just cancel, and similarly for a_2. It would therefore seem to be a reasonable assumption that the equilibrium distance δ_o between the adhesive and adherend is approximately equal to the average of a_1 and a_2, i. e.,

$$\delta_o = \tfrac{1}{2}(a_1 + a_2) .$$

In terms of N_1 and N_2, this becomes

$$\delta_o = \frac{1}{2}\left(\frac{1}{N_1^{1/3}} + \frac{1}{N_2^{1/3}}\right) = \frac{N_1^{1/3} + N_2^{1/3}}{2 N_1^{1/3} N_2^{1/3}} .$$

Substituting this into Eq. (32) yields

$$\phi_m = \frac{4}{3}\pi\left(\frac{1}{3}\right)^{1/2} \frac{I_1 I_2}{I_1 + I_2} \alpha_1 \alpha_2 \frac{N_1^2 N_2^2}{(N_1^{1/3} + N_2^{1/3})} . \qquad (33)$$

This expression gives the strength of an adhesive bond in terms of quantities available in tabular form for a variety of substances.

It is of some interest to determine δ_m, the value of δ at which $p = p_m$. From Eq. (28) and the equation preceding (30), one obtains

$$\delta_m = \left(\frac{2}{5} \times \frac{15}{2} \delta_0^6 C_1 \times \frac{1}{C_1}\right)^{1/6} = (3)^{1/6} \delta_0 = 1.20\, \delta_0 .$$

Hence the maximum restoring force is obtained when the separation is increased by only 20%. This bears out what was said previously regarding the rate of fall-off of the intermolecular forces with distance and justifies the various assumptions and approximations made on this basis.

5. Cohesive Strength due to Dispersion Force

On the basis of Eq. (33), the cohesive strength of a material may be determined, assuming that the dispersion force is alone responsible for the cohesive force. With $I_1 = I_2 = I$, $\alpha_1 = \alpha_2 = \alpha$, $N_1 = N_2 = N$, Eq. (33) becomes

$$p_c = \frac{\pi}{12}\left(\frac{1}{3}\right)^{1/2} I \alpha^2 N^3 = 0.151\, I \alpha^2 N^3 . \qquad (34)$$

This result will be used below to calculate the cohesive strength of aluminum.

6. Numerical Results

As a first application of the above analysis, the cohesive strength of aluminum will be calculated, using Eq. (34). From the Handbook of Chemistry and Physics, $I = 5.96$ ev $= 9.55 \times 10^{-12}$ ergs. The mass density is given by the same source as $\rho = 2.699$ gm/cm^3. Since the atomic weight is 26.97 and

hence the mass of an aluminum atom is $26.97 \times 1.66 \times 10^{-24}$ gm $= 4.47 \times 10^{-23}$ gm, the number of atoms per cm^3 is

$$N = \frac{2.699 \text{ gm/cm}^3}{4.47 \times 10^{-23} \text{ gm}} = 6.03 \times 10^{22} \text{ cm}^{-3}.$$

The molecular polarizability α is not readily available from tables except for a few elements and compounds. It can be estimated in several ways. According to Jackson*, α is of the order of the molecular or atomic volume (in the Gaussian system of units). Let σ be the radius of the aluminum atom. Thus, by the above assumption

$$\alpha = \frac{4}{3}\pi\sigma^3.$$

From the Handbook of Chemistry and Physics, the value of σ may be taken as $0.5\ \text{Å} = 5 \times 10^{-9}$ cm; hence,

$$\alpha = \frac{4}{3}\pi \times 1.25 \times 10^{-25} \text{ cm}^3 = 5.24 \times 10^{-25} \text{ cm}^3.$$

Another way of estimating α is to use the Clausins-Mosotti relation which is given by Jackson as

$$\alpha = \frac{3}{4\pi N}\frac{\epsilon - 1}{\epsilon + 2},$$

where ϵ is the dielectric constant. Although this relation holds best for gases and is less exact for liquids and solids, it may be used to ascertain the order of magnitude of α. The Handbook of Chemistry and Physics gives $\epsilon = 2.4$. Hence

$$\alpha = \frac{3}{4\pi \times 6.03 \times 10^{22}}\frac{1.4}{4.4} = 1.26 \times 10^{-24} \text{ cm}^3.$$

---

* J. D. Jackson, Classical Electrodynamics, Wiley 1962

Using the value of α obtained by the first method in Eq. (34), the cohesive strength is

$$p_c = 0.151 \times 9.55 \times 10^{-12} \text{ ergs} \times 2.75 \times 10^{-49} \text{ cm}^6 \times 2.19 \times 10^{68} \text{ cm}^{-9}$$

$$= 8.68 \times 10^{7} \text{ dyne cm}^{-2} = 1.26 \times 10^{3} \text{ psi.}$$

With the value of α from the Clausius-Mosotti relation, the corresponding result is

$$p_c = 0.151 \times 9.55 \times 10^{-12} \times 1.587 \times 10^{-48} \times 2.19 \times 10^{68}$$

$$= 5.01 \times 10^{8} \text{ dyne cm}^{-2} = 7.25 \times 10^{3} \text{ psi.}$$

Comparing either of these two values of p_c with the tensile yield strength of aluminum which is approximately 2×10^5 psi, it is clear that the dispersion force plays a minor role in the cohesive strength of aluminum.

As a second example, consider the bonding of aluminum to some adhesive. For aluminum, the following values of ionization potential, polarizability, and density will be used:

$$I_1 = 9.55 \times 10^{-12} \text{ erg}, \quad \alpha_1 = 1.26 \times 10^{-24} \text{ cm}^3, \quad N_1 = 6.03 \times 10^{22} \text{ cm}^{-3},$$

For the adhesive, the following typical large-molecule values will be used:

$$I_2 = 2 \times 10^{-11} \text{ 34g}, \quad \alpha_2 = 2.5 \times 10^{-24} \text{ cm}^3, \quad N_2 = 3 \times 10^{22} \text{ cm}^{-3},$$

These values are to be inserted into Eq. (33). The calculation is most conveniently performed in several steps:

$$N_1^{1/3} + N_2^{1/3} = 3.92 \times 10^{7} \text{ cm}^{-1} + 3.15 \times 10^{7} \text{ cm}^{-1} = 7.07 \times 10^{7} \text{ cm}^{-1}$$

$$\frac{N_1^2 \, N_2^2}{(N_1^{1/3}+N_2^{1/3})^3} = \frac{3.63 \times 10^{45} \text{ cm}^{-6} \times 9 \times 10^{44} \text{ cm}^{-6}}{3.53 \times 10^{23} \text{ cm}^{-3}} = 9.26 \times 10^{66} \text{ cm}^{-9}$$

$$\frac{I_1 I_2}{I_1 + I_2} = \frac{1.91 \times 10^{-22} \text{ erg}^2}{2.96 \times 10^{-11} \text{ erg}} = 6.45 \times 10^{-12} \text{ erg}$$

$$\alpha_1 \alpha_2 = 3.15 \times 10^{-48} \text{ cm}^6$$

$$\frac{4}{3}\pi \left(\frac{1}{3}\right)^{1/2} = 2.42$$

$$\therefore \; p_m = 2.42 \times 6.45 \times 10^{-12} \times 3.15 \times 10^{-48} \times 9.26 \times 10^{66}$$

$$= 4.55 \times 10^{8} \text{ dyne cm}^{-2} = 6.59 \times 10^{3} \text{ psi.}$$

The measured strength of bonds between epoxy resins and aluminum is generally in the range 5 - 10 x 10^3 psi. The analysis presented here thus appears to give correct order-of-magnitude results. More exact agreement cannot be expected from this simple treatment when applied to such complex polymeric adhesive substances as the epoxy resins.

7. Conclusions

The preceding analysis determines the force of adhesion between two sheets of materials assumed to be ideally flat and assuming also that the molecules of the two media interact only via the Lennard-Jones (6-12) potential. The analysis is of value in that it brings out the important physical parameters

entering into the bond strength, such as the polarizability and ionization potential. On this basis the superior bonding quality of aluminum oxide over that of pure aluminum, for example, can be understood, as both the polarizability and ionization potential of an aluminum oxide molecule are larger than those of an aluminum atom.

On the other hand, the analysis does not take into account the deviations from ideal conditions which adversely affect the bond strength. For example, the bonding surfaces may not be absolutely flat, resulting perhaps in insufficient contact between adhesive and adherend. High humidity conditions may result in the deposition of a layer of water molecules on the bonding surfaces. Since the cohesive strength of water is almost zero, this will obviously reduce the bond strength. Other factors affecting bond strength are improper wetting of the adherend by the adhesive, bond-line impurities, and static charge in the bond-line. A quantitative correlation between such factors and the bond strength is perhaps best obtained empirically.

BIBLIOGRAPHY

1. J. C. Slater, Quantum Theory of Matter, McGraw-Hill 1951.
2. F. London, Trans. Farady Soc. 33, 8 (1937).
3. W. H. Keeson, Physik. Zeitschrift 22, 129 (1921).
4. P. Debye, Physik. Zeitschrift 21, 178 (1920).
5. J. O. Hirschfelder, C. F. Curtiss, and R. B. Bird, Molecular Theory of Gases and Liquids, Wiley 1954.
6. H. B. G. Casimir and D. Polden, Phys. Review 73, 360 (1938).
7. S. J. Czyzak, Adhesion and Adhesives: Fundamentals and Practice, Wiley 1954.
8. J. D. Jackson, Classical Electrodynamics, Wiley 1962.

APPENDIX 2

ENVIRONMENTAL TEST CONDITIONS

TEST REPORT

6401 OAKTON STREET • MORTON GROVE, ILLINOIS

Report No. 551194

DESCRIPTION OF TEST:

HIGH VACUUM

Requirements:

The test samples shall exhibit no visible evidence of physical damage or bond deterioration as a result of the test described below.

Test Procedure:

Eight (8) test samples, described below, were placed on a cold plate in an ultra-high chamber, at room ambient conditions.

Flat Plates	Honey-comb Structures
D-24	B-35
CE-22	A-89
BE-31	C-30
AE-79	D-23

The chamber was sealed, the vacuum pump turned on, and the start time noted. After two (2) hours of pumping, pressure and temperature were recorded, and liquid nitrogen flow through the cold plate was started. Twenty-four (24) hours after the start of pumping, pressure and temperature were recorded. This data recording was repeated at 5-minute intervals for a 15-minute period. The chamber was returned to ambient conditions, and the samples were removed and visually examined.

The test described above was repeated on nine (9) other test samples, described below, with the following exceptions:

(a) Liquid nitrogen flow was started after the chamber pressure started to level off with respect to time.

(b) The final 5-minute data-interval period was 120 minutes.

Flat Plates	Honey-comb Structures	Cylinder Block
D-25	C-29	—
AE-80	A-90	
BE-27	D-22	
CE-23	B-38	

GENERAL DATA SHEET

TYPE PAR.

Ultra-High Vacuum #1

TEST NO
551194

-320°F and Highest Vacuum

DATE
5/17/65

MATERIAL
Eight (8) Metal Samples

AMB TEMP RH
21.1°C 48%

MANUFACTURER
MRD Division, General American Transportation Corp.

W NO

TESTED BY
F. Wegrzyn

LAB SUP CHECK

ENGRG CHECK
C. Elliott

Time	Pressure	Temperature	Date	Event
0925	Sea Level	+77°F	5/17/65	Start pumping
11:25	2.8×10^{-5}	+77°F	5/17/65	Start LN_2 Flow
09:25	2.0×10^{-6}	-279°F	5/18/65	Begin record period
09:30	9.8×10^{-7}	-287°F	5/18/65	+5 min.
09:35	2.0×10^{-6}	-288.5°F	5/18/65	+10 min.
09:40	1.5×10^{-6}	-297.5°F	5/18/65	+15 min. End record period.

Visual examination on the samples showed external damage or parting in the adhesives from the metals.

D-24	B-35
CE-22	A-89
BE-31	C-30
AE-79	D-23
Flat Plates	Honey Combs

DESCRIPTION OF TEST:

Report No. 551194

HIGH VACUUM (Cont'd.)

Description of Test Apparatus:

Ultra-High Vacuum Chamber, ITL, M/N A-1035, S/N 135
Sea level to 1 x 10^{-8} mm. Hg, ±1%; last calibration: 12/30/65
Pumping speeds:
Mechanical pump, Type DK90, 53 cfm
Diffusion pump, Type PMC-144, 620 liters/second

Potentiometer, Minn.-Honeywell, M/N 126W3, S/N 345, 0-71 millivolts, ±0.5%; last calibration: 4/26/65

Thermometer, Cenco, M/N 19325-1, -20°C to +110°C, ±1%

Test Results:

No visible evidence of physical damage was noted on any of the test samples. See the data sheets for actual pressures and temperatures attained.

GENERAL DATA SHEET

TEST SPEC PAR

Ultra-High Vacuum #2

TEST NO.
551194

TEST CONDITIONS
-320°F and Highest Vacuum

DATE
5-20-65

MATERIAL
Nine (9) Metal Samples

TEMP RH
22.2°C 45%

MANUFACTURER
MRD Division, General American Transportation Corp.

MFR'S MAT'L

TESTED BY
F. Wegrzyn

LAB SUP CHECK

ENGR CHECK
C. Elliott

Time	Pressure	Temperature	Date	Event
10:00	Sea Level	+77°F	5/19/65	Start pumping
12:20	1.2×10^{-5}	+77°F	5/19/65	Start LN_2 Flow
10:00	1.3×10^{-6}	-298.7°F	5/20/65	Begin record period
10:05	9.2×10^{-7}	-298.5°F		+5 min.
10:10	9.0×10^{-7}	-298.2°F		+10 min.
10:15	8.0×10^{-7}	-298.2°F		+15 min.
10:20	7.0×10^{-7}	298.2°F		+20 min.
10:25	9.8×10^{-7}	299.4		+25 min.
10:30	1.0×10^{-6}	299.4		+30 min.
10:35	1.5×10^{-6}	302.8		+35 min.
10:40	7.2×10^{-7}	300.1		+40 min.
10:45	10×10^{-7}	299.4		+45 min.
10:50	9.9×10^{-6}	300.1		+50 min.
10:55	7.6×10^{-7}	299.4		+55 min.

GENERAL DATA SHEET

TEST
Ultra High Vacuum #2

SPEC

PAR:

TEST NO.
551194

CONDITIONS
-320°F at highest vacuum

DATE
5-20-65

MATERIAL
Nine (9) Metal Samples

TEMP RH.
23.3°C 43%

MANUFACTURER
MRD Division, General American Transportation Corp.

W NO.

INSTRUMENTS

TESTED BY
F. Wegrzyn

LAB SUP CHECK.

ENGRG CHECK
C. Elliott

Time	Pressure	Temperature	Date	Event
11:00	8.9×10^{-7}	-299.4	5-20-65	+60 min.
11:05	1.4×10^{-6}	-308.2		+65 min.
11:10	10×10^{-7}	302.7		+70 min.
11:15	8.6×10^{-7}	302.7		+75 min.
11:20	8.0×10^{-7}	300.1		+80 min.
11:25	9.8×10^{-7}	304.6		+85 min.
11:30	1.1×10^{-6}	308.2		+90 min.
11:35	1.2×10^{-6}	308.2		+95 min.
11:40	9.9×10^{-7}	302.7		+100 min.
11:45	9.9×10^{-7}	302.7		+105 min.
11:50	9.0×10^{-7}	304.6		+110 min.
11:55	8.2×10^{-7}	308.2		+115 min.
11:60	8.0×10^{-7}	308.2		+120 min.

GENERAL DATA SHEET

TEST: **Ultra High Vacuum #2 (cont'd)** | SPEC | PAR.

TEST NO: **551194**

CONDITIONING: **-320°F at highest vacuum**

DATE: **5-20-65**

MATERIAL: **Nine (9) Metal Samples**

TEMP: **23.3°C** RH: **43%**

MANUFACTURER: **MRD Division, General American Transportation Corp.**

M NO:

INSTRUMENTS

TESTED BY: **F. Wegrzyn**

LAB SUP CHECK:

ENGRG CHECK: **C. Elliott**

Visual examination of the samples showed no deterioration or damage to the bonding material.

Flat Plates	Honey Comb	Solid Block
D-25	C-29	-
AE-80	A-90	
BE-27	D-22	
CE-23	B-38	

APPENDIX 3

ULTRASONIC EMISSION TEST DATA

Metal to Metal Test
FM 1000 - Good Bond
bond failure at 11,932 psi

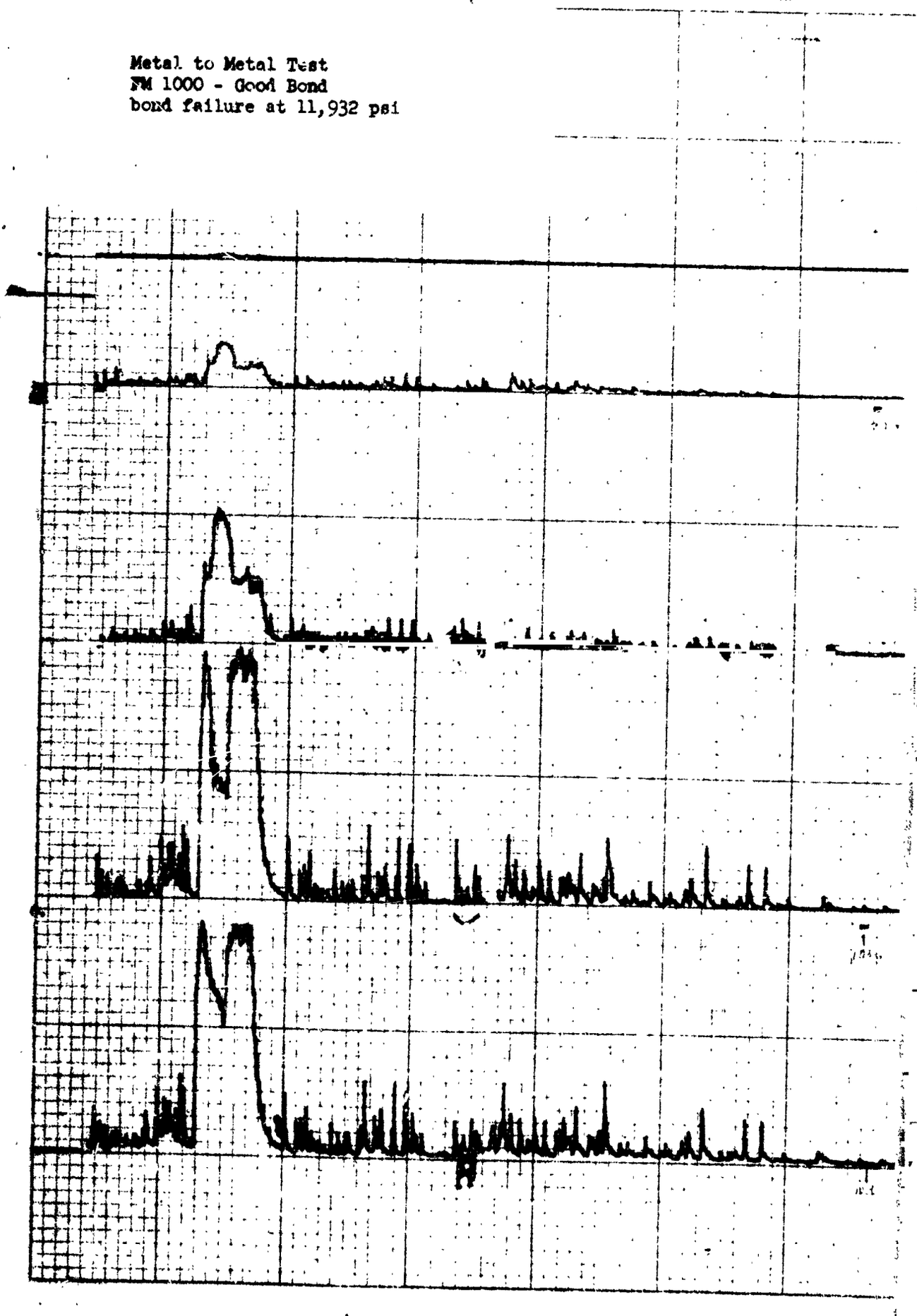

2

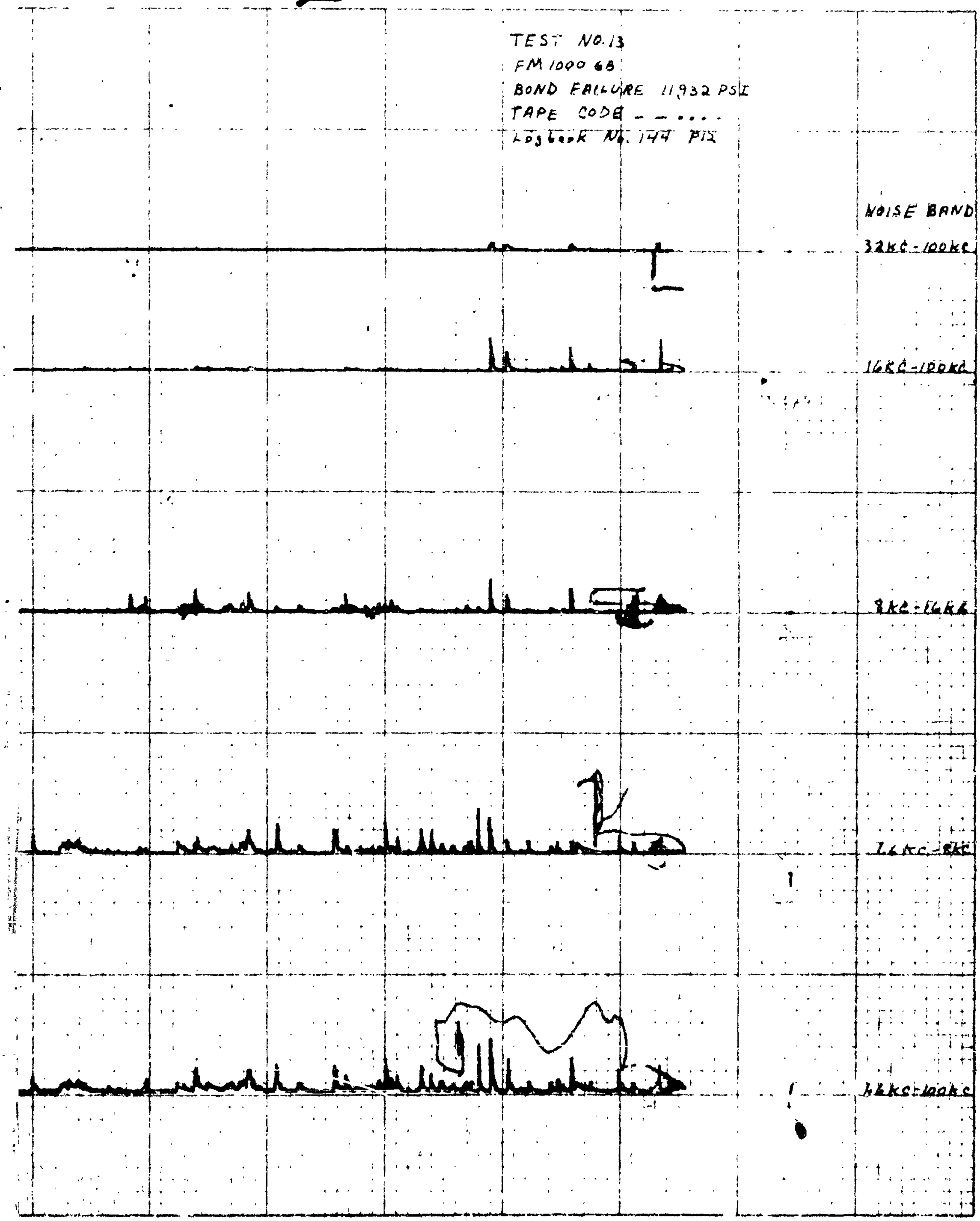

TEST NO. 13
FM 1000 6B
BOND FAILURE 11,932 PSI
TAPE CODE — — . . . .
Logbook No. 144 P12
NOISE BAND
32KC-100KC
16KC-100KC
8KC-16KC

Metal to Metal Test
FM 1000 -.10% contaminated
bond failure at 2460 psi

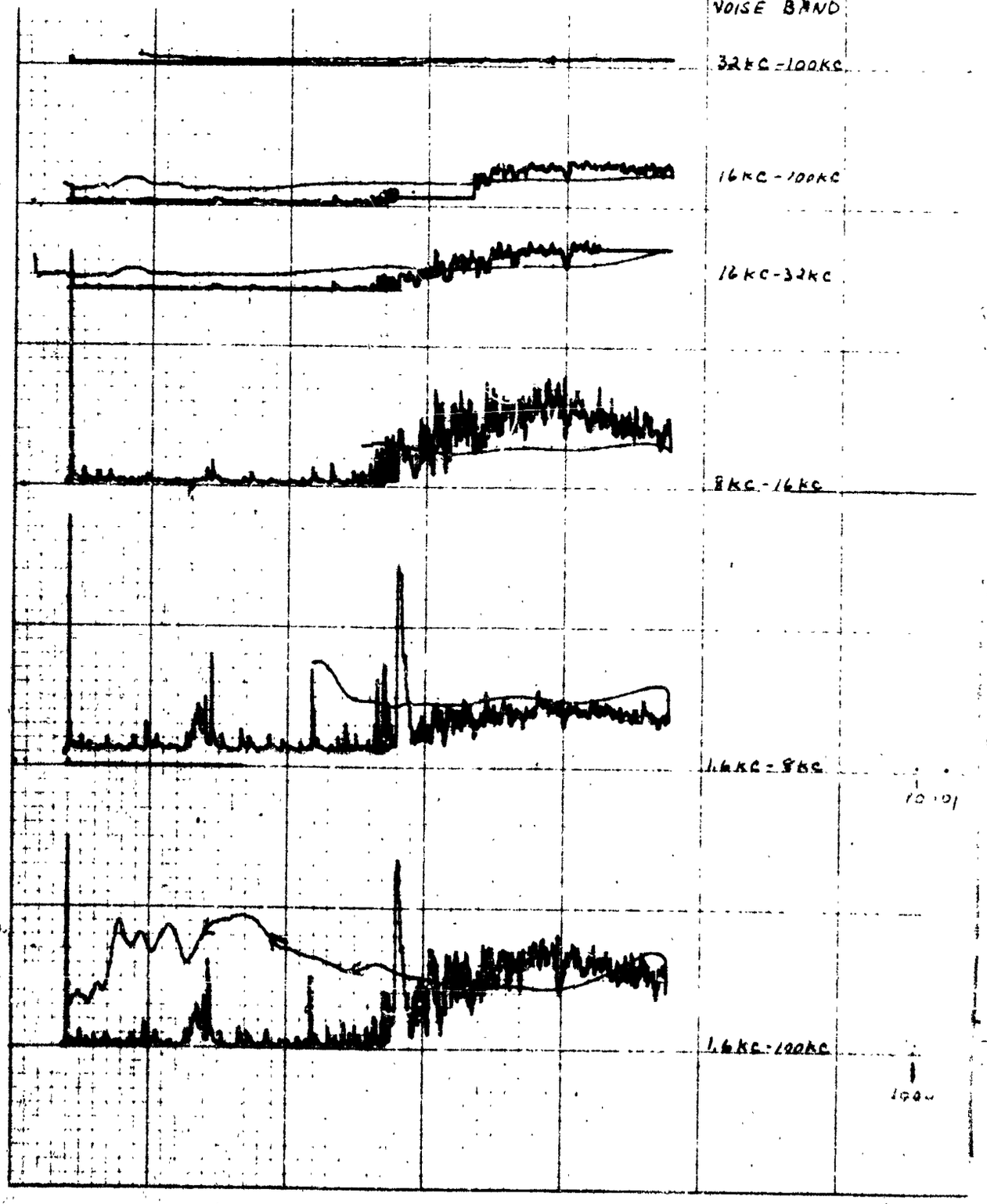

K&E 10 X 10 TO THE INCH 359-5L
KEUFFEL & ESSER CO

2

TEST NO. 16
FM 1000-C65-10
BOND FAILURE 2460 PSI
TAPE CODE ---.....
Logbook No 144 P12

Metal to Metal Test
HT 424 - Good Bond
failure at 3100 psi

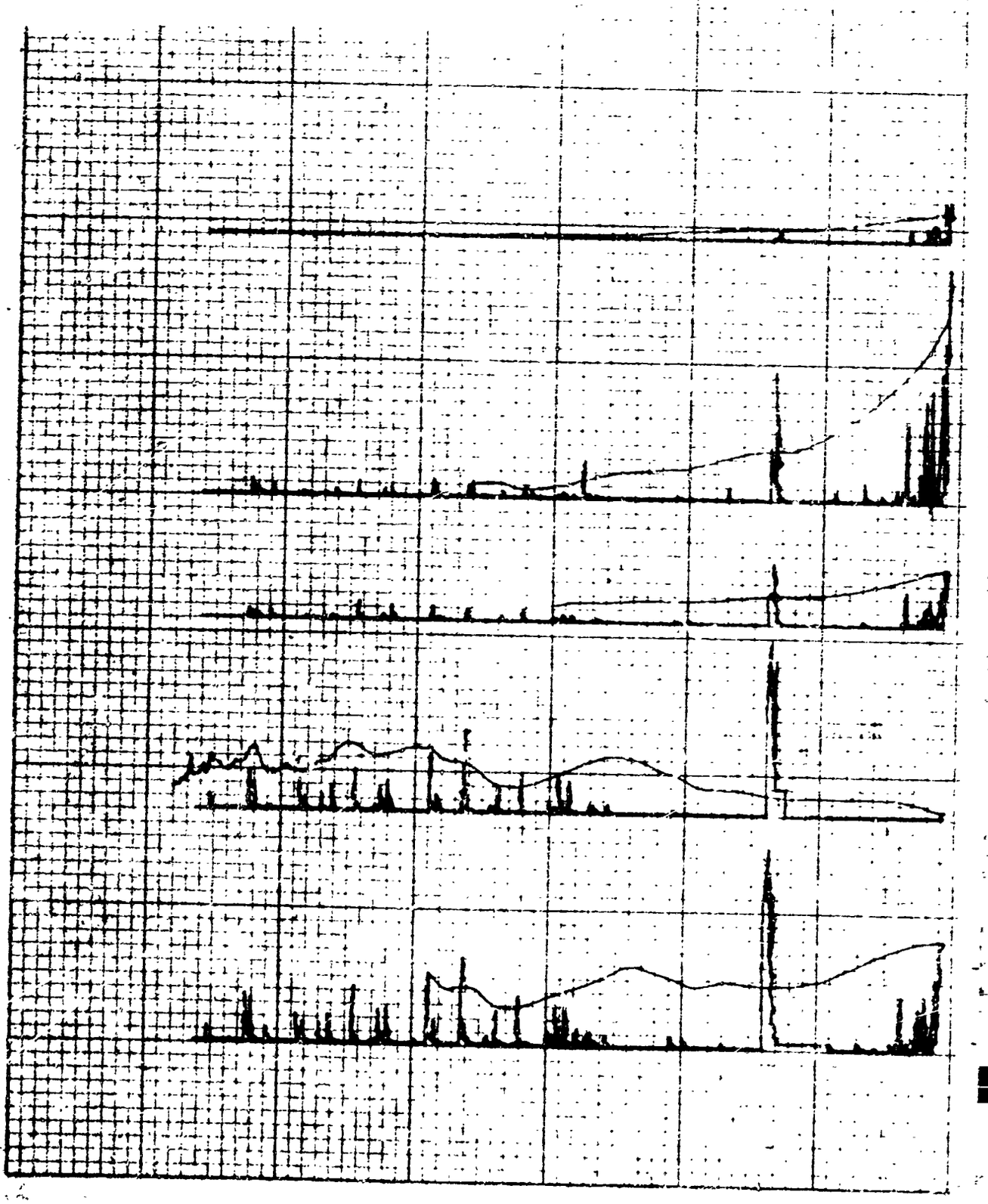

Noise Band
32-100 KC
16-100 KC
8-16 KC
4.6-8 KC
1.6-100 KC

Metal to Metal Test
HT 424 - 30% contaminated
failure at 4010 psi

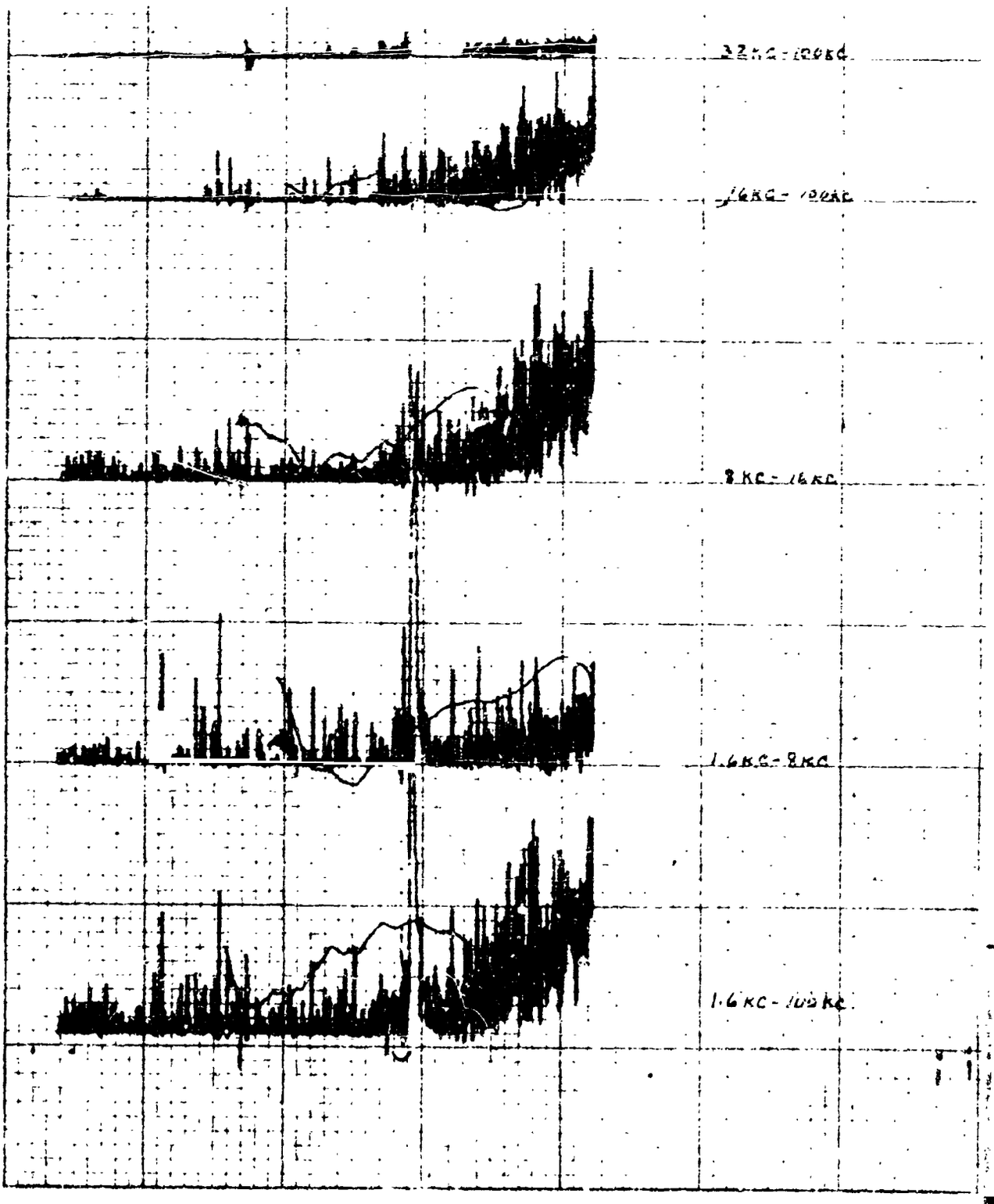

TEST NO. 15
4T424 C65-70
BOND FAILURE 2260 PSI
TAPE CODE
Log book NO 114 P12.
(Demodulator time constant
For this test only .01 sec)

Metal to Metal Test
HT 424 - 40% contaminated
bond failure at 2260 psi

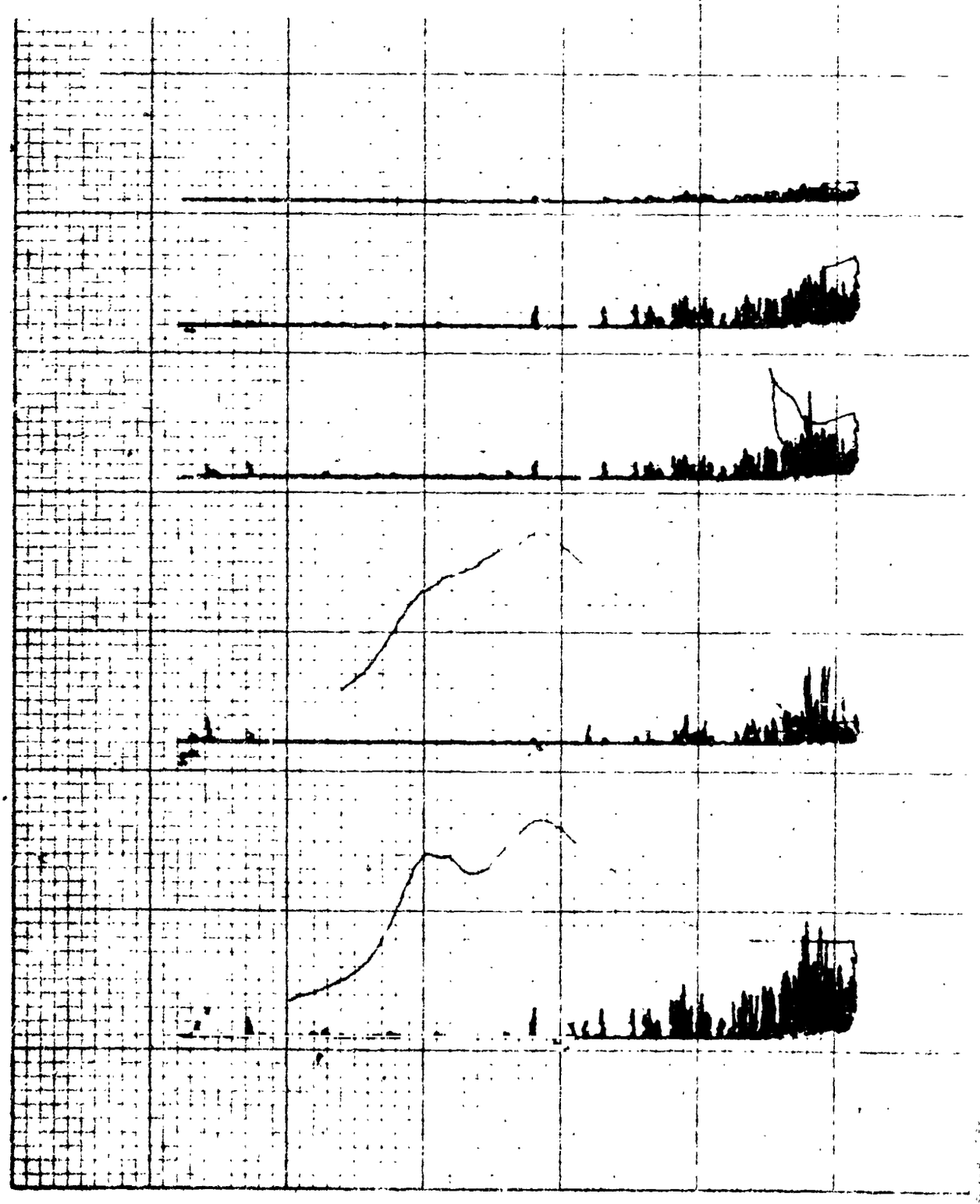

10 X 10 TO THE INCH 359 5L
KEUFFEL & ESSER CO.

2

TEST NO 9
MB329 GB
BOND Failure 45-65 psi
TAPE CODE. ... ←
LOGBOOK NO. 144 P12

NO SE 30 19

32KC - 100KC

16KC - 100KC

8KC - 16KC

1.6KC - 8KC

1.6KC - 100KC

Metal to Metal Test
MB 329 - Good Bond
bond failure at 4565 psi

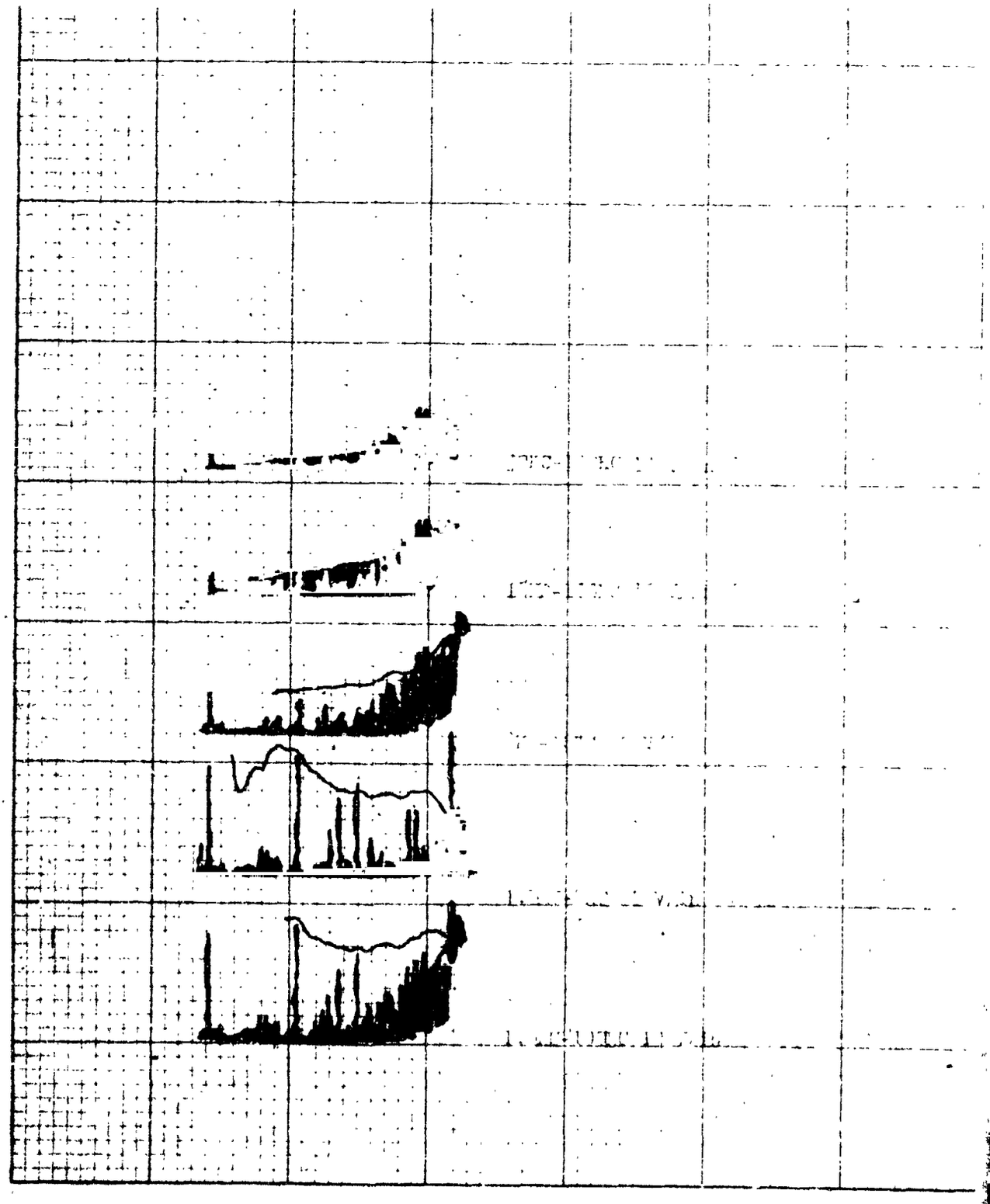

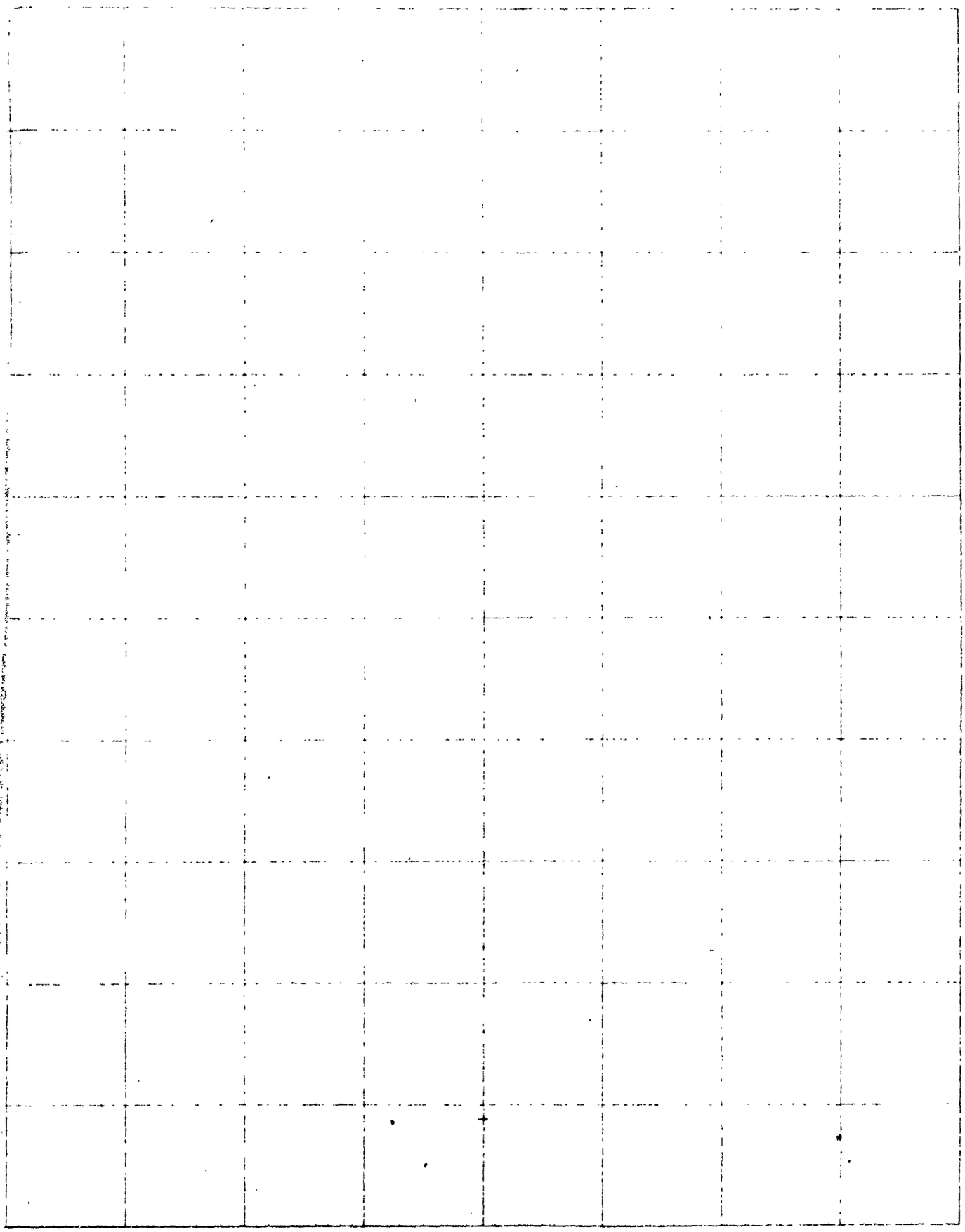

Metal to Metal Test
MB 329 - 10% contaminated
bond failure at 2355 psi

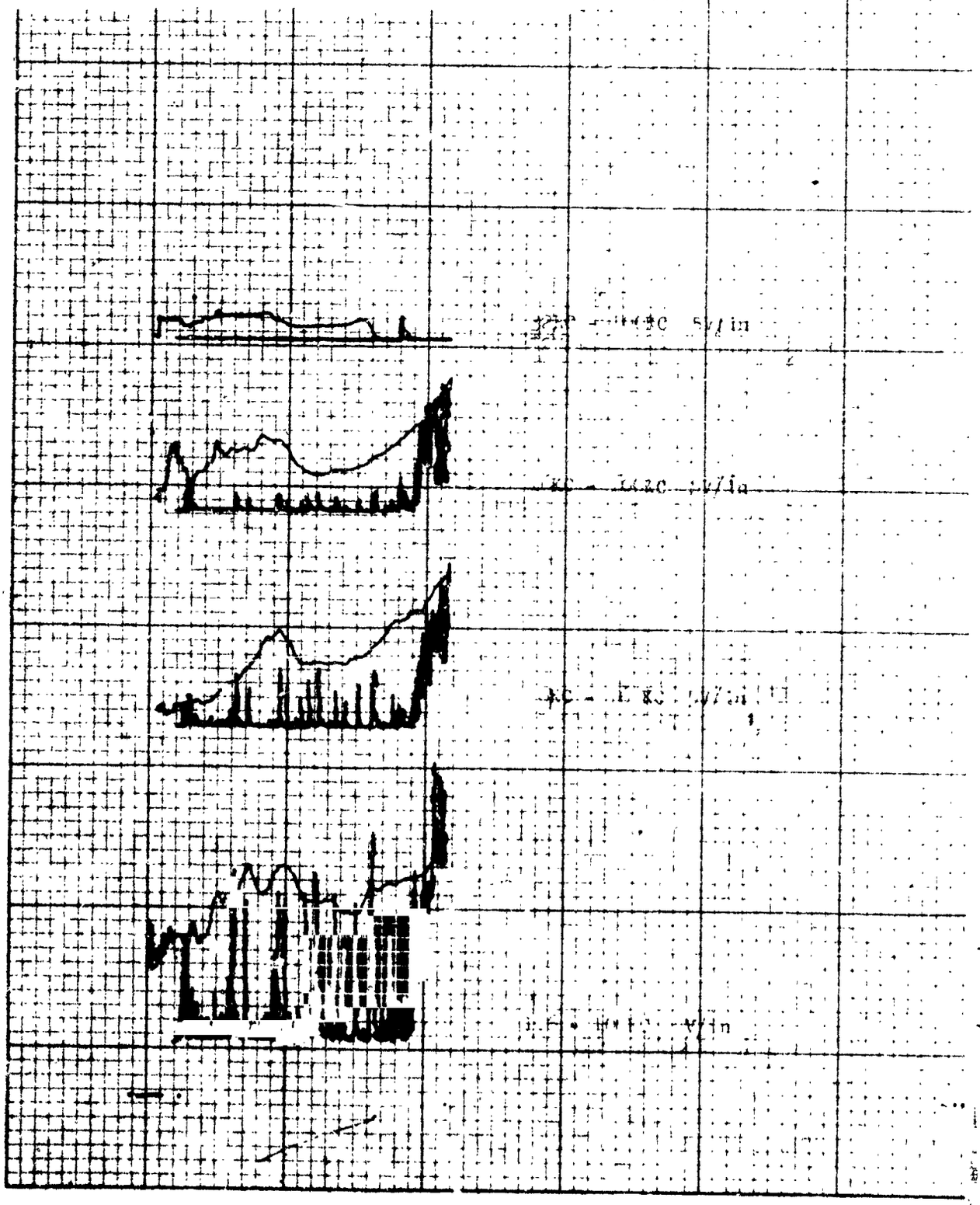

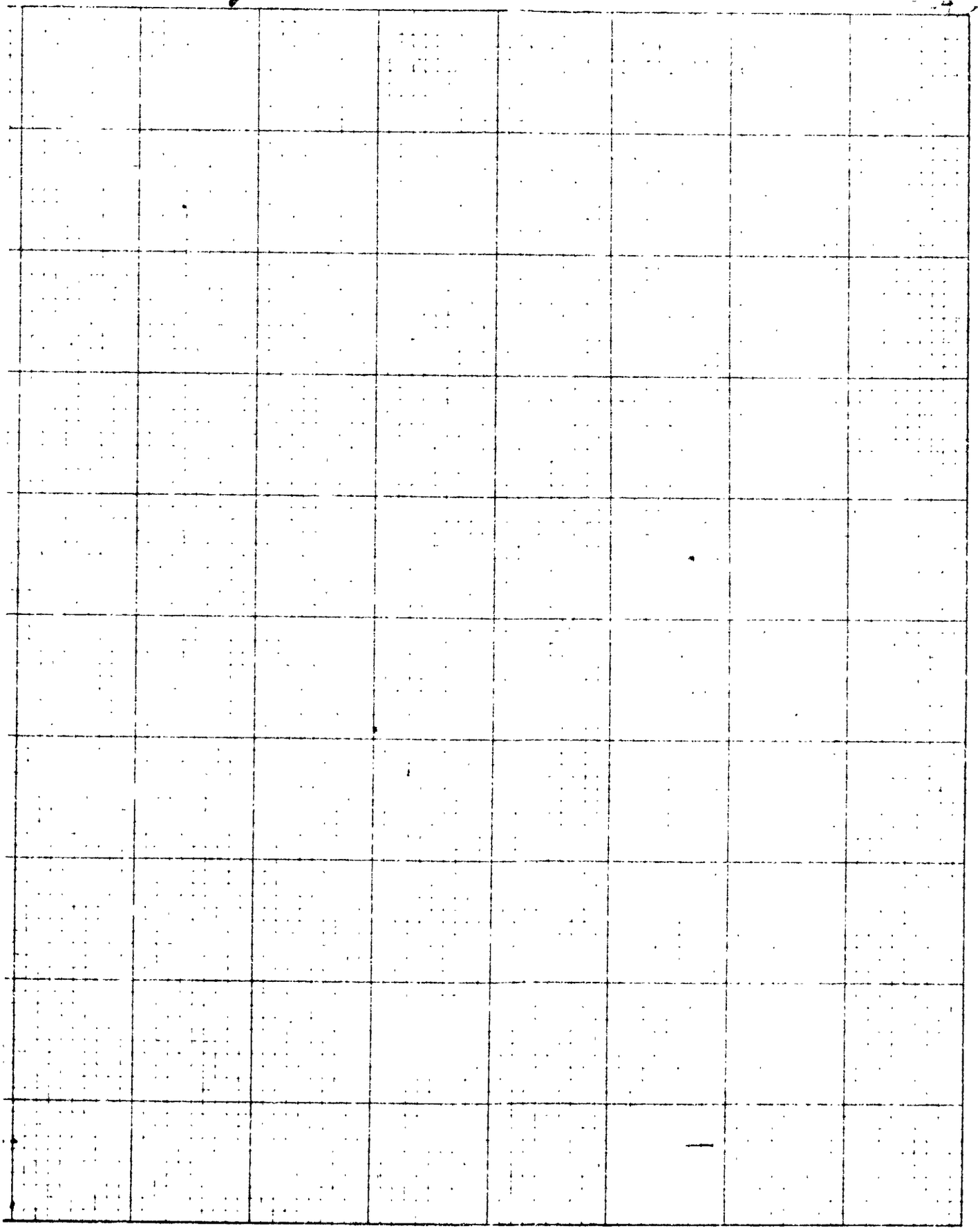

Metal to Metal Test
ME 329 - 30% contaminated
bond failure at 1230 psi

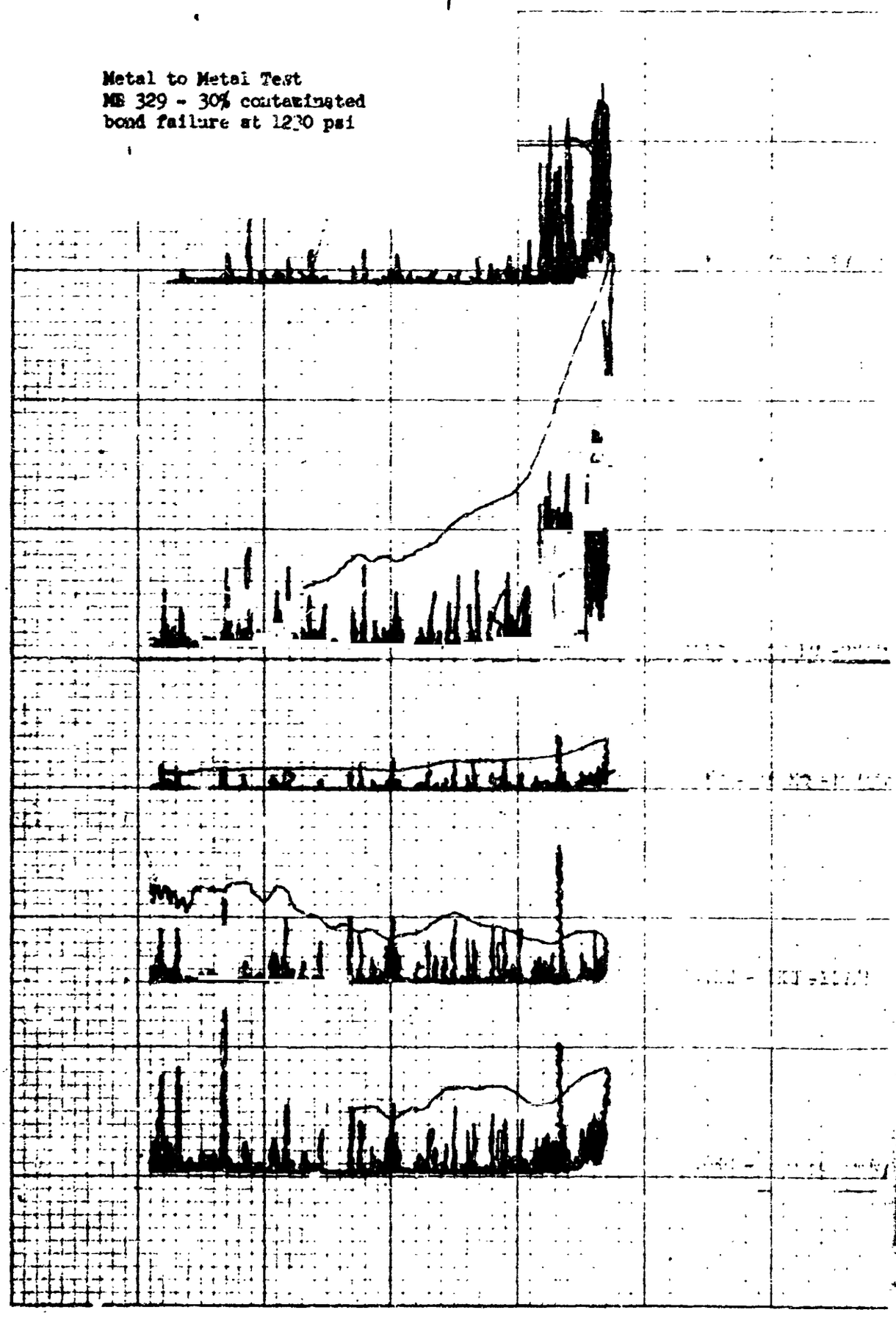

2

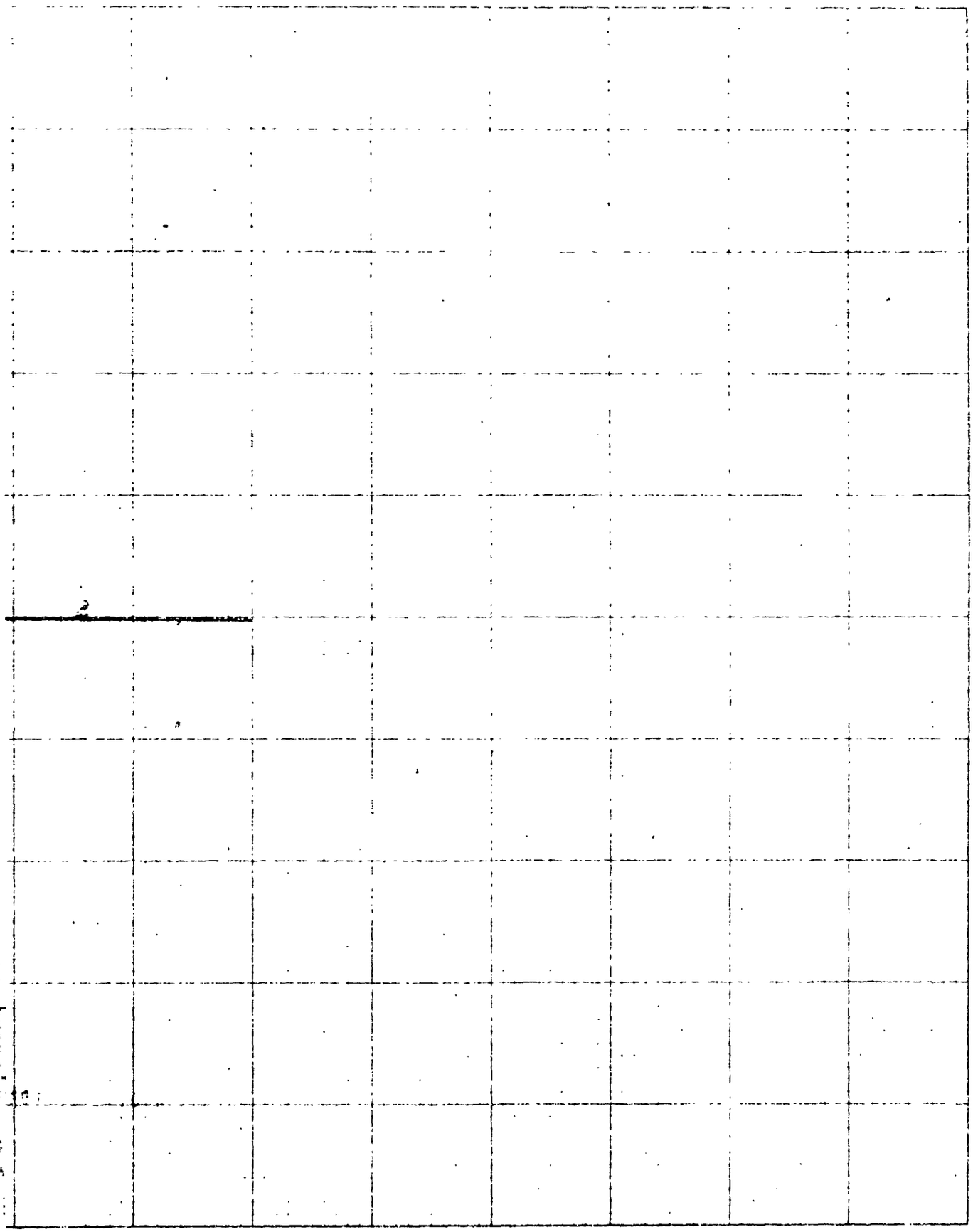

Test of Honeycomb Panel
HT 424 - Good Bond
8/26/65
Bond failure at 405 psi

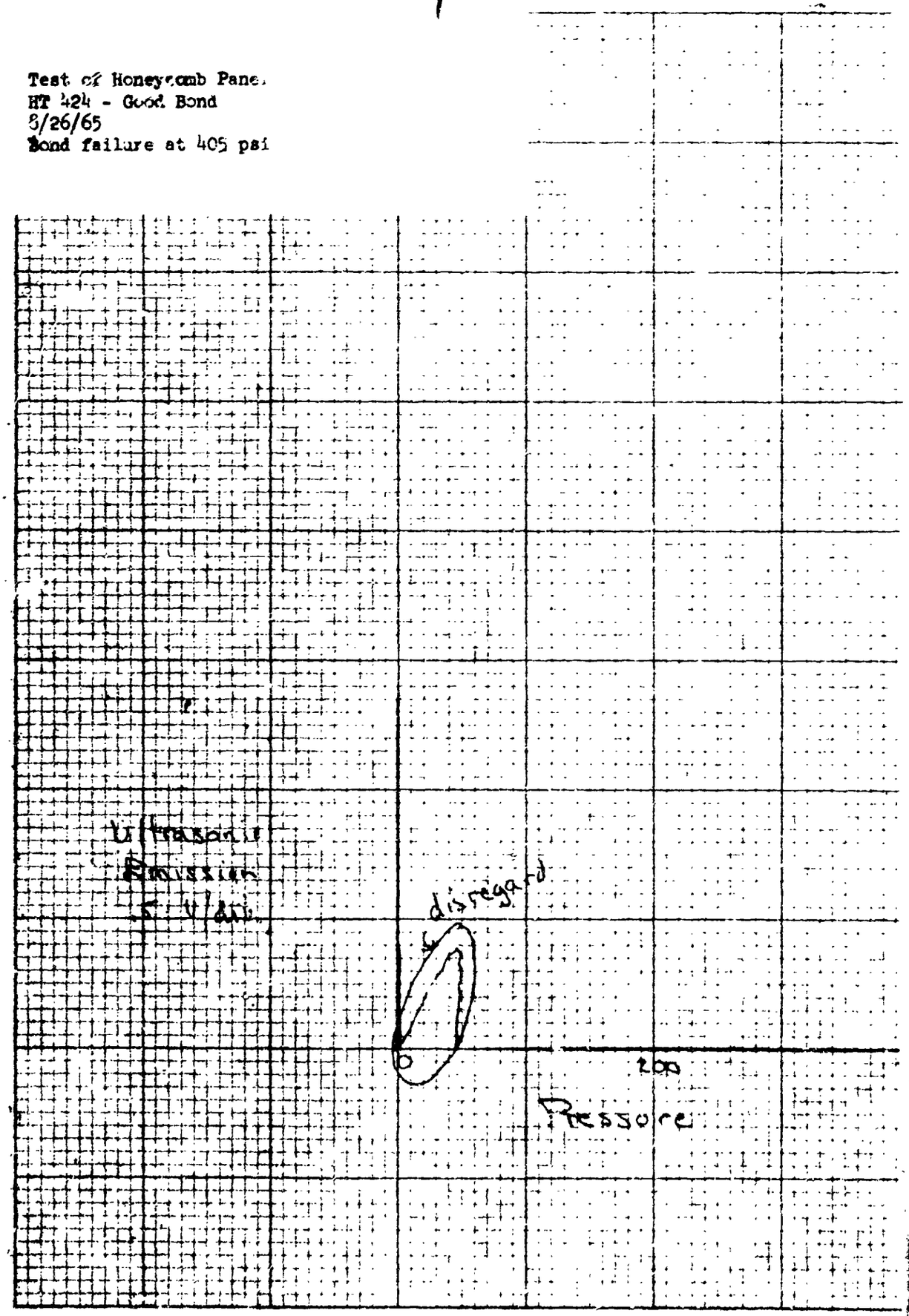

2

Test of honeycomb panel
HT424 – Gold Bond
8/26/65
Broken at 405 psi

Test of Honeycomb Panel
HT 424 - 20% contaminated
8/26/55
bond failure at 305 psi

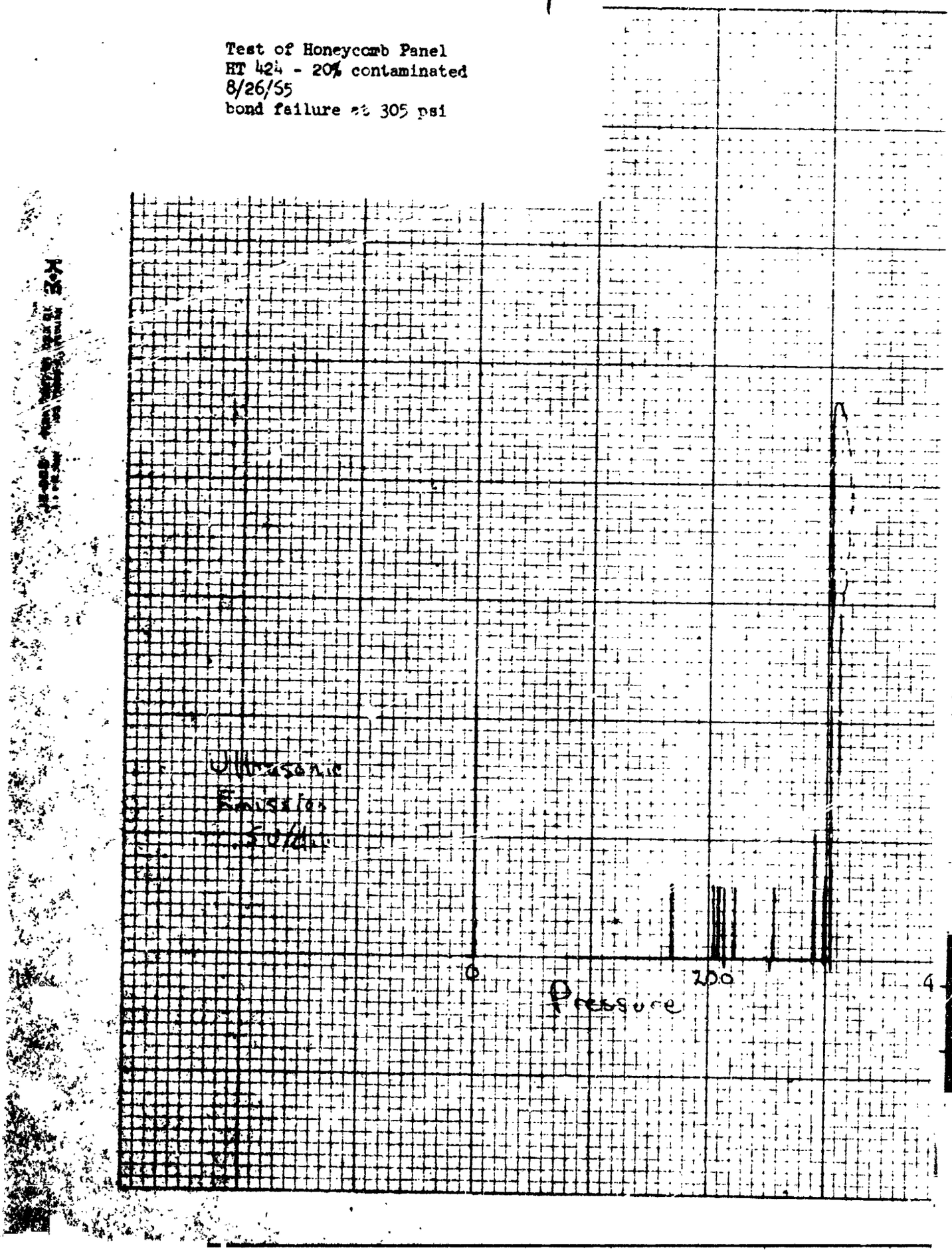

2

Test of honeycomb panel

HT 424 - 20% contaminated

8/26/65

Broken at 305 psi

Test of Honeycomb Panel
MB 329 at Good Bond
8/24/65
bond failure at 650 psi

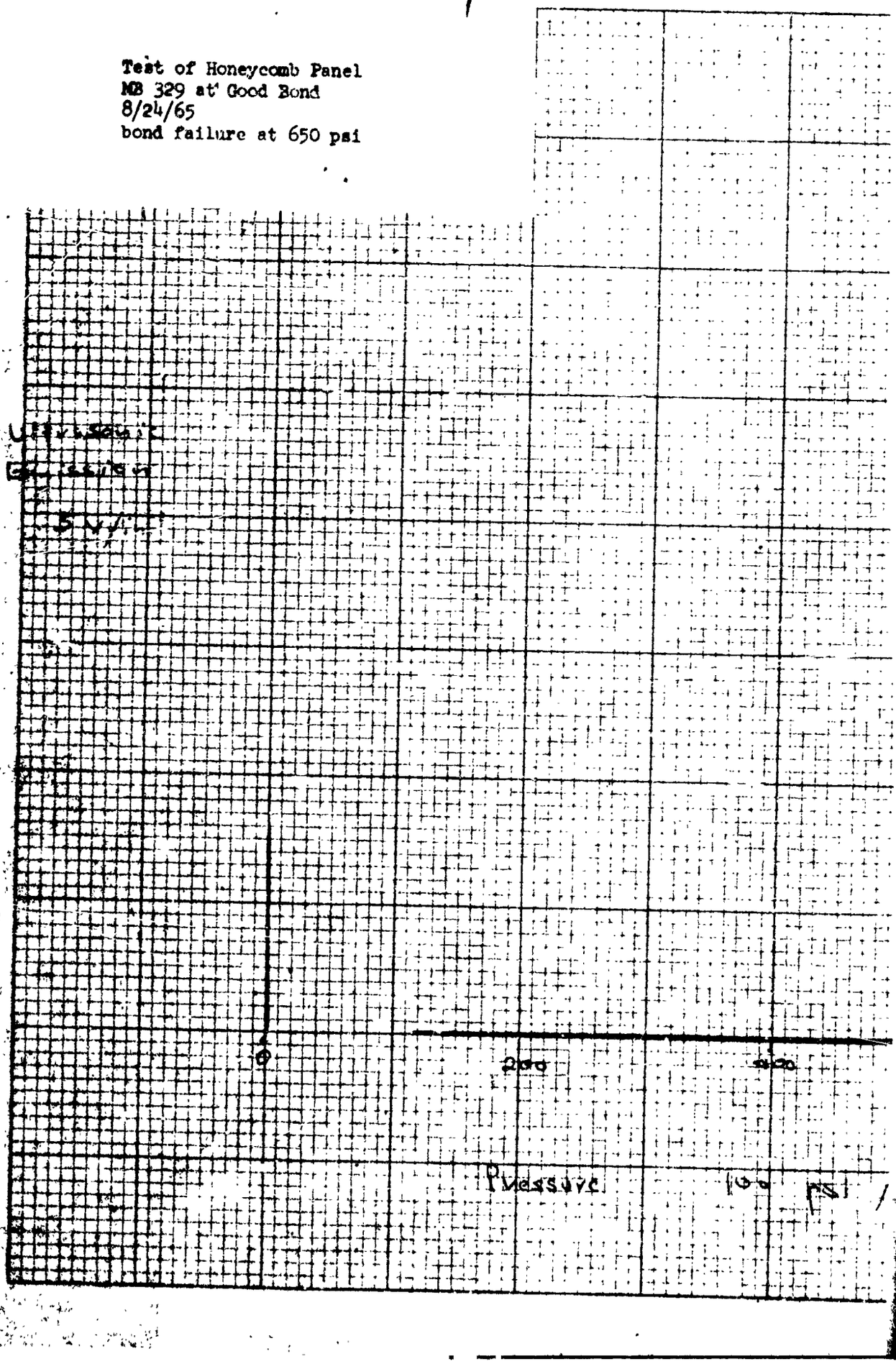

2

Test of honeycomb panel

HB 32 ft - Good Bond

Aug 24 1965

Ultimate Failure 650 psi

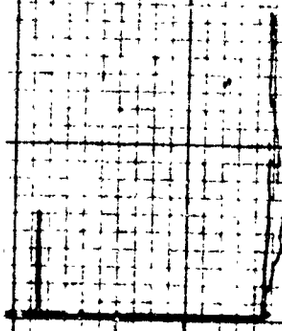

Test of Honeycomb Panel
MB 329 - 20% contaminated
8/25/65
bond failure at 619 psi

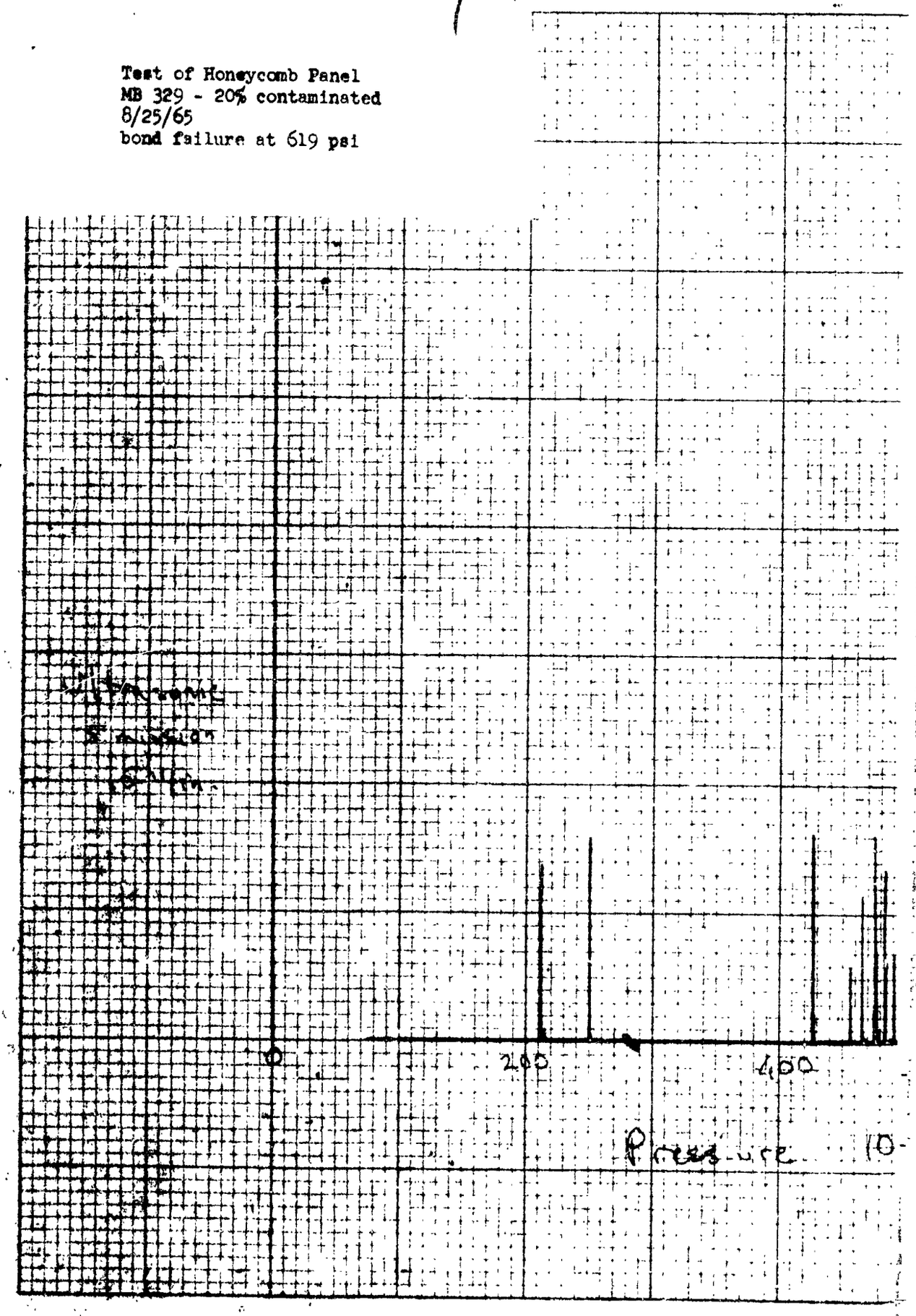

2

Test of honey comb panel

MB 329 — 20% Contaminated

Aug. 25 1965

Failure at 619 psi

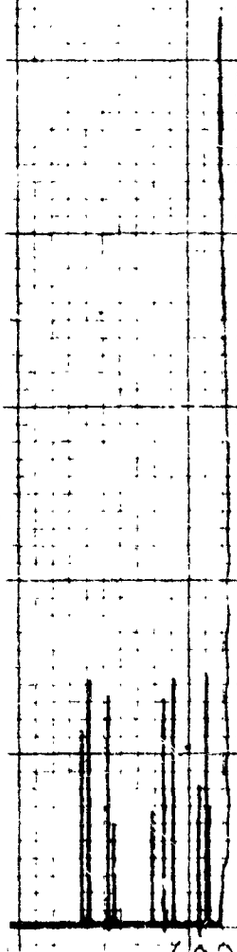

Test of Honeycomb Panel
HT 424 - Good Bond
8/26/65
bond failure at 560 psi

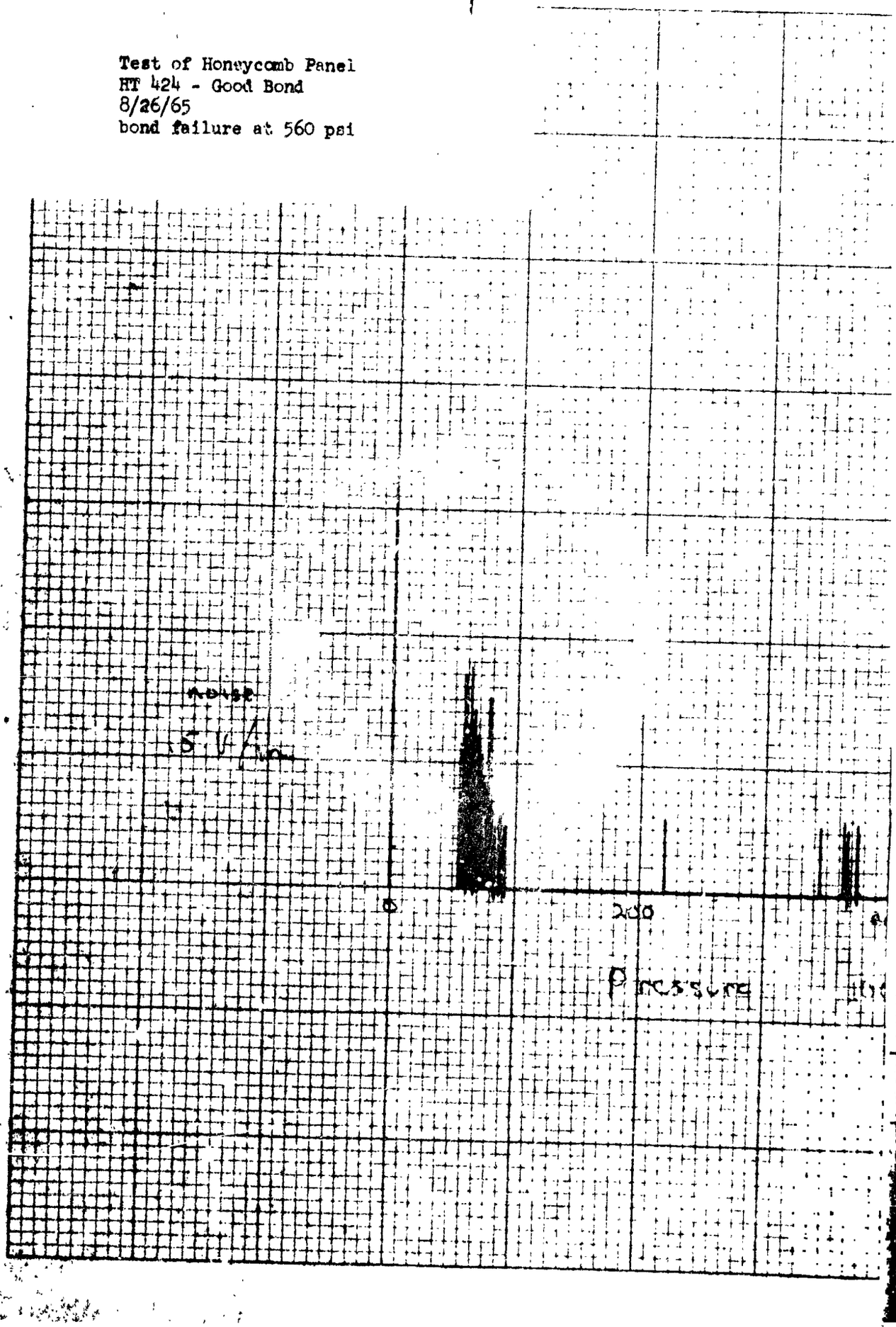

2

Test of honeycomb panel

Sample #B-45 — pneumatic honeycomb
9/26/65 HT424

broken at 560 psi

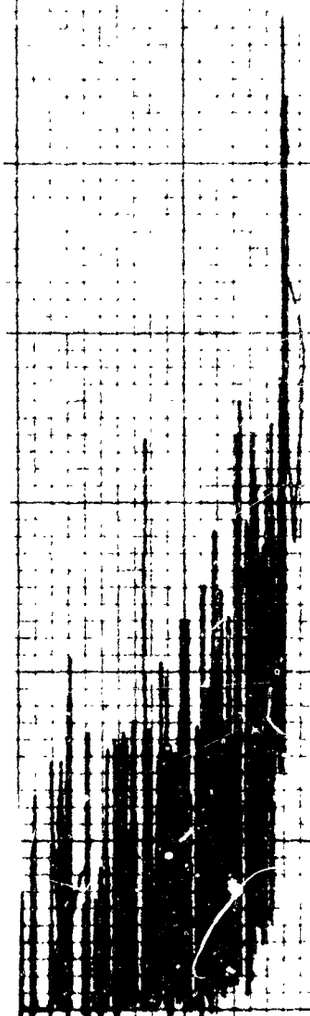

Test of Honeycomb Panel
HT 424 - Good Bond
8/26/65
Suspected bond failure at 525 psi
pressure failure at 525 psi

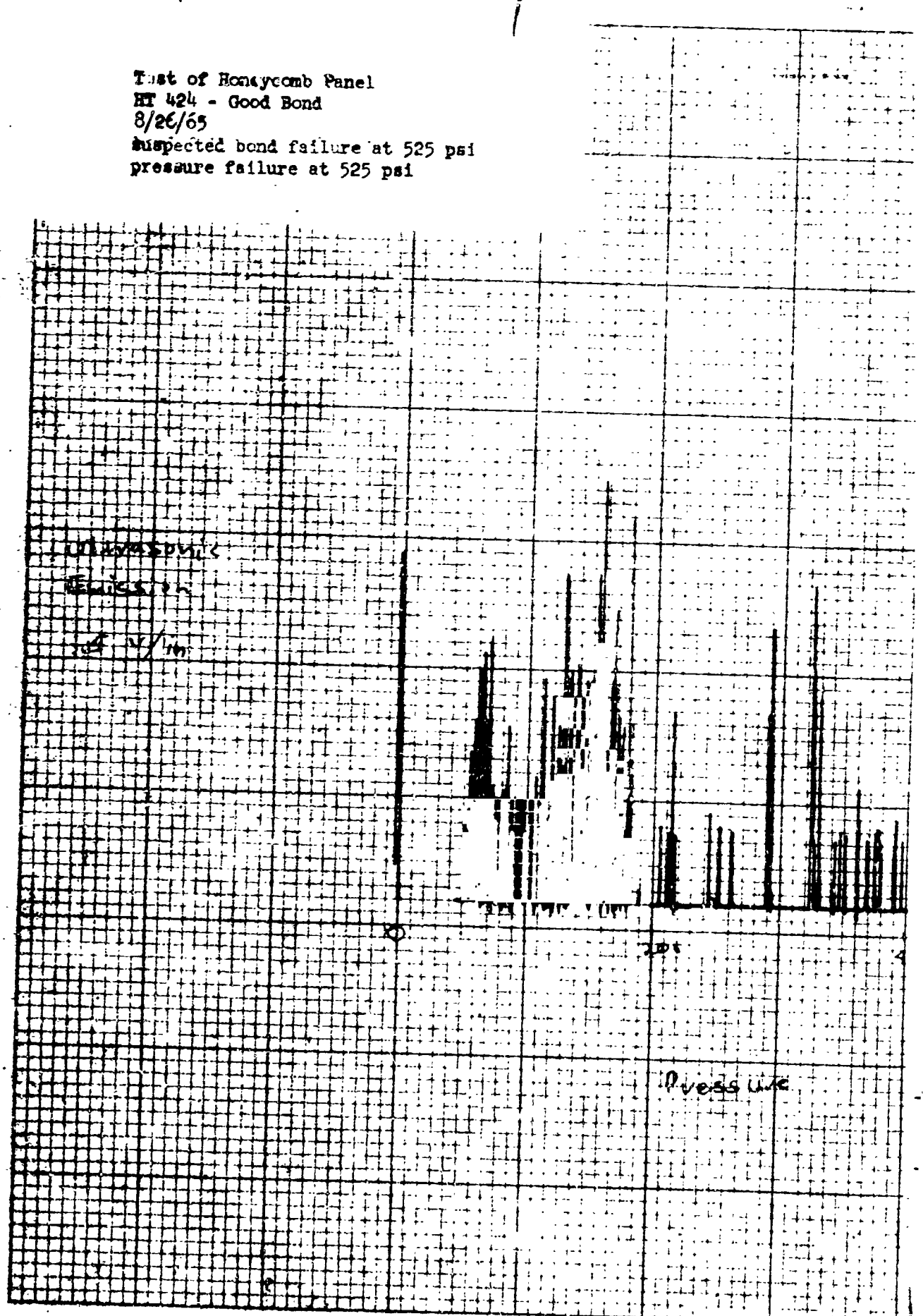

2

Test of Honeycomb panel

Sample B43 - Phenolic Honeycomb

Aug 26 1965 HT424

Suspected Honeycomb failure ≈ 55 psi

Pressure Failure = 525 psi

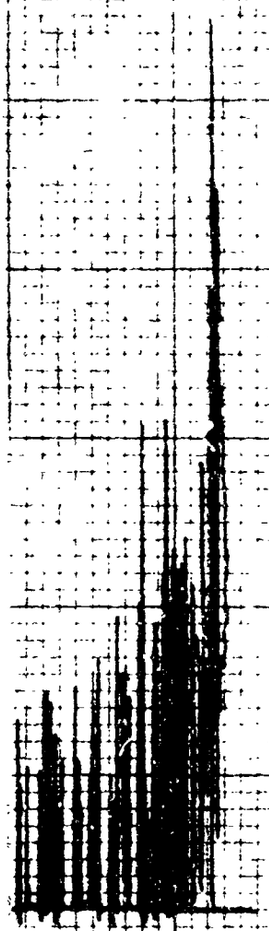

900

100 psi / in

Test of Honeycomb Panel
MB 329 - Good Bond with .030" face sheet
8/26/65
bond failure at 700 psi

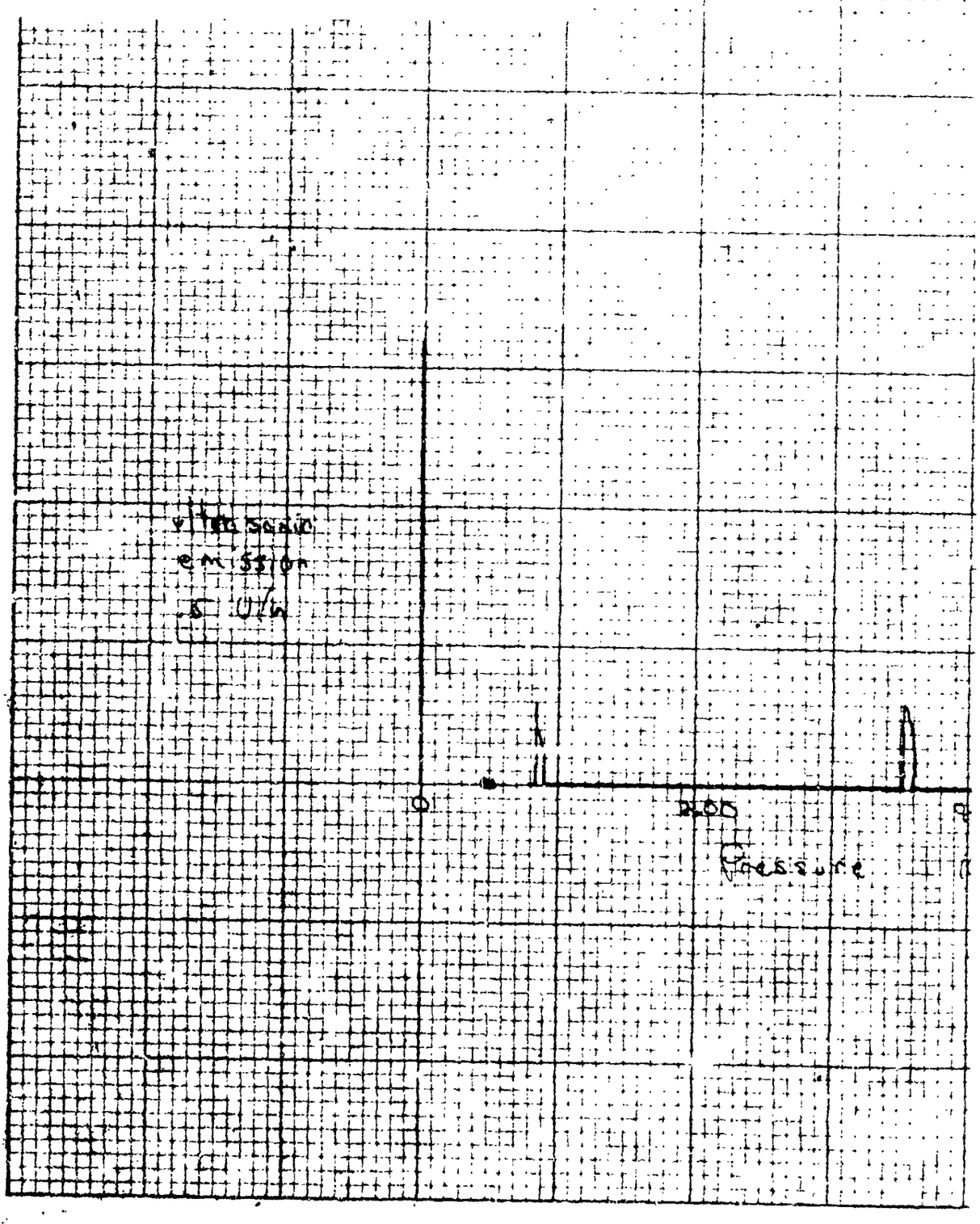

2

Test of honeycomb panel

Sample # C+5

MB 329 .030 inch

~~Place sheet~~

8/24/60 Face sheet

yield 700 psi

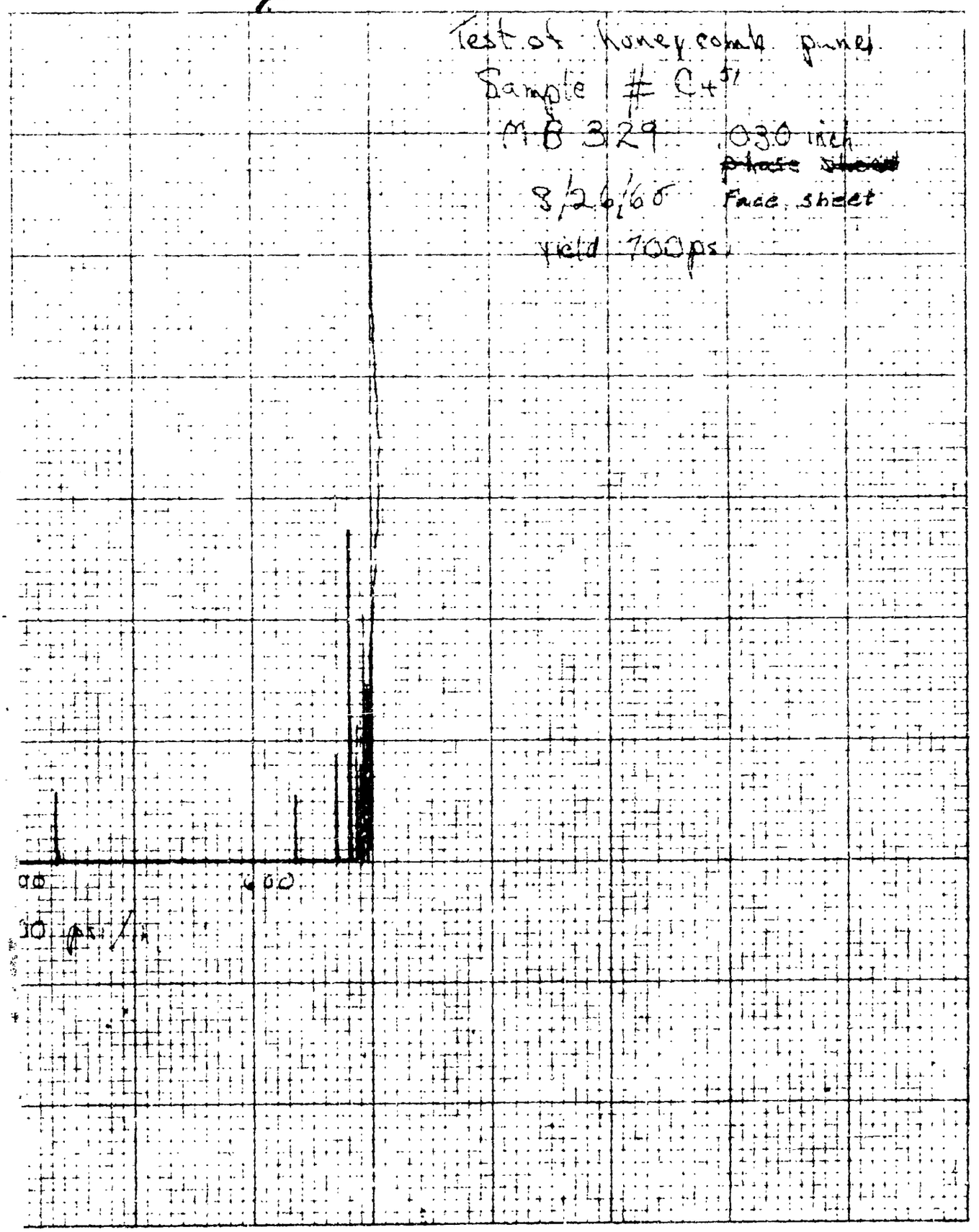

Test of Honeycomb Panel
FM 1000 - Good Bond
8/26/65
bond failure at 405 psi

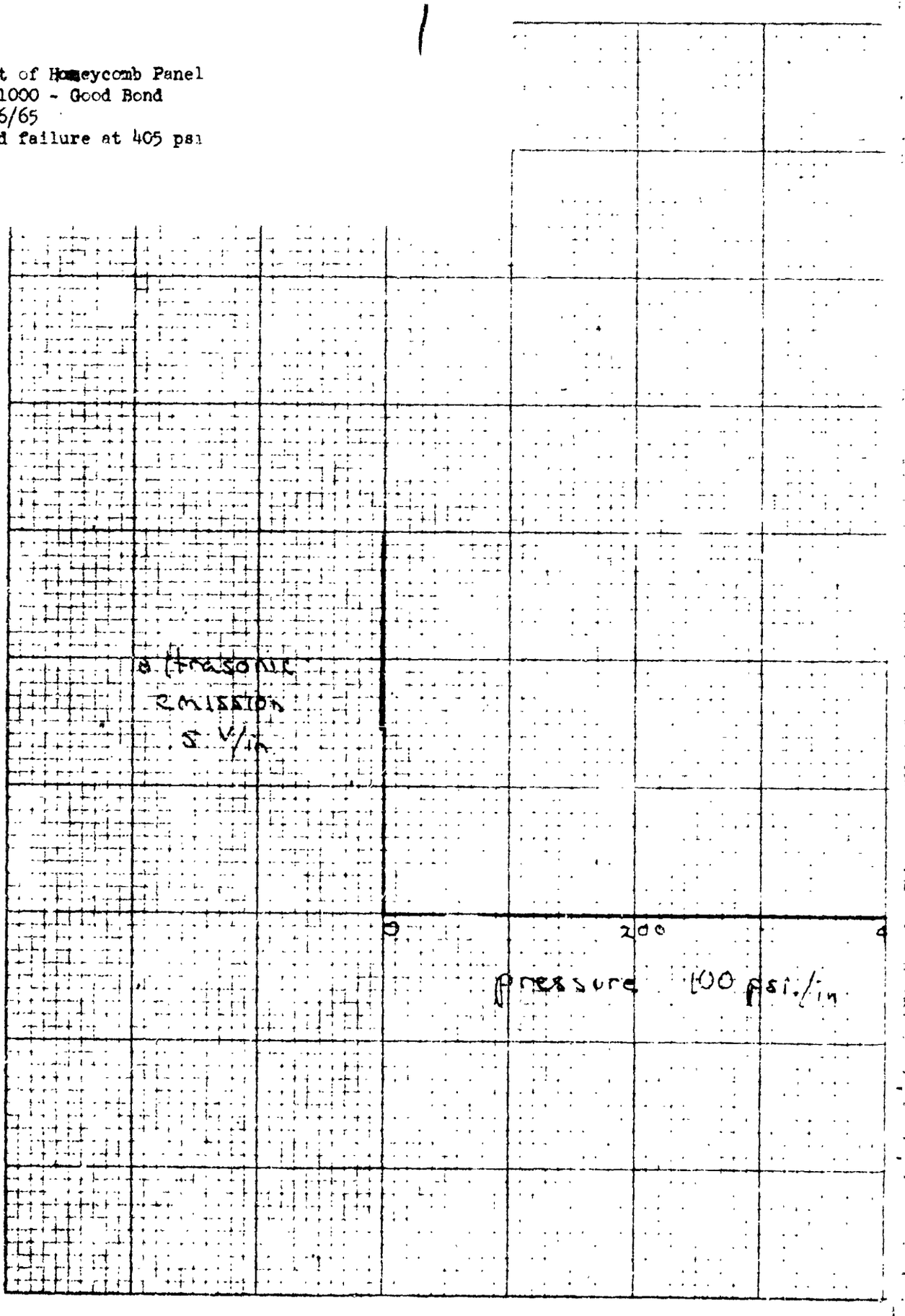

K&E 10 X 10 TO THE INCH 359-SL KEUFFEL & ESSER CO.

Test of honeycomb panel
FM 1000 – Good Bond
8/26/65
bond yield ~~406 psi~~

Test of Honeycomb Panel
FM-1000 - 20% contaminated
8/26/65
suspected bond failure at 260 psi
pressure failure at 307 psi

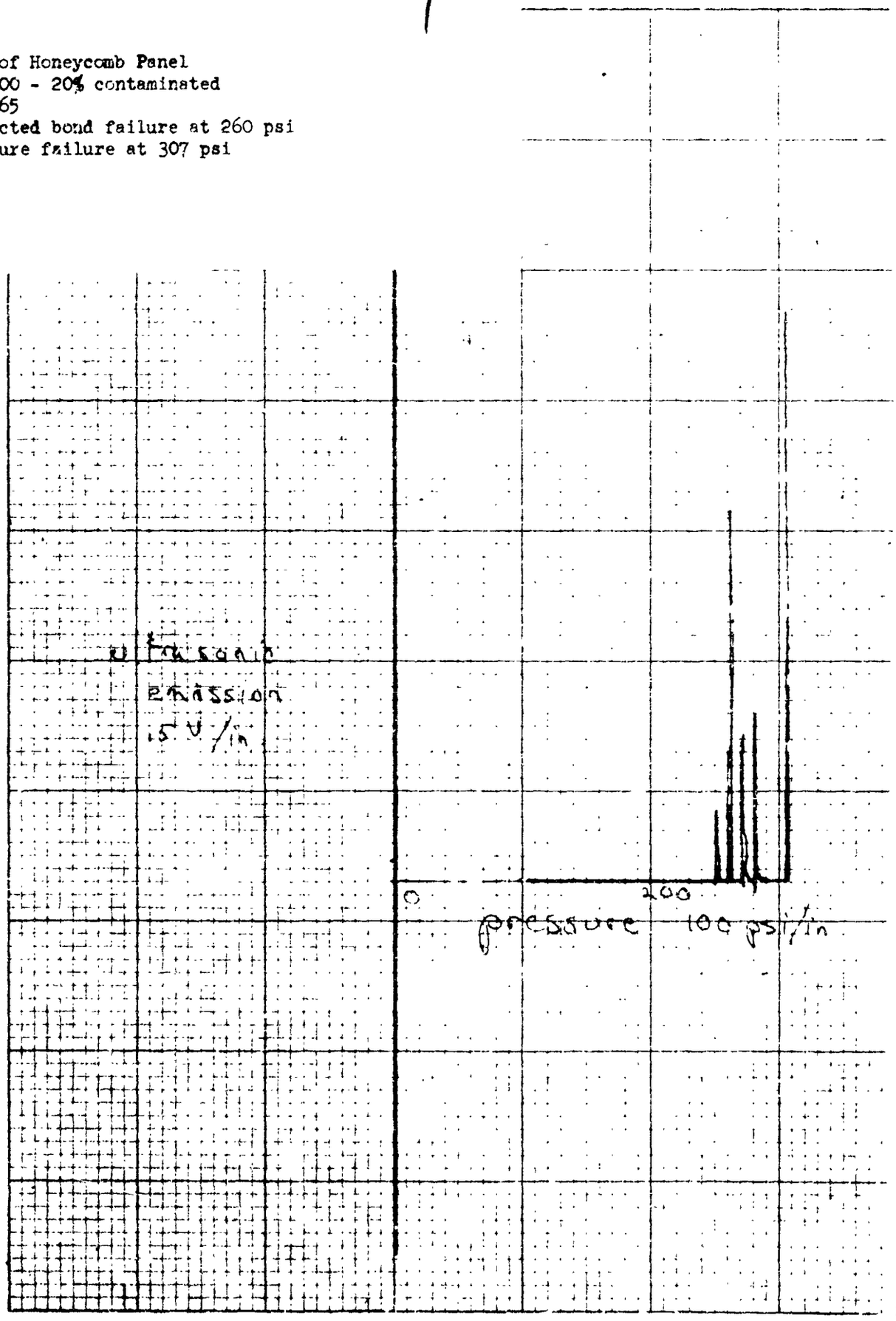

2

Test of honeycomb panel

FM 1000 — 20% contaminated

8/26/65

bend yield 260 psi

pressure yield 307 psi

APPENDIX 4

OPERATION OF THE ULTRASONIC EMISSION DETECTOR

The Ultrasonic Emission Detector is a heterodyne ultrasonic receiver designed to operate in the 27 to 37 KHz frequency region for use in the ultrasonic NDT procedures previously described. Figure 14 (Block Diagram of Ultrasonic Emission Detectors) will be used to explain its operation.

Ultrasonic energy impinging upon the transducer will result in an electrical signal being transmitted to the Ultrasonic Emission Detector. The first stage of signal processing consists of an amplifier with a voltage gain of 5000 about a center frequency of 31 KHz with a usable range of 5 KHz on either side of the center frequency. This restricted bandwidth effectively filters out noise and spurious signals.

The next stage of signal processing converts the 27 to 37 KHz signals to signals of under 6 KHz, within the range of human hearing. This is accomplished by hetrodyning the output of the first amplifier with a local oscillator of 32 KHz. Of the sum and difference frequencies produced the difference will be within the desired audio range. A potentiometer is provided on the rear panel to adjust the amplitude of the local oscillator for maximum mixing efficiency. This control is adjusted to the point where background noise is just audible with maximum headphone volume.

The final stage of signal processing consists of signal presentation. The signal from the mixer is made available for meter or chart recorder presentation by a pulse detector with an integration time of about .1 second. This output is available on the rear panel. In addition, signals from the mixer are amplified for headphone use by an audio amplifier with a gain of 5000; this output is available on the front panel. A potentiometer adjustment of headphone volume is also located on the front panel.

Construction of the Ultrasonic Emission Detector was undertaken with a high regard for portability and field use. Removable modular design was used to facilitate repairs. In addition, a spare module receptical was provided for easy storage of a replacement module. The four basic modules are: (their circuit diagrams are given in the following figures)

1) Amplifier - Figure B
2) Oscillator - Figure C
3) Mixer and Pulse Detector - Figure D
4) Headphone Amplifier - Figure E

This instrument was used in the tests presented in Table 4.

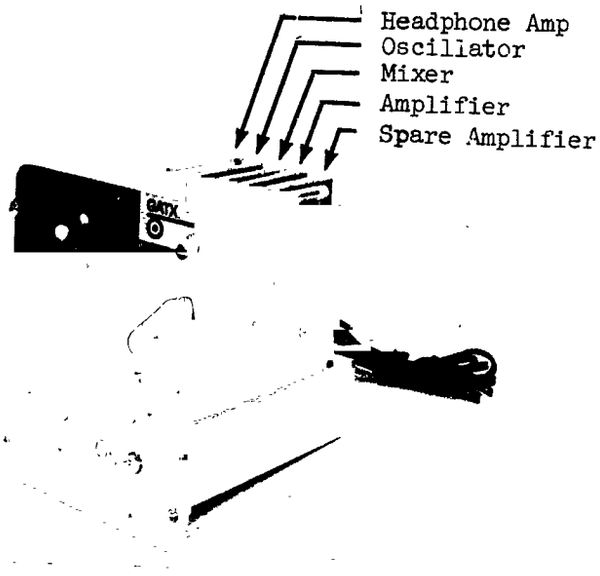

Ultrasonic Emission Detector

Figure A

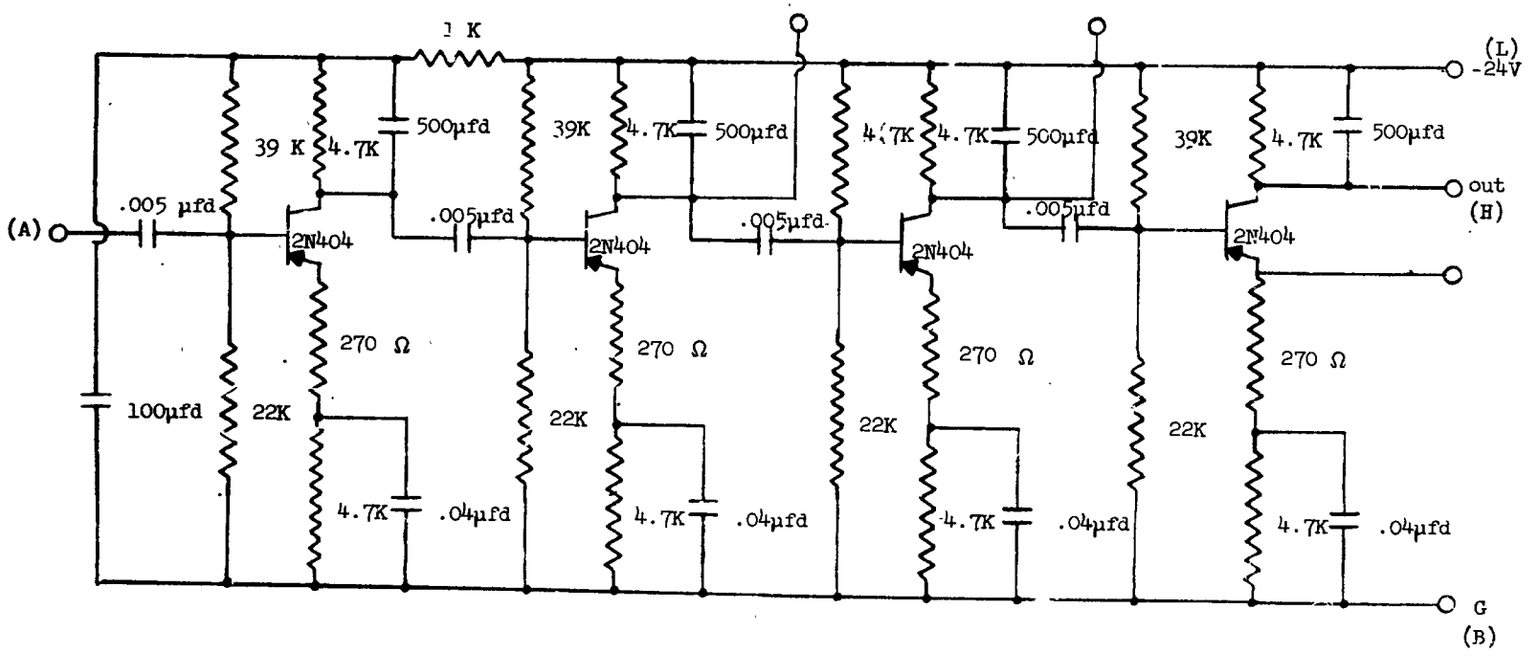

AMPLIFIER - Fig. B

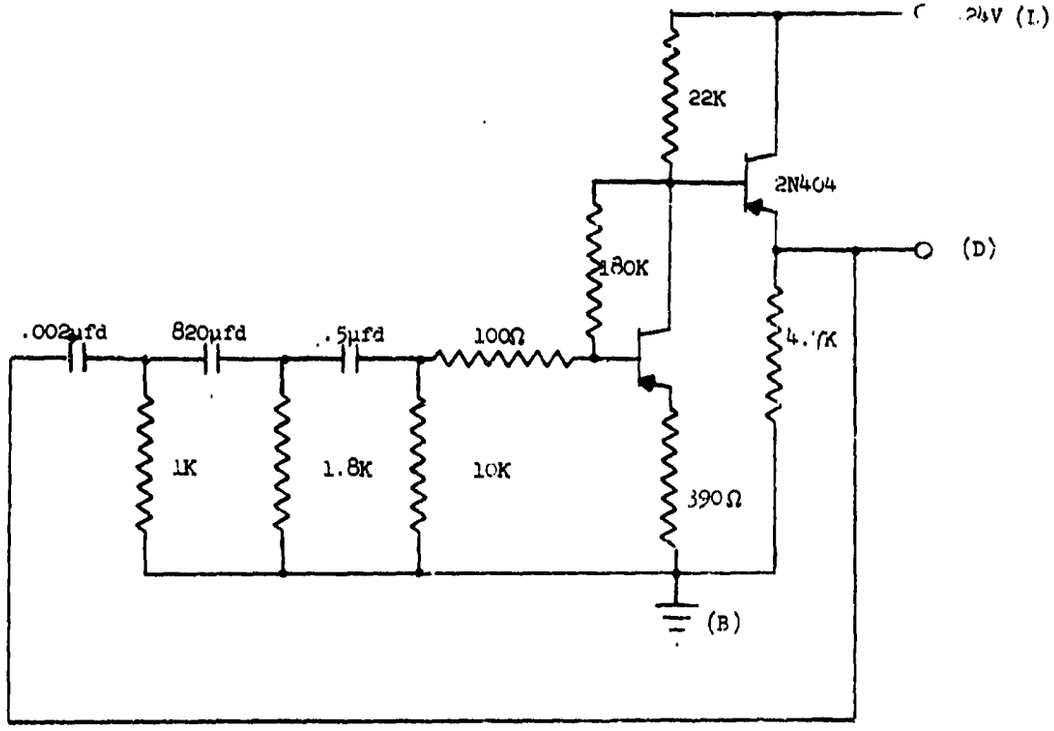

PHASE SHIFT OSCILLATOR

Fig. C

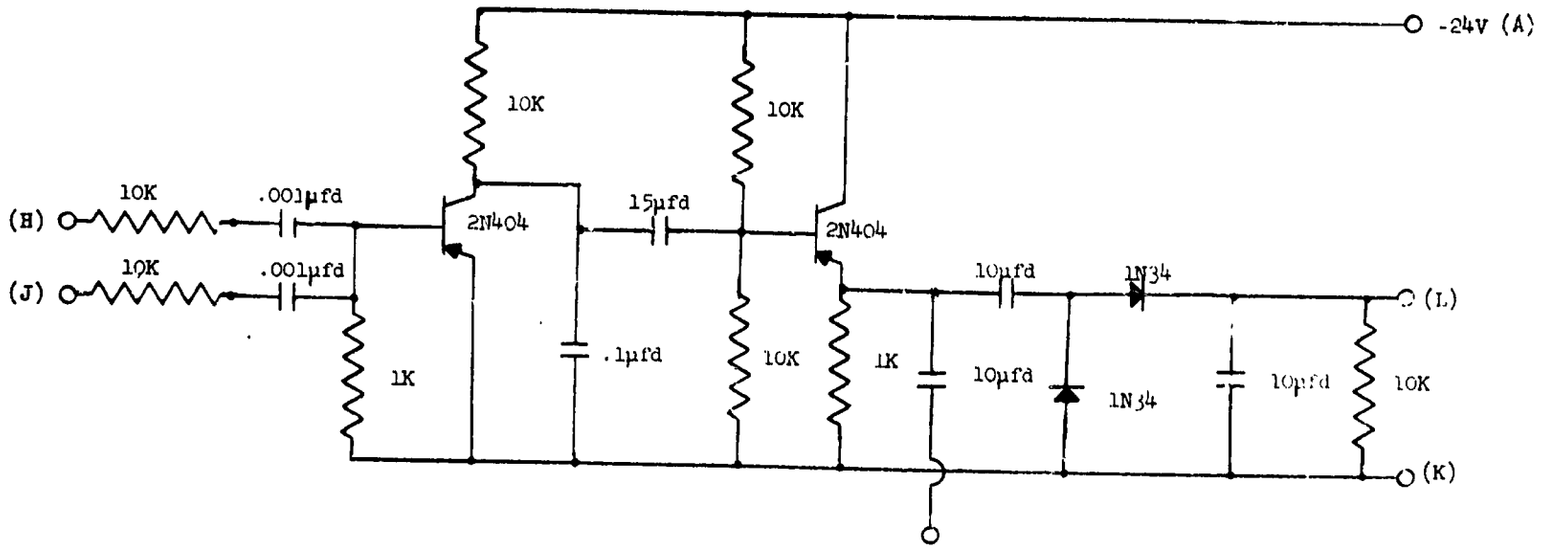

MIXER AND PULSE DETECTOR

Fig. D

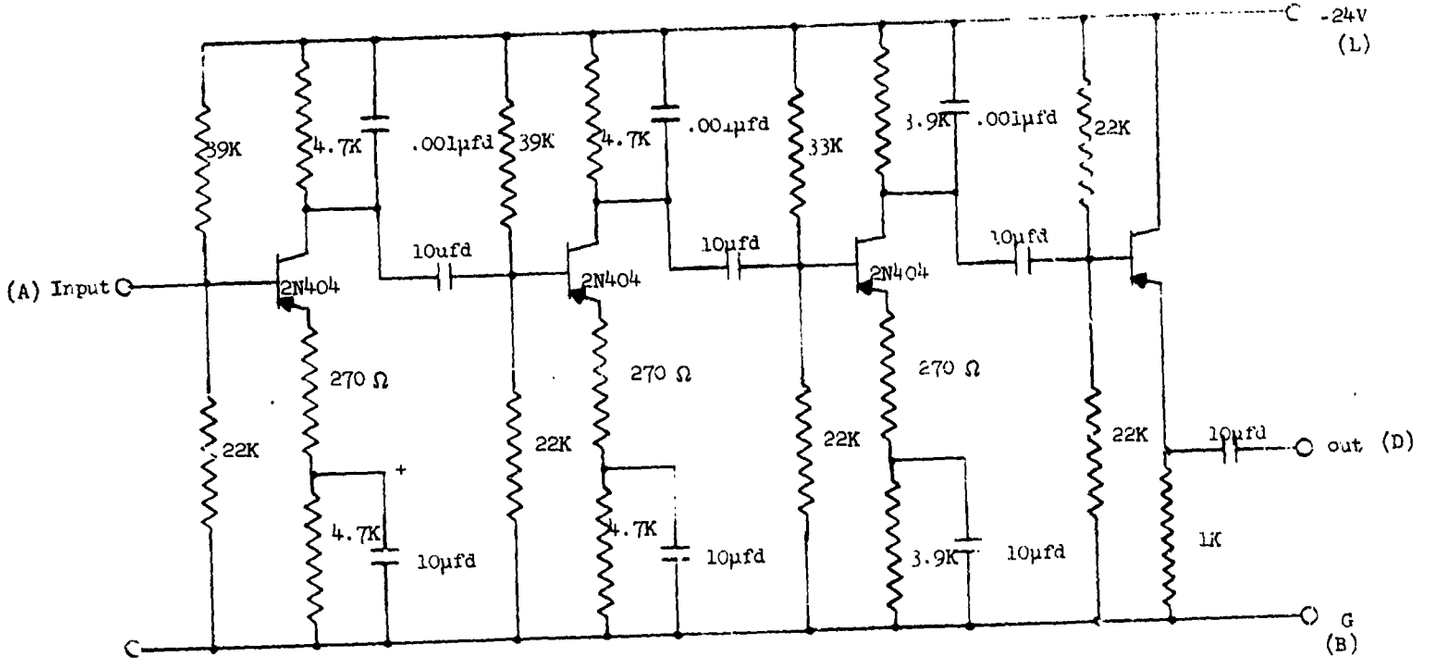

HEAD PHONE AMPLIFIER

Fig. E